THE MECHANICAL DESIGN AND DEVELOPMENT OF A KRYPTON GAS TARGET SYSTEM FOR THE PRODUCTION OF RUBIDIUM-81

C.J. Stevens

Research Project presented in partial fulfilment

for the Masters Diploma in Technology at the

Cape Technikon

1992

Internal Supervisor: D.J. Sinclair M.Sc.(Eng.) B.Sc.(Mech. Eng.)

External Supervisor: G.F. Steyn Ph.D.(Stell.)

DECLARATION

I, the undersigned, hereby declare that the work contained in this thesis is my own original work and has not previously in its entirety or in part been submitted at any technikon for a masters diploma in mechanical engineering.

Signature: _____   Date: _30/10/92_

ACKNOWLEDGEMENTS

THE MECHANICAL DESIGN AND DEVELOPMENT OF A KRYPTON GAS TARGET SYSTEM FOR THE PRODUCTION OF RUBIDIUM-81

Charles Joseph Stevens

National Accelerator Centre, P.O. Box 72, Faure, 7131, South Africa

Abstract

This research project involved the design, development and manufacture of a krypton gas target system for the production of the radioisotope Rubidium-81 at the National Accelerator Centre (NAC).

The newly designed system had to be linked to the existing production facilities, which set certain restraints and fixed parameters to the design approach. The high-pressure krypton-filled gas target was designed to link up to the existing transport system which is used for the transportation of all targets to and from the target bombardment station and the hot-cells where processing takes place. Radiation resistant materials had to be selected for the target, as it would be exposed to high radiation doses during bombardment in the target bombardment station. Target cooling aspects also had to be taken into consideration due to the heat generated during bombardment.

A cryopump system for transferring the krypton gas from a gas storage reservoir to the gas target and back during loading and unloading was developed. A further development was a system which would retrieve the formed radioisotopes in a water suspension after bombardment. This demanded the design of a set of spray nozzles which were mounted inside the gas target chamber, a suitable water circulating pump and filters to trap the suspended radioisotopes . Due to the high radiation levels, which are, of course, dangerous to operating personnel, the whole system was constructed inside a hot-cell, and thus required the design of a fully remote control system together with gas monitoring and safety components. The processing system itself required many switching and monitoring operations which have to be carried out accurately and sequentially and this further demanded making use of a microcomputer control system.

Material strengths, manufacturing methods, performance and selection of the various components in the system were investigated, as well as the respective routine maintenance and repair aspects.

DIE MEGANIESE ONTWERP EN ONTWIKKELING VAN 'N KRIPTONGASSKYFSTELSEL VIR DIE VERVAARDIGING VAN RUBIDIUM-81

Charles Joseph Stevens

Nasional Versnellersentrum, Posbus 72, Faure, 7131, Suid-Afrika

Samevatting

Hierdie navorsingsprojek het die ontwerp, ontwikkeling en vervaardiging van 'n kriptongasskyfstelsel vir die produksie van die radioisotoop Rubidium-81 by die Nasionale Versnellersentrum (NVS) behels.

Die nuut-ontwerpte sisteem moes by die bestaande produksiefasiliteite inskakel, wat die ontwerpbenadering met bepaalde beperkinge en vasgelegde parameters belas het. Die hoëdruk kriptongevulde gasskyf is ontwerp om by die bestaande transportstelsel aan te pas wat gebruik word vir die vervoer van alle skywe na en van die skyfbombardeerstasie en die warmselle waar prosessering plaasvind. Stralingsbestande materiale moes vir die skyf uitgesoek word aangesien dit tydens bombardement in die bombardeerstasie aan hoë stralingsdosisse blootgestel sal word. Aspekte van skyfverkoeling moes ook in ag geneem word as gevolg van die hittevrystelling tydens bombardement.

'n Kriopompstelsel om die kriptongas van 'n gasopgaartenk na die gasskyf en terug te verplaas tydens die proses van laai en ontlaai, is ontwikkel. 'n Verdere ontwikkeling was 'n stelsel wat die gevormde radioisotope na bombardement in 'n watersuspensie herwin. Dit het die ontwerp van 'n stel spuitstukke wat binne die gasskyfkamer gemonteer is, 'n geskikte watersirkuleerpomp en filters om die gesuspendeerde radioisotope vas te keer, geverg. Vanweë die hoë stralingsvlakke, wat natuurlik gevaarlik is vir bedryfspersoneel, is die hele stelsel binne-in 'n warmsel ingerig, wat vereis het dat 'n stelsel wat ten volle afstandsbeheerd is, tesame met gasmonitering en veiligheidskomponente, ontwerp moes word. Die prosesseringstelsel self verg talle skakelings- en moniteringsaksies wat akkuraat en opeenvolgend uitgevoer moet word, en dus ook vereis het dat daar van 'n mikrorekenaarbeheerstelsel gebruik gemaak word.

Materiaalsterktes, vervaardigingsmetodes, werkverrigting en die keuse van verskeie komponente in die stelsel is ondersoek, sowel as die onderskeie roetine instandhoudings- en herstelaspekte.

CONTENTS

CHAPTER 5 – RESULTS

APPENDICES

LIST OF FIGURES

LIST OF FIGURES (cont.)

LIST OF TABLES

DEFINITION OF TERMS AND CONCEPTS

Activity

The rate of radioactive transformations (radioactive decays) in a given source or sample (i.e. the intensity of the radioactive source or sample).

Carrier free radioisotope

This refers to a radioisotope produced to have a very high specific activity. Carrier free strictly implies the absence of unactivated or stable isotopes of the same element as that of the desired radioisotope. In practice, the term is also used when only very low levels of stable isotopes are present in the final product.

Cyclotron

A highly sophisticated machine used for the acceleration of charged particles such as protons, deuterons and alpha-particles.

Electronvolt (eV)

This is the energy an electron would gain when accelerated across a potential difference of one Volt. The units electronvolt (eV), kilo-electronvolt (keV) and Mega-electronvolt (MeV) are more convenient than the S.I. unit, Joule.

Generators

A radioisotope generator is little more than a supply of a moderately long-lived parent radioisotope which decays to a required short-lived radioisotope.

Half-life

The average time interval required for one-half of any quantity of identical radioactive atoms to undergo radioactive decay (i.e. the time interval required for the activity of a source of any single radioactive substance to decrease to one-half). The half-lives of the known radioisotopes vary from less than a millionth of a second to more than a billion years.

Hot

In the radioactive sense of the word, it means highly radioactive and consequently poses a radiation hazard to personnel.

Ion exchange resin/generator columns

In most radioisotope generators the parent radioisotope is absorbed on a support material, such as an ion exchange resin, which is packed in a small column. The short-lived daughter radioisotope may be eluted with different solvents from the support material.

Isotope

One of two or more atomic species of an element having identical number of protons in the nucleus, but different number of neutrons. Thus, while chemically indistinguishable, they differ in mass and radioactive behaviour.

mCi/μAh

Millicurie per micro-ampere-hour. The activity of a radioactive source or sample is conveniently expressed in millicuries (1 millicurie = $3,7 \times 10^7$ radioactive transformations or decays per second). Radioisotope production yield is specified in units of mCi/μAh where μAh is the unit used for the accumulated charge received by the target during bombardment with a charged-particle beam.

CHAPTER 1

MOTIVATION AND OUTLINE

1.1 INTRODUCTION

The National Accelerator Centre (NAC) is a multidisciplinary facility of the Foundation for Research Development (FRD), set up in 1977 to provide for:

(1)   Basic and applied research using particle beams.

(2)   Particle radiotherapy for the treatment of cancer.

(3)   Production of radioactive isotopes for nuclear medicine, industry and research.

The NAC is organised so as to bring together people working in medical, biological and physical sciences who are interested in the use of accelerated particle beams, thus providing opportunities for research in these separate disciplines and also stimulating mutual interest in the interdisciplinary areas.

The NAC facility is designed to make available a wide variety of cyclotron-produced radioisotopes, which cannot, in general, be produced in a nuclear reactor. Cyclotron-produced radioisotopes are also usually very pure, i.e. "carrier-free" isotopes, and are often used as tracers to monitor various body functions. Highly sophisticated equipment such as gamma-cameras and positron tomographs are then used to detect and form images showing the tracer locations. This is one of the techniques used in diagnosing and localizing malignant tumours.

The main function of the NAC's Radioisotope Production Group, at present, is to produce various radioisotopes and to deliver them in their required forms to hospitals in South Africa.

The group's programme essentially consists of two components:

(1)   Research and development.

(2)   Routine production.

The research and development component involves chemistry, physics and engineering activities.

In order to obtain perspective of the production procedures, a brief explanation of the facility lay-out and production sequence is given (see Fig. 1):

(1) The first step in the production of a specific radioisotope is the preparation of the target material— solid, liquid or gaseous— into a form suitable for bombardment with the proton beam. Solid targets of various materials are prepared by one or more of the following processes: cutting, machining, cold or hot sintering. Because of the heating of targets under irradiation, all targets have to be water-cooled, and therefore all water soluble or highly corrosive target materials have to be encapsulated. Solid targets or target capsules are mounted in standardized target holders, while liquid and gas target materials have to be contained in special target holders with high integrity, since leakage can cause serious contamination problems.

(2) Since radioisotope production targets become highly radioactive when irradiated, they are a radiation health hazard to personnel and therefore have to be handled remotely. For this purpose target holders are transported by means of a remotely-controlled target transport system. The transport system comprises a microcomputer control system, motorized trolleys and transportation rails connecting the target bombardment station (in the irradiation vault) to the hot-cell complex, parking loop and target storage area [Hum88].

After preparation, the targets, in their holders, are transported to the target bombardment station (see below).

(3) The target bombardment station [Mil89a] is a complex microcomputer-controlled system which consists of three rotary target magazines behind one another, mounted inside a cylindrical radiation shield (see Fig. 2). Each magazine has a capacity to load five target holders and a maximum of three targets can be bombarded in tandem. A pneumatic robot arm facilitates transfer between the transport trolleys and the target magazines, and a pneumatic pusher arm connects the targets to the beamline. Cooling water to the target holders is also provided via the pusher arm. The various targets are bombarded for different time periods, varying from approximately 20 minutes to 15 hours.

(4) After bombardment, the target holders are transported to one of the reception hot-cells, where the target material is removed from them.

TARGET BOMBARDMENT STATION

TRANSPORT SYSTEM

TARGET STORAGE

PARKING LOOP

MOTORIZED
TROLLEY

TARGET PREPARATION

RECEPTION HOT CELLS

PROCESSING
HOT CELLS

PACKAGING AND
DESPATCH

DISPENSING AND
QUALITY CONTROL
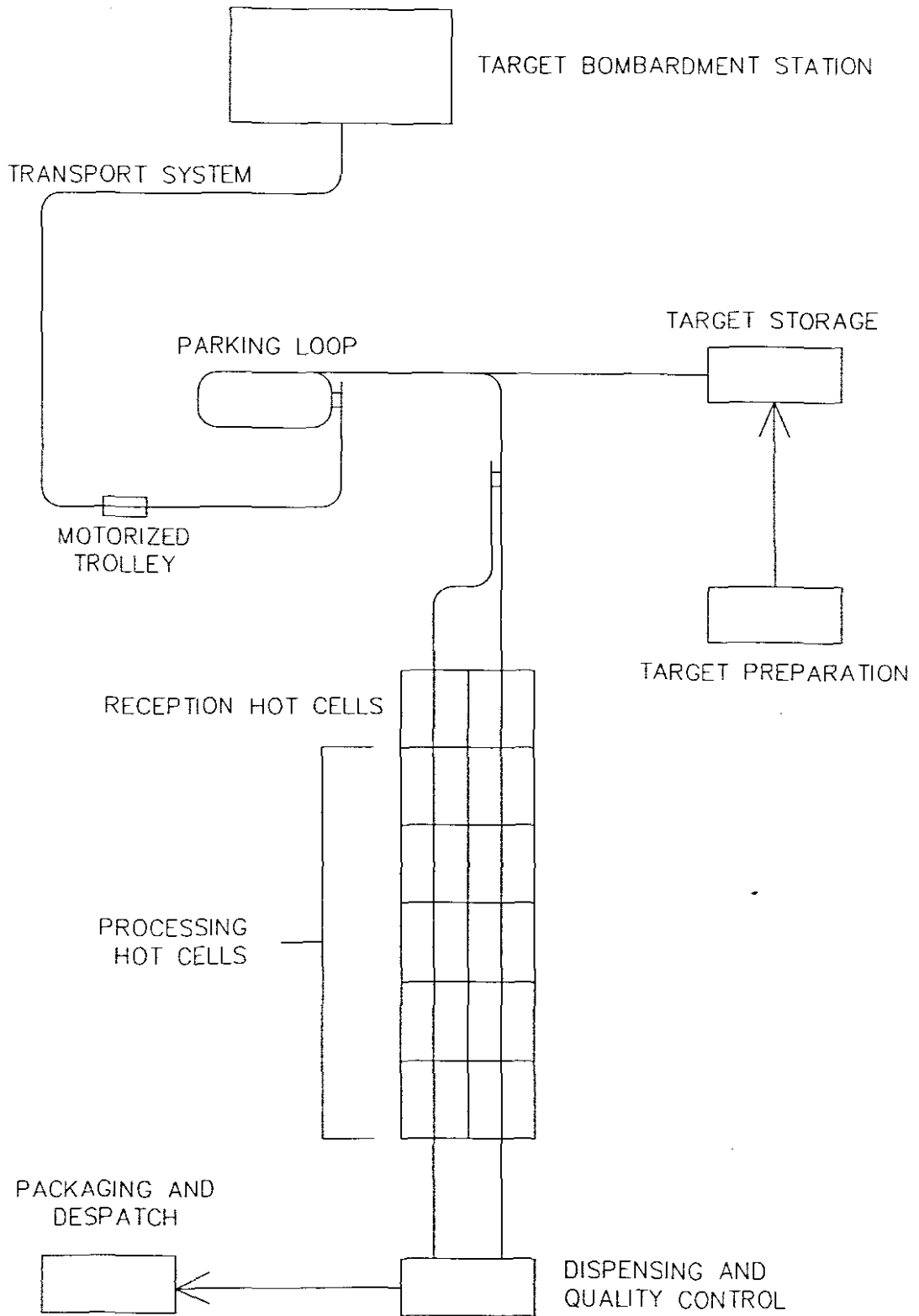
Fig. 1:   *Schematic production facility lay-out.*
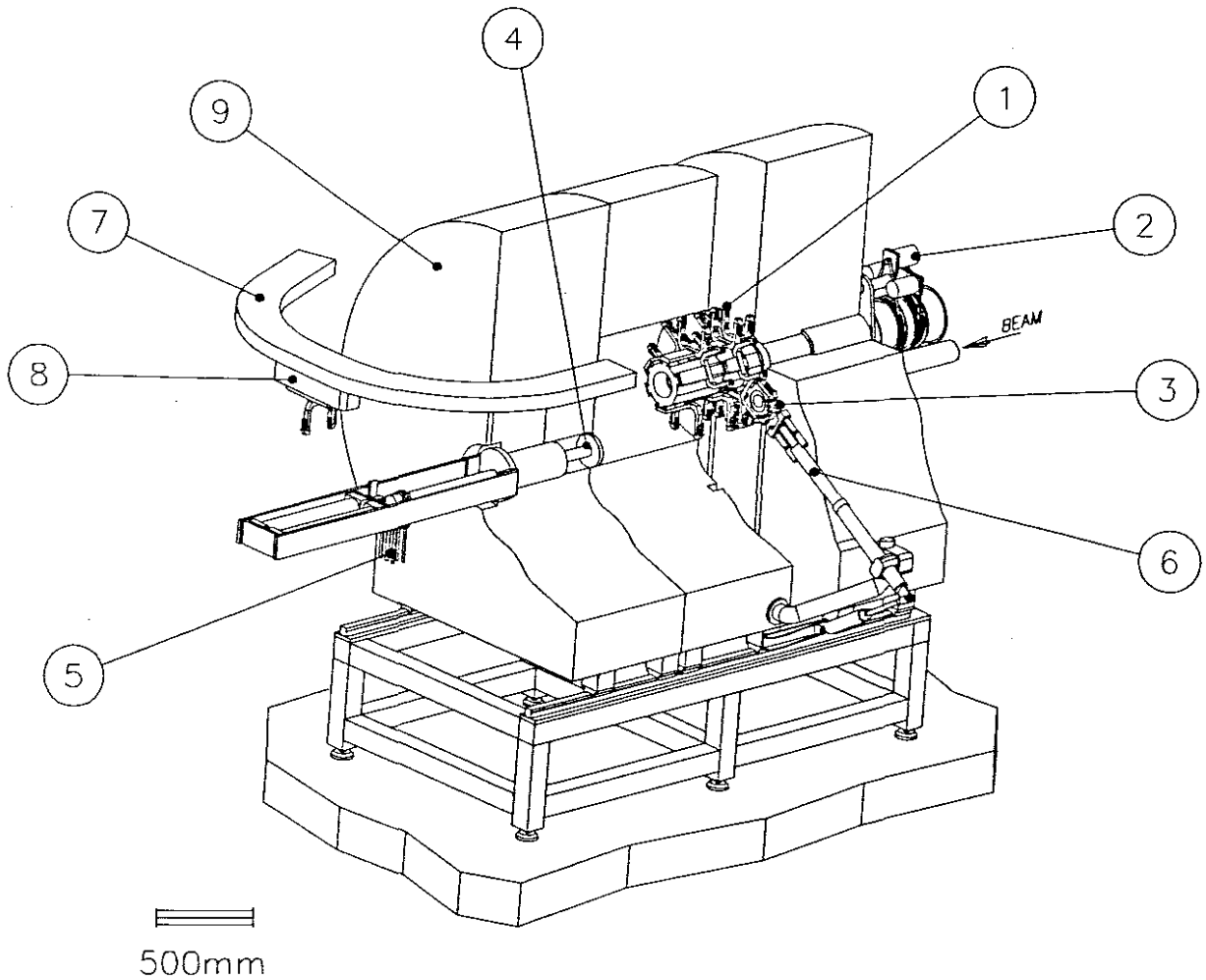
Fig. 2: *Perspective view of the target bombardment station [Mil89a], showing the rotary target magazines (1) and their motor drives (2), target in load/unload position (3), target pusher arm (4), with cooling water lines (5), target transfer robot arm (6), electric−rail target transport system (7), with trolley (8) and neutron attenuation shield (9).*

(5) The chemical separation of the desired radioisotopes is performed in the chemical processing hot–cells. These hot–cells are lead shielded chambers where "hot" chemistry is performed under negative pressure atmospheric conditions.

(6) After separation, the radioisotopes are transported to the dispensing laboratory where the pharmacist performs the dispensing in aseptic conditions and performs the quality control, i.e. checks the chemical purity, radionuclidic purity, etc. of the final product.

(7) After dispensing, the vials containing the radioisotopes are sealed and then packed in lead pots and tins, before being dispatched to the various local hospitals or D.F. Malan airport, for transport to remote hospitals.

1.2 MOTIVATION

Rubidium–81 (^{81}Rb) is an important cyclotron–produced radioisotope with applications in diagnostic nuclear medicine. Having a half–life of 4.58 hours, it decays to its short–lived daughter radioisotope, krypton–81m (^{81m}Kr), having a half–life of 13,3 seconds [Ste91]. The ^{81m}Kr is a radioactive noble gas, and is widely utilized as a lung ventilation diagnostic agent. Scintigraphs of the lungs are taken with a gamma–camera after administration of the above–mentioned radioisotope by inhalation of a ^{81m}Kr/air mixture. Because of the very short half–life of ^{81m}Kr, it can only be supplied to hospitals in the form of ^{81}Rb/^{81m}Kr–generators, the ^{81m}Kr being produced continuously by the decay of the ^{81}Rb. These generators are produced twice weekly at the NAC, and distributed to hospitals all over South Africa.

With the 66 MeV proton beam which is routinely available at the NAC for radioisotope production as well as neutron therapy irradiations, only two main production routes can be utilized for the production of ^{81}Rb/^{81m}Kr–generators [Ste91]. The first route is via proton–induced nuclear reactions on rubidium, by the irradiation of a suitable rubidium–containing target such as rubidium chloride (RbCl), while the second route is via proton–induced nuclear reactions on krypton, by irradiation of a krypton gas target. The second of these two routes has several distinct advantages.

The main problem in using rubidium target material is that the ^{81}Rb can, of course, not be chemically separated from the stable Rb of the target matrix. All the Rb in the target therefore has to be loaded onto the ion–exchange resin in the generator columns. This results in physically bigger generators, requiring more lead shielding during

transport and therefore higher packaging and transport costs. However, since the targetry and target processing equipment are relatively simple, in contrast to that needed for a krypton gas target, this route was chosen for the initial production of [81]Rb at the NAC.

A krypton gas target has the main advantage of ensuring a carrier-free final product, that can be loaded onto very small generators. Furthermore it offers, in principle, a much higher production rate than can be achieved with a RbCl-target. A target with a length of 200 mm, filled to a pressure of 1400 kPa, has a typical yield at end of bombardment (EOB) of $\sim$ 25 mCi/μAh when bombarded with a beam current of 30 μA, in contrast to a typical yield of 6,8 mCi/μAh at EOB (for a beam current of 40 μA) currently being achieved at the NAC with a RbCl-target under similar irradiation conditions [Ste91]. The weekly beam time requirement of 2 $\times$ 2 hours for the RbCl-target will thus be reduced to about 2 $\times$ 25 minutes for the gas target, taking radioactive decay into account. The resultant saving in beam time of $\sim$ 3,5 hours is significant, and can be well used for other irradiations (on a full weekly beam time schedule).

For the above-mentioned reasons it was decided to invest in the design, development and construction of a krypton gas-target and processing system for the production of [81]Rb at the NAC, and eventually to phase out the use of RbCl-targets. Furthermore, it was realised that such a project would also greatly contribute to establishing gas target technology at the NAC. The general need for economical, flexible and reliable gas target systems which are compatible with the existing bombardment facilities had been identified from the outset, but time constraints did not previously permit the development of the rather specialised technology involved.

1.3   OUTLINE OF THESIS

The contents of this thesis are divided into six chapters, and information regarding the same items in the following chapters may easily be retrieved by making use of the cross-referencing numbering system. Item heading numbers will be the same throughout the thesis except for the first digit, which indicates the chapter number.

Chapter 2 ("Literature Study") looks at previous work that was done on the subject and all relevant knowledge is considered for guidelines or usage in determining the detailed design objectives of this project.

Chapter 3 ("Formulation of Design Objectives") lays down all design requirements, considerations and parameters within which the project was finally initiated. The chapter is divided into the various component sections and each is separately formulated.

Chapter 4 ("Investigations") covers in-depth investigations and designs of the gas target system. Each system component is separately investigated whilst considering all the interrelationships between the various components.

Chapter 5 ("Results") analyzes results obtained from the investigations. Both positive and negative results which eventually led to the final designs are indicated.

Chapter 6 ("Conclusions") ends the thesis by indicating the objectives that have been achieved and further points out recommendations and possible future development work on the krypton gas target system.

Metric units are used throughout the thesis except where supplier products are specified in imperial units. All pressure values indicated are gauge pressures and absolute values will be indicated as such.

CHAPTER 2

LITERATURE STUDY

Specialized gas target technology has also been developed by various overseas laboratories and the production methods adopted prove to be fairly varied, depending on local requirements and conditions.

The general production methods used, however, involve the following:

(1) Inserting the gas into a leak-tight vessel at a predetermined pressure.

(2) Connecting a water, gas or liquid nitrogen cooling system to remove heat generated by the beam.

(3) Bombarding the gas through a thin window at the entrance side of the vessel.

(4) Releasing the gas after bombardment.

(5) Opening or leaving the vessel closed and rinsing or steaming the inside which contains the produced radioisotope deposits.

(6) Retrieving the water or steam used for rinsing for further processing or loading onto the generators.

The gas target construction also seems to follow a basic design: The gas is mostly contained in stainless steel or aluminium vessels, varying from 20 mm to 600 mm in length and 20 mm to 150 mm in diameter. The vessel entrance windows are constructed from various high strength materials, varying in thickness and diameter. The rear section of the vessel usually consists of a thick beam-stop to completely stop the beam. Cooling of the window and body of the vessel is achieved by means of cooling jackets or channels through which the cooling medium flows.

Unfortunately, relevant documents and reports acquired from many overseas centres generally do not cover technical aspects in great detail. The techniques used at four different centres are, however, known in enough detail to be summarized here:

TRIUMF – CANADA

The target used at this institute consists of two separate chambers coupled to a beamline, allowing two gases to be bombarded simultaneously [Bur79, Rut85]. There are three helium cooling chambers located such that there is one at the upstream and downstream ends of the target and one separating the two target chambers. Thus the target has six windows, each constructed from Inconel 600 and having dimensions 75 mm diameter by 127 μm thick. Hydrostatic tests produced a window burst pressure of 4100 kPa. The windows are cooled with the helium at a pressure of 1000 kPa and a flow rate of 57 ℓ/min. The helium cooling chambers are each 22 mm in length.

The target chambers each being 73 mm in length, are connected to the radiochemistry laboratories by two 3 mm diameter by 100 m long stainless steel tubes and the gas is pumped through continuously at a flow rate of 2 ℓ/min. The targets being bombarded at 450 MeV and $20 - 95$ μA currents, are designed for a working pressure of 1000 kPa. When gas bombardment is not required, the target can be retracted by ~ 200 mm in order to avoid unnecessary activation of the windows during other bombardment applications.

If the beam is accidentally steered off the centre of the target, it will hit the 3 mm thick cylindrical target walls and may cause heat dissipation of several kW. To compensate for this likelihood the cylindrical walls are water-cooled at a flow rate of 5 ℓ/min. Beam-trip points are interlocked to each of the helium cooling and water cooling systems and both the flow rate and temperature are monitored in each system.

UNIVERSITY OF OSLO – NORWAY

This cyclotron centre bombards krypton gas with protons at ~ 30 MeV and with beam currents of $10 - 15$ μA [Bjo84]. The target chamber is filled at 1000 kPa, and during irradiation the pressure increases by 50% due to heating. In order to keep the gas volume at a minimum, while avoiding loss of beam intensity and activation of the chamber walls, the chamber is conically-shaped, the diameter at the entrance being 25 mm, the length 300 mm and the diameter at the beam-stop 45 mm (see Fig. 3). The total volume of the chamber is 300 cm^3.

The target chamber material used is stainless steel and the inner surface has been carefully polished, both mechanically and chemically, in order to obtain a smooth surface which could be uniformly wetted. The back-plate contains a beam-stop in the
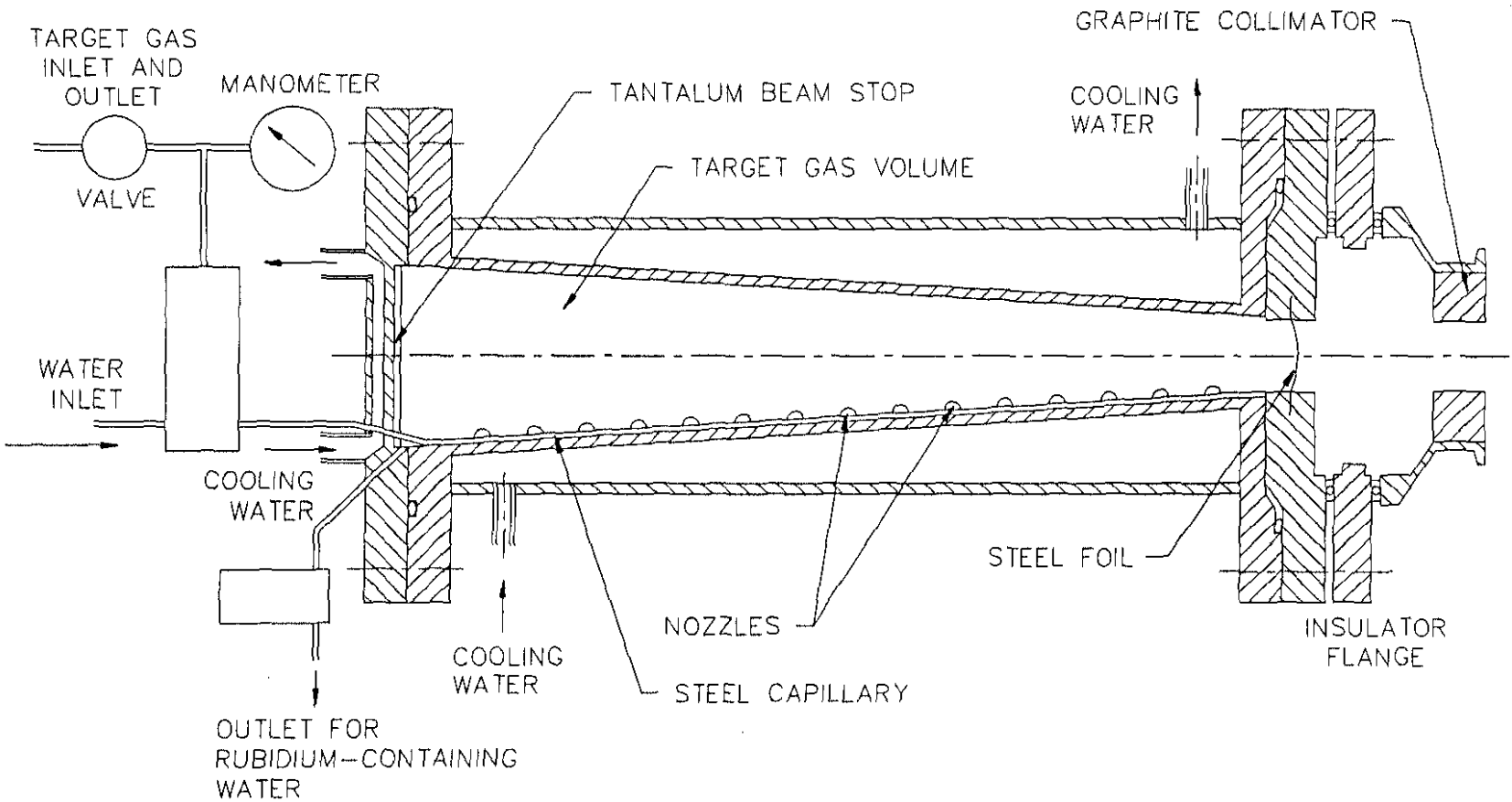
Fig. 3:   Cross-section of the conically-shaped gas target used at the Oslo cyclotron [Bjø84].

form of a 1,5 mm thick tantalum disc. A steel capillary entering through the back-plate is located in the bottom of the target chamber over its entire length. On the capillary, fifteen tiny nozzles with hole diameters of 0,2 mm are mounted at 20 mm interdistances. Through these nozzles water is sprayed on the inner walls of the chamber. The same capillary is also used for loading and unloading of the target gas. The chamber wall and tantalum beam-stop are cooled by flowing water.

The high-pressure target gas is separated from the vacuum in the beamline by a 20 mm diameter by 25 μm thick stainless steel foil. Since the beamline position is also used for several other purposes, it is imperative that the production apparatus can be easily disconnected and removed. The target therefore is coupled to the end of the beamline, via a bellow, by means of snap-on vacuum flanges. The target chamber itself is mounted on a production rig which may be adjusted both horizontally and vertically. The production rig carries the target, the gas and water systems, valves, pumps, storage vessels and waste reservoir. It is mounted on wheels for easy disconnection and removal from the beamline (see Fig. 4).

The main gas reservoir consists of a high-pressure cylinder with pressure regulator. Before the target chamber is loaded with gas, it is evacuated to a pressure well below 0,1 kPa. The gas is then fed into the chamber until the desired pressure is obtained. After irradiation the target gas is transferred by cryopumping into a small storage pressure vessel placed in liquid nitrogen. The stored gas is re-used at the next production run.

Demineralized and distilled water is contained in a 1 ℓ glass reservoir. After the irradiated target gas has been stored in the small pressure vessel, air is let into the target chamber. In air the rubidium converts to rubidium-oxide which is readily soluble in water. Compressed air is applied to force the water through the capillary nozzles and the rubidium-containing water is subsequently temporarily stored in a glass storage vessel. From this vessel the liquid may be loaded onto five generator columns.

The various operations are executed remotely by means of a video camera and a push-button electrical box operating the pumps and solenoid valves.

WATER RESERVOIR

COMPRESSED AIR

TARGET

BEAM

DISPENSER VOLUME

STORAGE PRESSURE
VESSEL

LIQUID NITROGEN

VACUUM PUMP

KRYPTON GAS
RESERVOIR

STORAGE VESSEL

LIQUID DISTRIBUTOR

WASTE WATER

GENERATORS
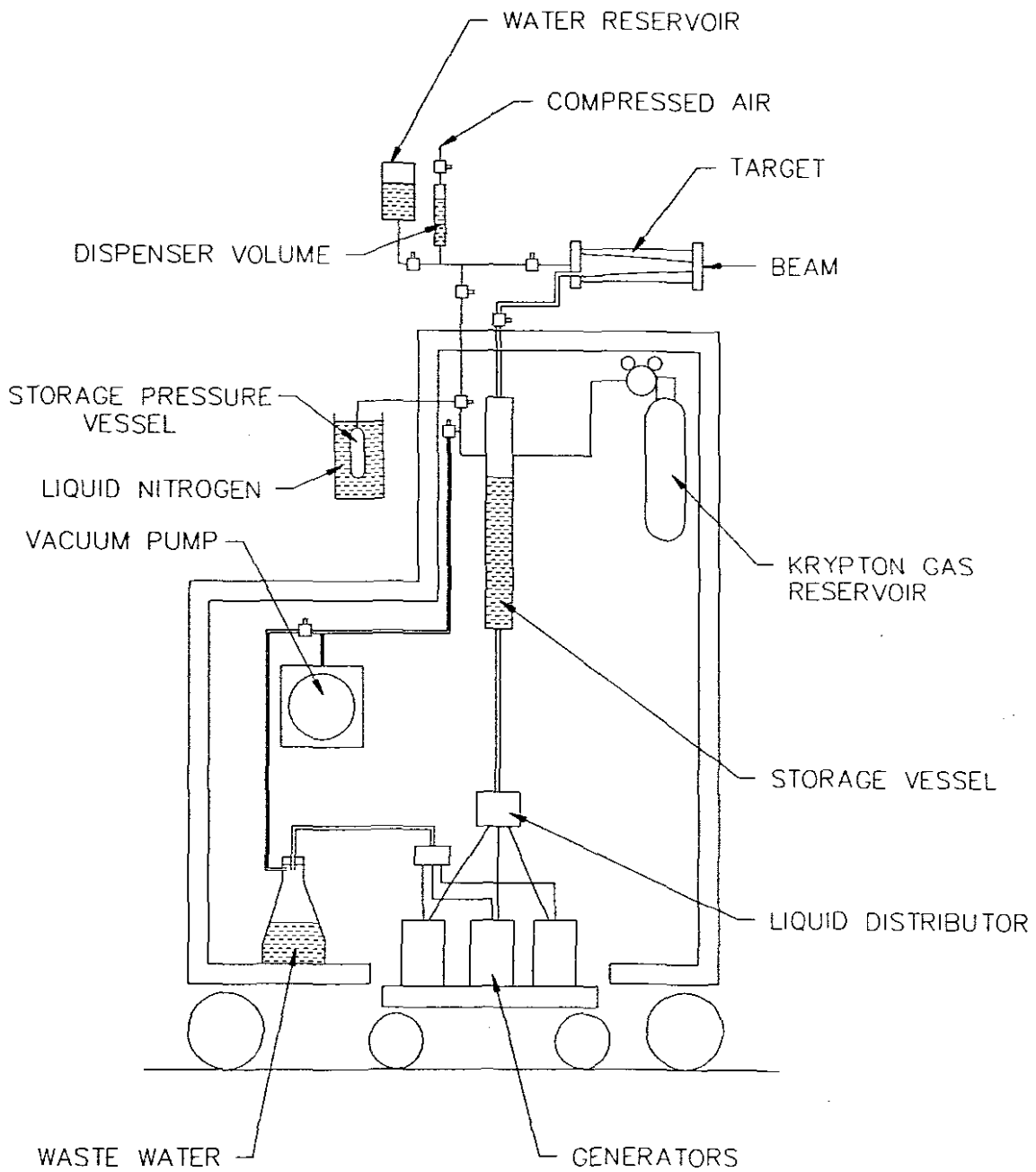
Fig. 4: *Diagram of the production rig used at the Oslo cyclotron [Bjo84].*

MRC CYCLOTRON UNIT, HAMMERSMITH HOSPITAL, LONDON - U.K.

The use of a 60 MeV proton beam for the production of rubidium from krypton gas was investigated [Wat86]. Initial experiments to measure the potential yield were carried out using an uncooled stainless steel target chamber (50 mm internal diameter by 530 mm long), lined with removable 0,05 mm thick aluminium foil. The target filling pressure of 1400 kPa was held by a 0,125 mm thick Cu/2% Be foil window with an entrance diameter of 25 mm. Following 20 minute bombardments with 58,9 MeV proton beams at very low currents of 100 nA, the krypton gas was released through two 0,22 μm membrane filters, a soda lime trap and an ion exchange trap. The aluminium liner was then dissolved in NaOH and the target chamber was washed out with diluted NaOH. A significant finding from this experiment was that >70% of the rubidium activities produced remained in the gas phase for at least 2 hours after the end of bombardment and was subsequently trapped by the first membrane filter.

Based on these experimental results, a production target was designed (see Fig. 5). The 150 mm diameter by 530 mm long target is also filled to 1400 kPa, and includes a 30 mm diameter beam entrance window. The target, which is constructed from aluminium in order to reduce the effects of activation, is surrounded by a water-cooling jacket and incorporates a pure aluminium beam-stop to absorb the residual proton energy. The front plate assembly contains a 0,125 mm thick Cu/Be target window foil and a 0,05 mm thick Cu/Be beamline window foil, both cooled by jets of helium gas.

This target is used extensively for full production purposes and bombarded with 20 μA, 58,9 MeV protons for an hour at a time.

Because of the large volume of krypton gas within this target (125 ℓ) it was necessary to devise a recovery system for the gas (see Fig. 6). This was achieved by making use of a remotely controlled cryopumping system.

Another consequence of the large target volume is the impracticability of recovering the rubidium by just filling or rinsing the target with water. The technique of spraying is also discounted because of the possible variability in the recovery yield due to inefficient wetting of the target chamber walls. An alternative approach, which is successful in routinely recovering 100% of the radioactivity in about 500 mℓ of water, is that of steam-rinsing the target. To ensure that all the rubidium is recovered, a filter is used on the gas outlet to capture the rubidium in the gas phase. By using a 0,45 μm thick silver membrane for this purpose, it is possible to steam-rinse the target gas through this filter.
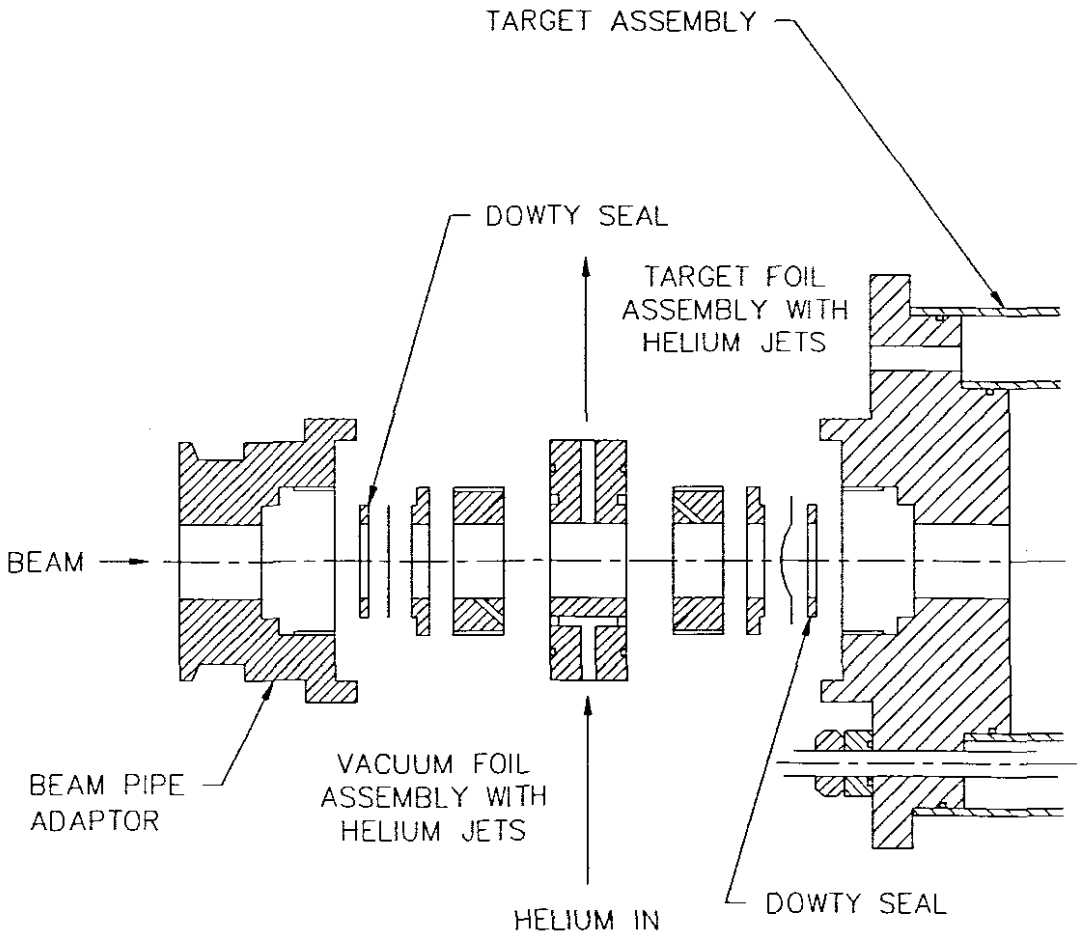
Fig. 5: *Cross-section of foil assembly and arrangement of helium cooling of the krypton gas target used at the MRC Cyclotron Unit [Wat86].*
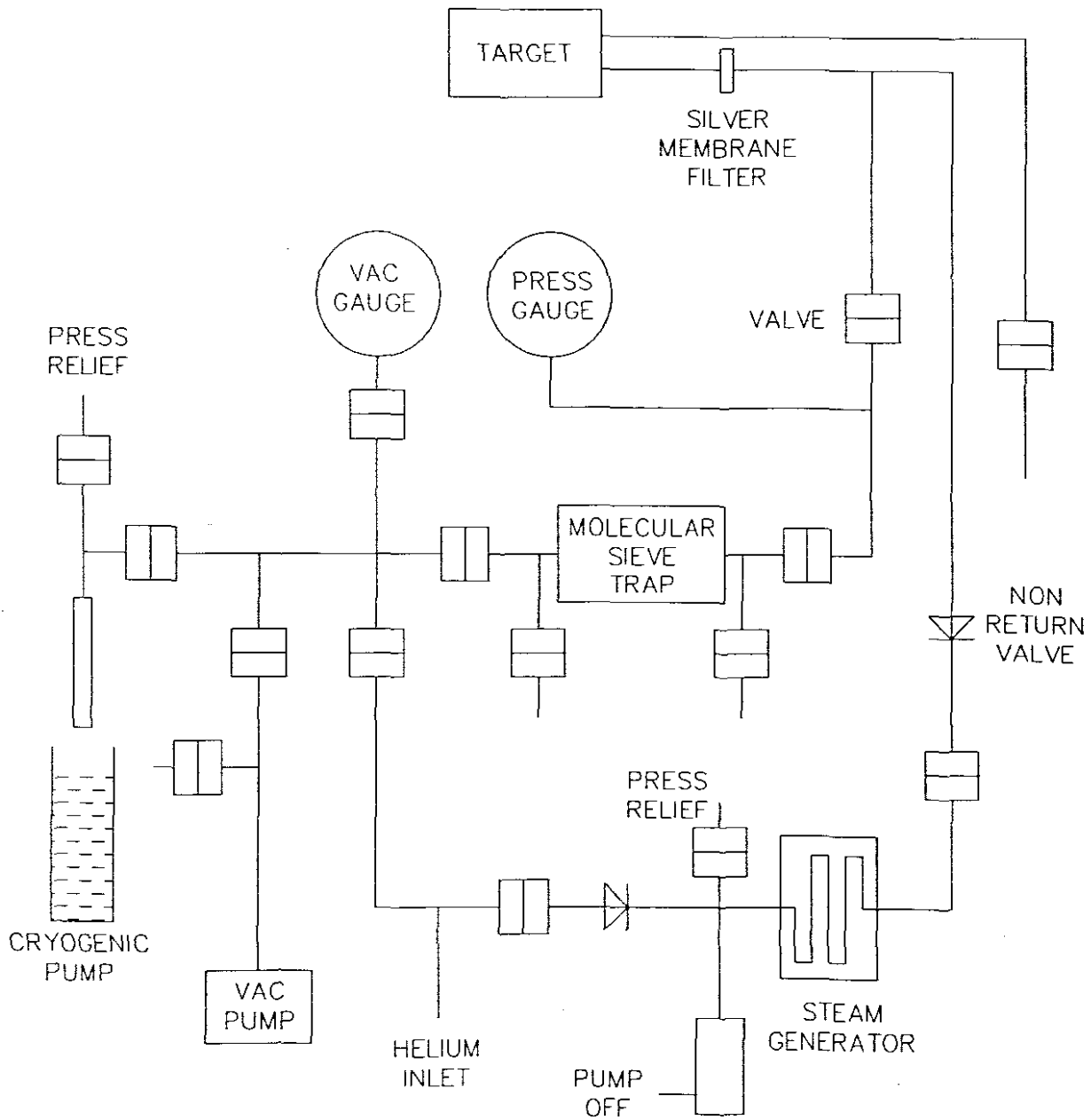
Fig. 6: *Schematic lay-out of production apparatus at the MRC Cyclotron Unit [Wat86].*

The target walls were initially treated with steam to produce a film of boehomite (complex hydroxide) in order to reduce the corrosive effects of regularly condensing steam onto the aluminium walls and leaving them partially wet between bombardments. The compromise of producing an aluminium target which has electrochemical deposited walls (chromium or nickel) was regarded to be the most suitable in this situation [Wat86], although at the time such a target had apparently not yet been constructed [Goo91].

INSTITUT FüR STRAHLEN UND KERNPHYSIK DER UNIVERSITäT BONN – WEST GERMANY

The gas target described is a fixed, high pressure gas cell designed to serve as a versatile thick deuterium target for high intensity neutron production [Von76]. The gas target essentially consists of three concentric tubes (see Fig. 7). The innermost tube is a gas cell of 13 mm inside diameter and 90 mm length. A 1 mm thick special alloy with high thermal conductivity was chosen for the construction of the inner tube. The middle tube is used for liquid nitrogen cooling and the outer tube is connected to a vacuum system to provide thermal insulation.

The gas cell is equipped with beam entrance and exit foils and a separate removable beam-stop. The beam-stop consists of a gold disc in a copper flange and is cooled to -30° C with methanol. It therefore does not contribute to the heating of the target gas. The beam entrance and exit foils are manufactured from 150 μm thick molybdenum. Each foil is placed between a sturdy stainless steel flange and a metal seal held in place with a retainer plate, and the assembly is bolted to the polished end face of the cell body. The beam is focussed onto the target by means of a 4-jaw tantalum collimator and the four overlapping pieces are individually insulated with 50 μm thick mica sheets. They are then mounted on the flange holding the entrance foil by means of screws insulated with shells made from boron nitride. This whole construction is bolted directly onto the beamline. The target volume is 12 cm^3, while the total volume of the external reservoir, consisting mainly of the high pressure hose and reducing valve, amounts to approximately 150 cm^3 and serves as a buffer preventing the pressure from rising too much when the beam heats the target gas, or when the cooling fails.

The target is bombarded with a 10 μA, 28 MeV deuteron beam, which corresponds to a bombarding energy of 25 MeV in the target gas. Under these conditions, the pressure rises by about 10% during bombardment.
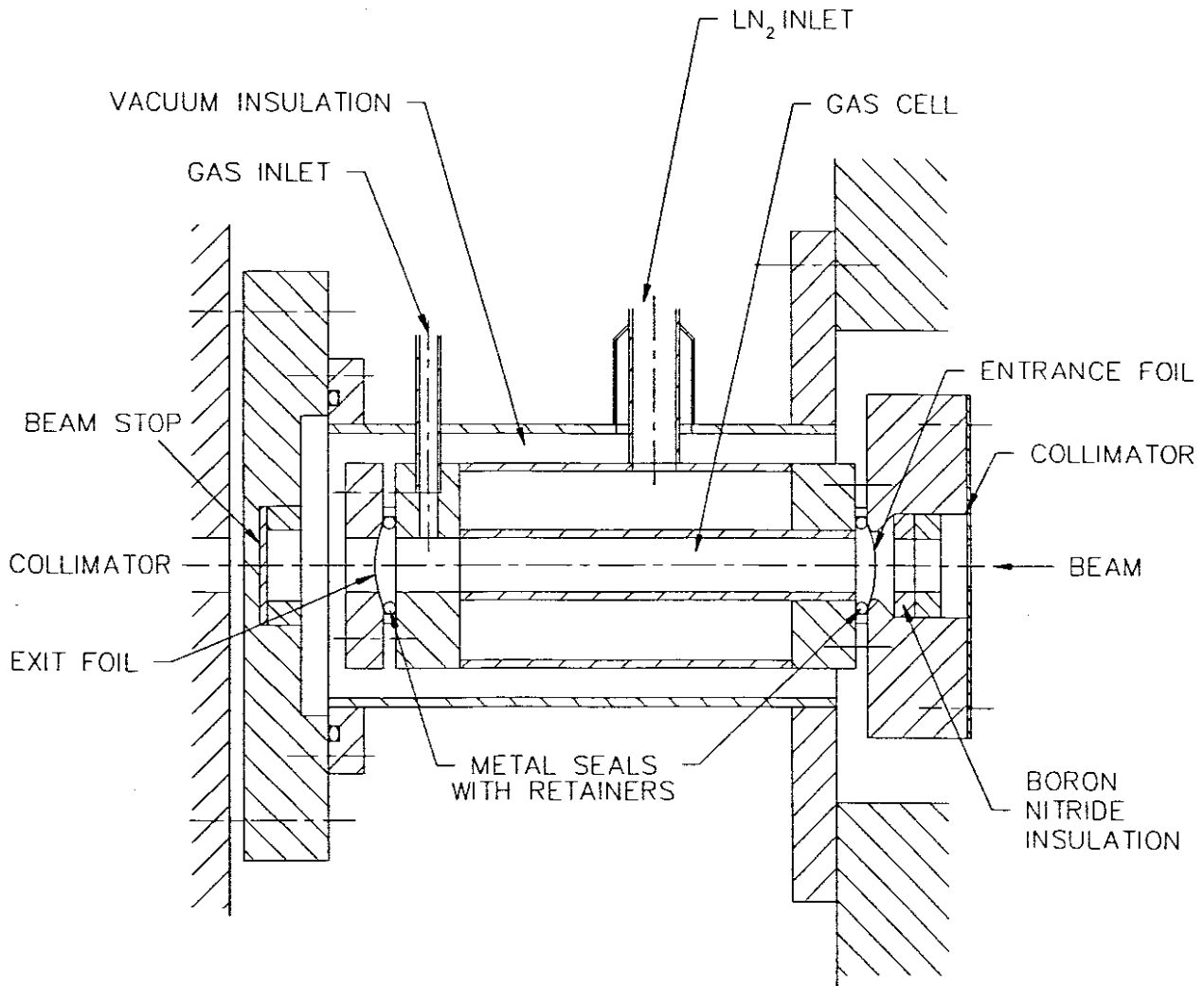
Fig. 7: *Cross-sectional view of the gas target used at Bonn University [Von76].*

CHAPTER 3

DESIGN OBJECTIVES AND PROJECT PLAN

3.1 GENERAL LAY-OUT AND PROCEDURES

Considering the specific local requirements and conditions and taking all previous applicable research into account (see Chapter 2), a proposed basic lay-out of the system was drawn up (see Fig. 8). The proposed operational sequence to be followed is as follows:

(1)   The gas target is coupled to the system by means of remotely controlled coupling valves.

(2)   A vacuum pump is activated and the entire system including the target is evacuated.

(3)   A predetermined quantity of krypton gas is inserted into the reservoir.

(4)   A gas pump then pumps the gas from the reservoir to the target.

(5)   The target is de-coupled and transported to the target bombardment station where it is bombarded for a certain period of time.

(6)   After bombardment the target is coupled to the system and the gas is pumped back to the reservoir.

(7)   The ^{81}Rb which has been deposited on the target inner surface and trapped on the filter is now rinsed off with water by means of a circulating pump.

(8)   The solution is forced out of the system and into a product vessel by means of compressed air.

(9)   The product is then finally transferred onto the generators via the generator loading system.

(10)   In preparation for the next production run, the system will be washed, air dried and vacuum dried.

Fig. 8: *Proposed basic krypton gas target system lay-out.*

KRYPTON

RESERVOIR

COUPLING VALVES

FILTER

GAS PUMP

TARGET

VACUUM PUMP

AIR LINE

H_2O SUPPLY

CIRCULATING PUMP

BASEMENT

GENERATOR
LOADING
SYSTEM

PRODUCT

19
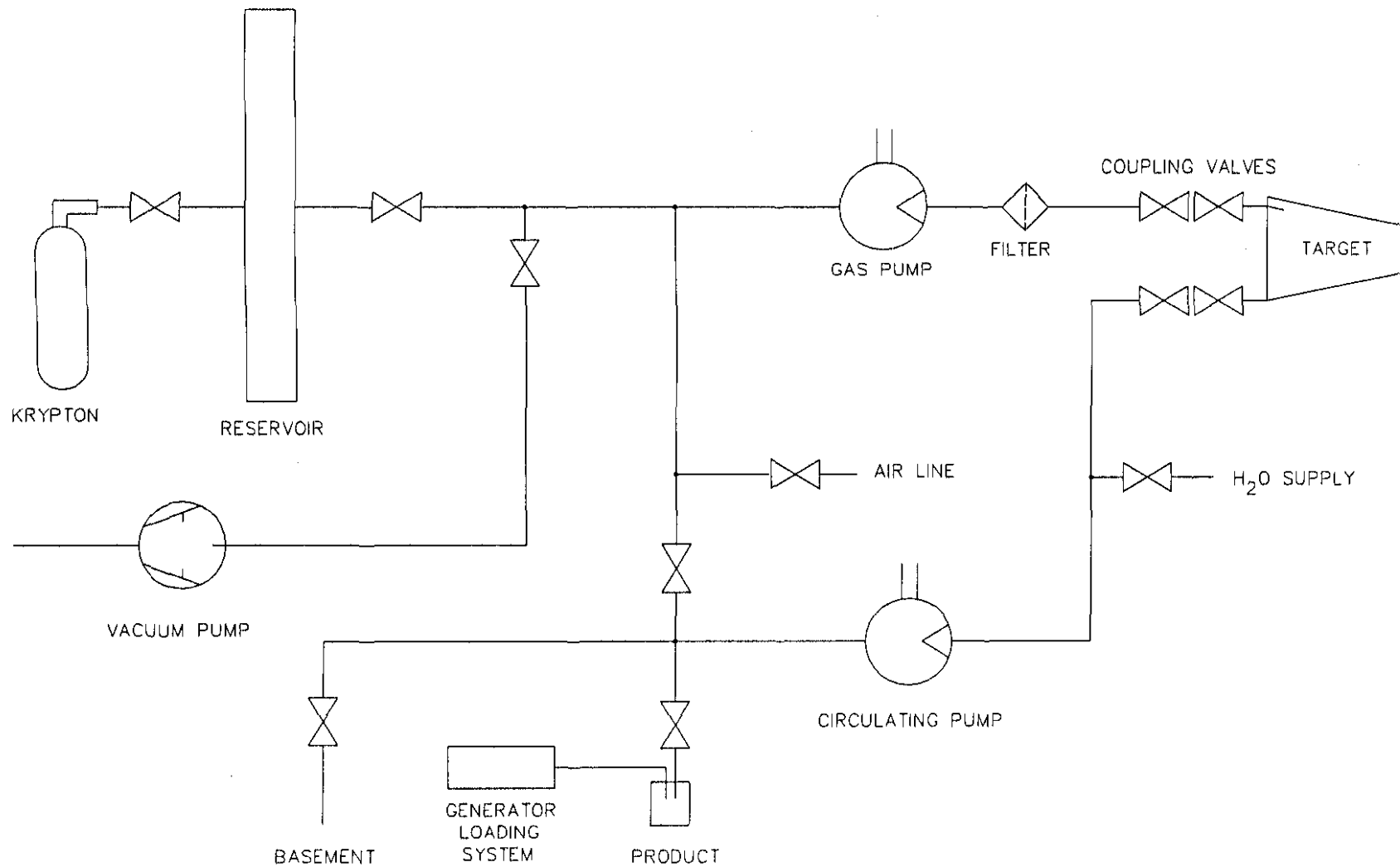
3.2 INDIVIDUAL COMPONENTS AND SYSTEMS

3.2.1 Test Target

Initially a test target needed to be designed and manufactured in order to:

(1) Ascertain what the beam profile in the final production gas target would look like.

(2) Check the basic operation of the gas pump (see par. 3.2.5).

(3) Check the design and operation of the coupling valves (see par. 3.2.7).

The test target would be used to determine the beam profile in both vacuum and pressurised krypton gas and thus to check the effect and angles of beam scattering though the entrance windows, cooling water layer and gas.

3.2.2 Production Gas Target

The various design considerations and objectives for the production gas target were the following:

(1) Profile design, maximum weight, assembly procedures and sequences.

(2) Selection of materials resistant to high radiation doses or ease of replacement of less resistant materials.

(3) Stresses applied on and within the target. The target would be subjected to estimated operating gas pressures of up to 3000 kPa.

(4) Construction of beam entrance window and beam-stop assembly.

(5) Provision for efficient water-cooling of the target and its integral components.

(6) Incorporation of coupling valves between the target and processing system.

(7) Mechanical compatibility with target bombardment station, transport system and hot-cell transfer and positioning system.

(8) Incorporation of a water spray arrangement for rinsing the target inner vessel.

(9) Ease and speed of maintenance.

(10) Surface finish of the inside of the target vessel. (This surface plays a vital role in the radioisotope recovery process. It needs to be smooth so that adhesion of radioisotopes is impaired during rinsing and the surface boundary layer also needs to be homogeneous and free of any abrasive polishing inclusions which can contaminate the radioisotopes.)

3.2.3   Spray System

After bombardment, the radioisotopes which have collected on the target vessel inner surface as well as those in suspension in the gas, are to be recovered as far as possible by means of rinsing with distilled water. A suitable spray system, possibly consisting of spray nozzles inside the gas target vessel, therefore had to be developed.

The water spray should wet all the inner surfaces of the target vessel and should also spray through the entire inner volume of the target to remove the radioisotopes in suspension quantitatively. It also had to be kept in mind that only a limited amount of water will be available for rinsing the target (see par. 4.2.4). Effective drainage and pressure losses in pipes also needed to be considered.

3.2.4   Circulating Pump

For processing convenience (see par. 4.2.4) the water used for rinsing the target is only 100 ml in volume, and it has to enter the spray nozzles at a fairly high pressure to give the required spray angles. A piston pump would probably be the most effective, since it could operate in bursts of relatively high pressure and small duration. A continuous flow in a closed loop, conforming to these parameters, would be practically impossible to achieve.

The physical size and weight of the pump also had to be considered, because of the limited interior space of the hot-cell. Another factor concerning the pump size was to minimize the internal dead volume in order to optimize the water flow and pressure.

3.2.5   Gas Pump

A gas pump was required for transferring the krypton gas from the reservoir to the target and vice versa. Standard methods of transferring gas from one point to another employ either a cryogenic pump or a gas pump. Whichever one was to be selected

however, the pump volume, flow, pressure, maintenance and construction materials needed to be considered.

3.2.6   Gas Reservoir

The purpose of the gas reservoir was to store the krypton gas during periods between irradiations. The same volume of gas was to be utilized for each irradiation, and would be transferred to and from the gas target via the gas pump.

Certain specifications were adopted for the gas reservoir, namely:

(1)   A specific internal volume is required, depending on the pressure and volume of krypton gas in the target.

(2)   Inlet, outlet and gas monitoring ports are required.

(3)   Servicing must be carried out with ease.

(4)   Materials used must not contaminate the gas.

3.2.7   Coupling Valves

A set of inlet and outlet coupling valves was required for coupling the processing system to the gas target. These valves were to seal an operating system pressure of 1400 kPa and their operations had to be controlled remotely. The target coupling valves also had to seal an estimated operating pressure of 3000 kPa during bombardment.

As there will be high radiation levels inside the gas target and processing system, reliability of these coupling valves is of utmost importance in order to avoid accidental leakage, which can cause serious radioactive contamination of the environment and operating personnel.

The valves were to be designed in such a manner that servicing and possible repairs could be carried out with speed and ease. This is vitally important because excessive radiation doses to maintenance personnel must be avoided.

The coupling valve materials selected should also not contaminate the gas in the system.

3.2.8   Pneumatic System

A pneumatic system to operate the valves and actuators in the krypton gas target system would be reliable, simple and easy to maintain, and seemed to be the obvious choice for remote control. The design of this system however, required the selection of the most versatile and effective pneumatic components resulting in the use of a minimum number of components. This is especially important because of the limited space in the hot-cell.

Further investigations regarding the pneumatic components included the overall operation lay-out, their mounting and their compatibility with the rest of the processing system.

3.2.9   Control System

Because of high radiation levels during processing, all the valves, actuators and mechanisms contained inside the hot-cell needed to be controlled remotely from a control panel or system outside the hot-cell. The system also had to include safety and status monitoring components. The control system generally had to be simple, reliable and easy to maintain. Further development work on the processing and operating systems would probably continue after completion of the project, and for this reason the control system's flexibility during any stage of operation is of paramount importance.

3.2.10   Hot-cell Lay-out

Careful consideration had to be given to the following aspects during the design and development of the hot-cell lay-out:

(1)   Ease and reliability of system operations.

(2)   Ease of visual inspection and monitoring of the system.

(3)   Radiation safety aspects.

(4)   Ease of routine maintenance, fault finding and repair.

(5)   Routes and connections to air, water, gas and electrical service lines.

(6)   Safety interlocks or signals due to failure of services.

(7) The remote-controlled coupling and de-coupling of the target to the gas processing system.

(8) Provision made for the recovery of the expensive krypton gas after bombardment.

3.2.11 Generator Loading System

An additional system was required to be incorporated for loading the product onto the generators. A generator loading system for the RbCl setup already existed and the design had to be investigated for inclusion into the krypton gas target system. The layout, mounting and remote control aspects of this system needed to be studied.

3.3 ROUTINE MAINTENANCE AND BREAKDOWN PROCEDURES

The system, being a routine production facility, would necessitate the drawing up of routine maintenance directives and schedules.

Due to different degrees of radiation exposure, mechanical vibration and wear, each component's maintenance cycle required their respective individual investigations.

In the event of a breakdown, specific removal, repair and assembly procedures should be followed, because the system would be radioactive. A detailed directive therefore needed to be drawn up for this purpose, and also to ensure that the quality of the final product is maintained.

Documentation containing component descriptions, serial/part numbers, name of company from which purchased and spares details had to be compiled for reference purposes during maintenance and repairs.

3.4 PROJECT PLAN

Before the commencement of the investigations it was necessary to draw up a project plan, in order to put the investigations into perspective and to streamline the project. In many cases the effective development of the various components could only be achieved in a certain order and for this reason the project was divided into five phases:

PHASE 1 – Beam profile test

Design and development of:

1.   Test target
2.   Coupling valves
3.   Beam profile measurements

PHASE 2 – Individual components

Design and development of:

1.   Production gas target
2.   Spray system
3.   Circulating pump
4.   Cryogenic pump
5.   Reservoir
6.   Pneumatic system
7.   Control system
8.   Generator loading system

PHASE 3 – Component Testing Phase

1.   Testing of all components for operation, compatibility and reliability during the operation of the system as a whole.
2.   Carrying out of corrections and modifications.

PHASE 4 – Hot–cell configuration

1.   Design of component mounting and manipulation inside the hot-cell.
2.   Assembly and remote control testing of all components.
3.   Carrying out of production trial runs.
4.   Optimizing the microcomputer control system hardware and software.

PHASE 5 – Documentation

Drawing up of routine maintenance, repair schedules/procedures and compiling the project literature.

CHAPTER 4

INVESTIGATIONS

4.1 GENERAL LAY-OUT AND PROCEDURES

As a starting point, the practicality and functionality of all the individual components in the basic lay-out proposed in Chapter 3 were investigated. A more detailed study of the various components will be dealt with at a later stage in this chapter.

After the above investigation was completed, a more realistic and practical lay-out, which would satisfy the system operations and sequence requirements, could be drawn up (see Fig. 9).

The operation sequence for the krypton gas target system is as follows:

(1)   For a clean, evacuated system, all valves open to atmosphere will be closed, all valves within the system opened, and the system pumped down by means of a vacuum pump (A) to a vacuum of ~ 0,1 kPa.

(2)   A cylinder of high-purity krypton gas (B) will be connected to the system via a krypton-purged flexible line.

(3)   Valve (6) will close and valve (1) will release the gas at a regulated pressure of ~ 100 kPa (abs) into the reservoir (C). Valve (1) will close when the reservoir has been filled to the required pressure.

(4)   Valves (4;9;19;20) will close and valves (5;6) will open and an in-line cryopump (D) will be activated.

(5)   The gas will freeze onto the cryopump, leaving a vacuum in the reservoir and connecting line.

(6)   Valves (5;21) will close, valves (19;20) will open and the cryopump will be de-activated.

(7)   The krypton will now return to the gaseous phase and fill the target (E) and connecting line to a pressure of ~ 1400 kPa, due to the difference in volume between the reservoir and target.

Fig. 9: *Krypton gas target system lay-out.*

27
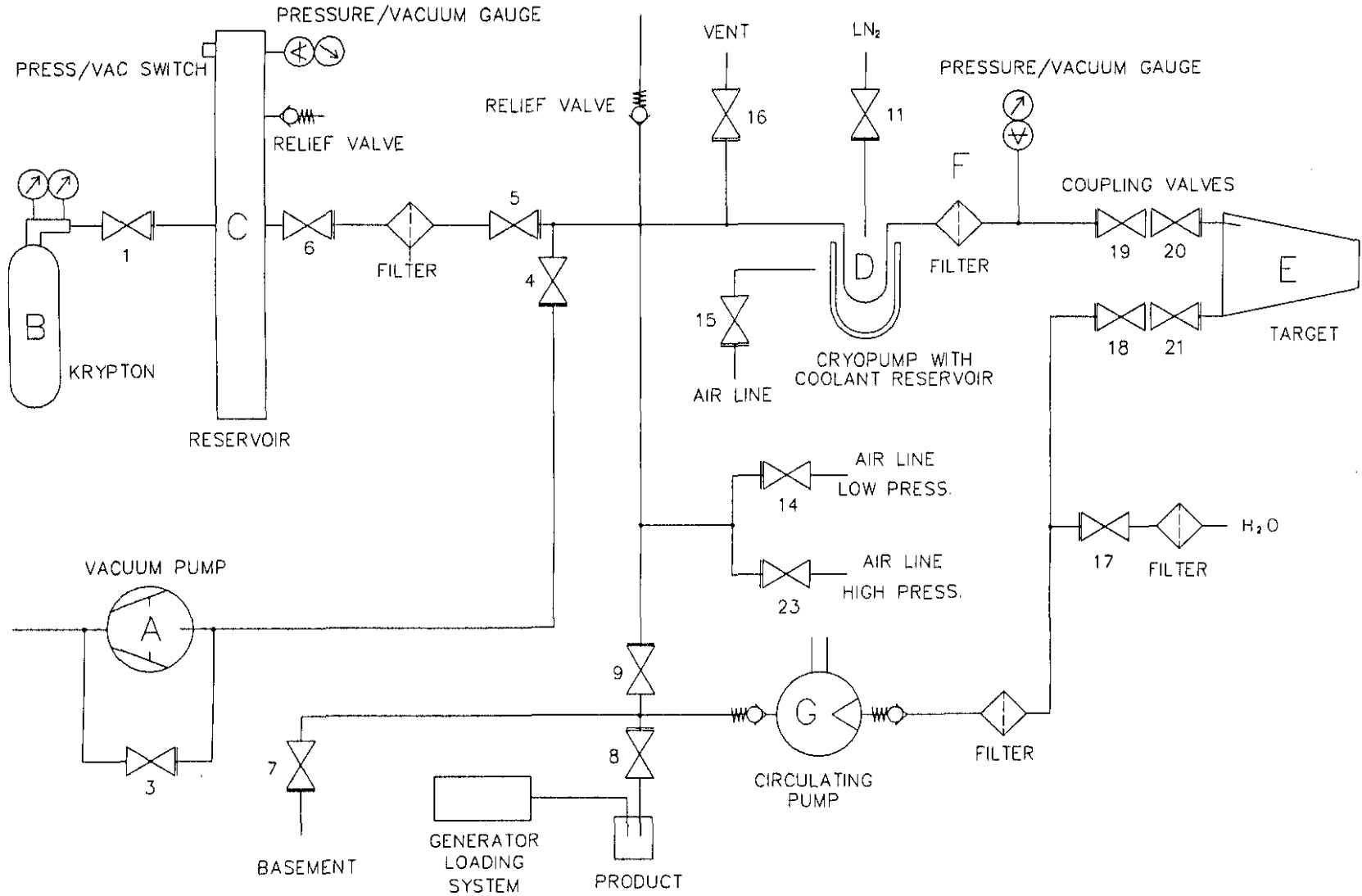
(8)   Once the target is filled, coupling valves (19;20) will close, the target will be de-coupled from the system and transported via the rail transport system to the production vault where it will be bombarded with the proton beam for a certain period of time.

(9)   After termination of bombardment, the target will be transported back to the target processing system in the hot-cell and re-coupled for further processing.

(10)   The coupling valves (19;20) will be opened and the krypton gas will be released to the activated cryopump via a filter (F). The cryopump and filter should trap the Rb that is still in suspension in the gas, and when valves (5;6) are opened, valve (19) closed, and the cryopump de-activated, relatively Rb-free krypton should flow back to the reservoir for future re-use.

(11)   The reservoir will be isolated by closing valves (5;6) and the target and cryopump will be vented by opening valves (16;19;20).

(12)   Valves (9;21) will be opened in preparation for the circulation of water for the recovery of the Rb on the target and systems inner surfaces.

(13)   Valves (9;18) will close and the circulating pump (G) will extract ~ 100 ml distilled water from the supply via valve (17).

(14)   Valve (17) will now be closed, (9;18) opened and the volume of water circulated through the target via a set of spray nozzles inside the target. Circulation will continue through the target and cryopump until all radioisotope deposits have been removed.

(15)   Valves (8;14) will open, valve (9) close and all radioisotopes in solution will be transferred to the product vessel by means of low-pressure (~ 300 kPa) compressed air.

(16)   The generator loading system is now used to transfer the solution onto the generators.

(17)   The circulating pump will again extract distilled water into the system, rinse the system and release the waste into the basement storage tank for radioactive waste via valve (7). This process will continue until all internal surfaces are clean.

(18)   Valves (7;23) will be opened and valve (9) closed, in order to dry the system with high-pressure compressed air (~ 600 kPa).

(19)   Once dry, all valves open to atmosphere will be closed, and any residual moisture removed by the vacuum pump.

(20)   The system is now ready for the next production run.

4.2 INDIVIDUAL COMPONENTS AND SYSTEMS

4.2.1 Test Target

The manufactured test target was hydrostatically tested at 6000 kPa on completion and installed on one of the experimental beamlines in the radioisotope production vault. A mounting cradle was constructed to support the test target and the coupling valves, which would be tested simultaneously.

4.2.1.1 Construction

A fairly large test target was designed so as to easily accommodate and measure the beam dispersion (see Fig. 10). A stainless steel main body of 150 mm diameter and 300 mm length was constructed, into which an aluminium cage containing six copper wires was mounted. The copper wires extended across the full diameter of the target chamber and were angularly offset with respect to one another so that the front wires did not screen the rear wires. All the wires needed to be exposed to the beam for accurate beam profile measurement.

A front stainless steel flange, which included a 1 mm thick window, was bolted and sealed onto the main body, and a rear stainless steel flange with an aluminium beam-stop was sealed to the main body by means of a chain clamp for quick removal.

Additional items mounted to the front and rear flanges were aluminium cooling jackets which were bolted on directly and sealed by means of O-rings.

Further additions to the main body were two 1/4" tube ports which would provide for pressure and vacuum gauges and two 1/4" tube ports which would connect to the vacuum and gas coupling valves.

4.2.1.2 Window Deflection

During the design of the test target, two important factors needed consideration: Firstly, a fairly accurate figure was needed for the window deflection at operating pressure, because this would determine by how much the cooling water layer thickness would decrease. This operating condition would then be used for beam degradation calculations. Secondly, accidental leakage from the 5,3 l test target could not be
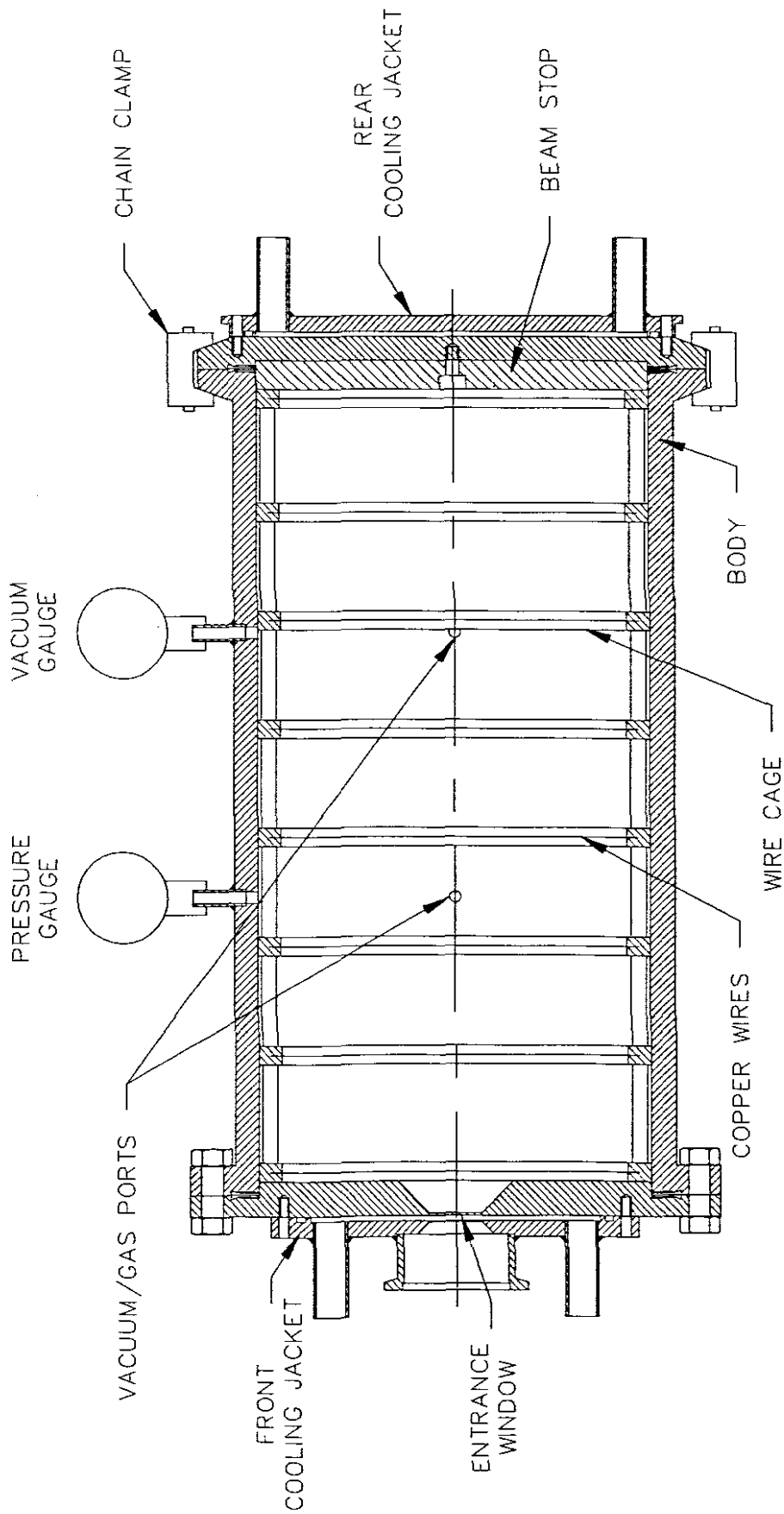
Fig. 10:   *Schematic representation of the krypton test target.*

tolerated due to the cost of krypton gas. The copper seals that were used are not generally very reliable if excessive deflections are encountered.

Calculating the deflections and stresses set up in the complex shape of the front flange could be very complicated and time consuming. For this reason it was decided to consult the Bureau for Mechanical Engineering (BMI) of the University of Stellenbosch for a finite element analysis of the front flange. The operating pressure in the test target was estimated to be in the region of 1400 kPa because the beam intensity would be sufficiently low so as to limit beam-heating of the target gas and BMI was therefore instructed to work on a safe pressure of 4500 kPa. For the analysis, one half of the front flange was considered, and 141 elements were selected in strategic positions (see Fig. 11). The information was fed into a finite element stress analysis program and the following results were obtained [Bmi89]:

(1)   The deflection at the centre of the window at 4500 kPa internal pressure would be 0,385 mm (see Fig. 12).

(2)   The Von Mises Stress contours of the window area indicated an internal stress of between 4381 and 4687 kPa at the outer central region of the window and a stress of between 3156 and 3462 kPa at the inner edge of the window (see Fig. 13).

4.2.2   Production Gas Target

The general lay-out design of the production gas target (see Fig. 14) was complicated by the different influencing factors that needed to be considered. One factor that played a limiting role was size. The gas target's size had to be compatible with all the existing equipment, which normally provided for much smaller target housings. After investigating the space that was available, the maximum outside dimensions were established as 150 mm wide × 150 mm high × 250 mm long.

Within this limited volume the target had to contain:

(1)   An inner vessel with a conical shape and size as determined by the test target experimental results: 25 mm front dia × 80 mm rear dia × 200 mm length (see par. 5.2.1).

(2)   A beam-stop with a minimum thickness in order to stop the beam before exiting the target.

(3)   Cooling for both the inner vessel and beam-stop, to remove the heat generated by the beam.
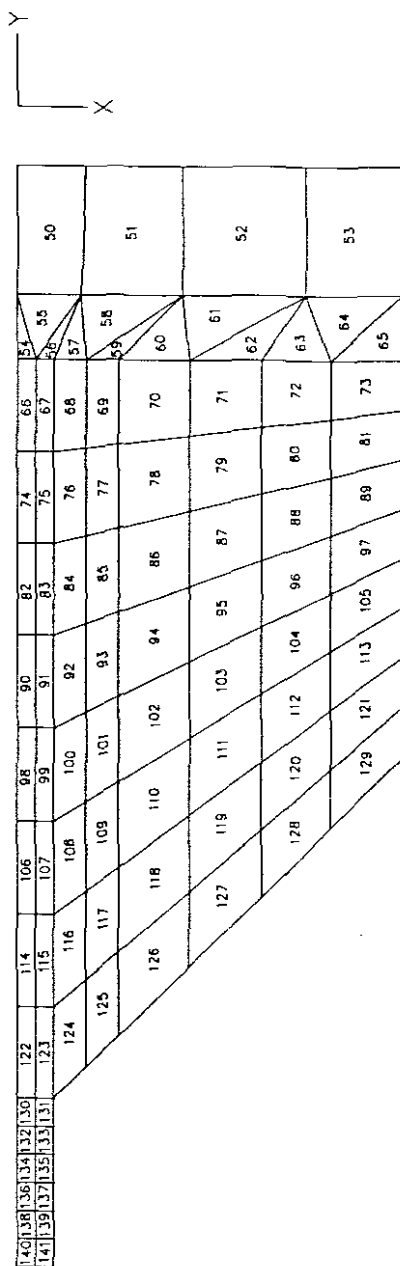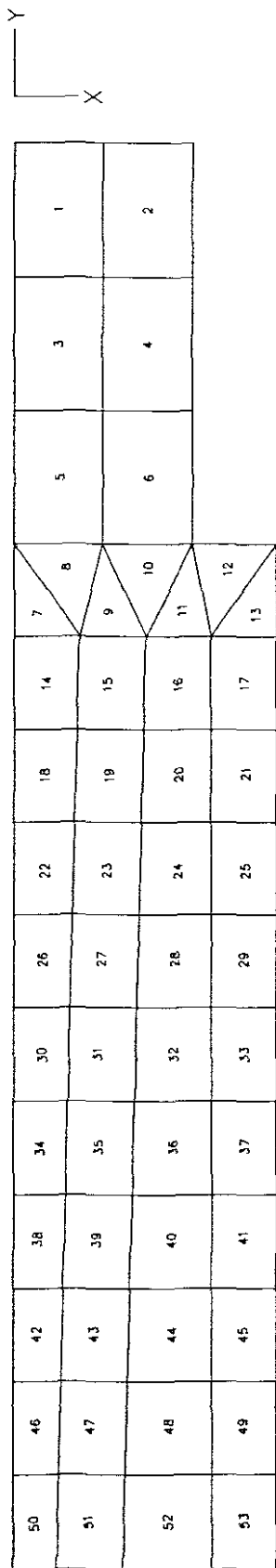
Fig. 11:   *Finite element positions on front flange [Bmi 89].*

ORIGINAL ⌊____⌋ 5.954
DEFORMED ⌊ __ ⌋ 0.385
TIME 1.000
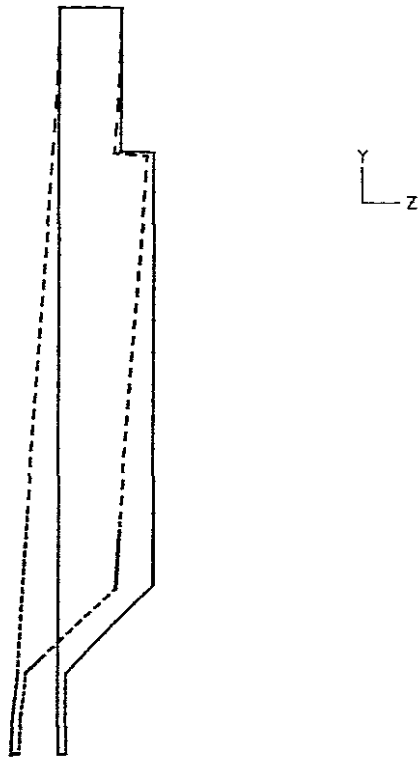
Differential Pressure· 20 mm Diameter at 4.5 MPa (BM 89/75)

Fig. 12: *Window deflection [Bmi 89].*

*** 20 mm Diameter at 4.5 MPa ... (BM89/79)***

bmi
stellenbosch

y

z

MPascal × 10²

	> 4.687
	4.381 − 4.687
	4.075 − 4.381
	3.769 − 4.075
	3.462 − 3.769
	3.156 − 3.462
	2.850 − 3.156
	2.544 − 2.850
	2.238 − 2.544
	1.932 − 2.238
	1.626 − 1.932
	1.319 − 1.626
	1.013 − 1.319
	0.707 − 1.013
	0.401 − 0.707
	< 0.401
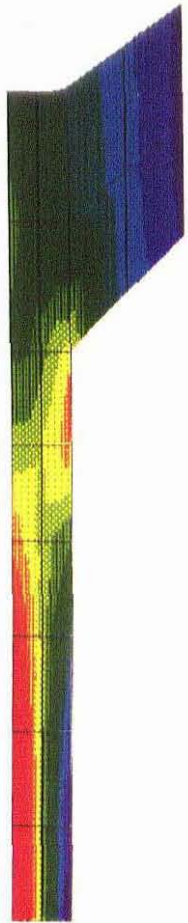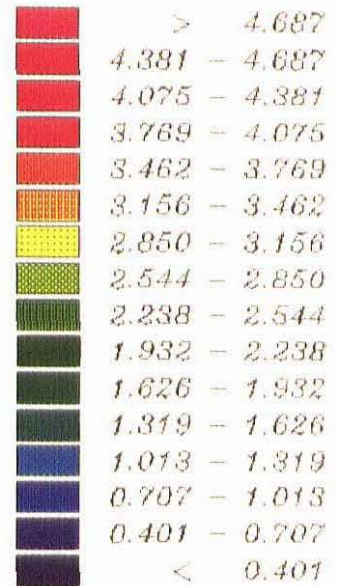
Scale

Von Mises Stresses

⊢————⊣ 1.0 : 0.1337

Fig. 13: — Von Mises Stress contours [Bmi 89].

34
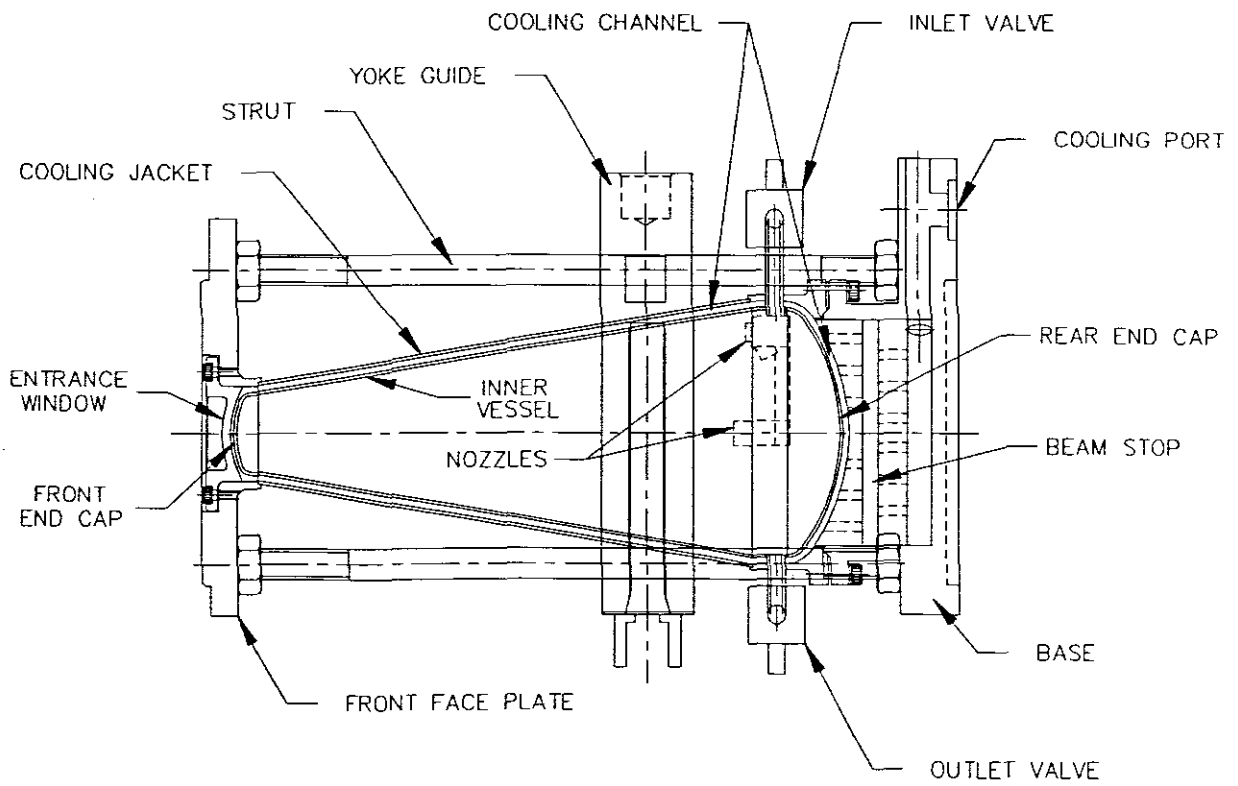
Fig. 14: *Production gas target lay-out design.*

(4) Struts to support the target from being crushed when the pusher arm pushes the target up against the beamline.

(5) Yoke-guides for the handling of the target by the robot arm, transport trolley and hot-cell hoist.

(6) A yoke lock for safeguarding the accidental release of the target from the target bombardment station or transport trolley yokes.

(7) Inlet and outlet valves for the transference of gas and water to the inner vessel.

A further critical factor was the strength-to-weight ratio. The target bombardment station and transport trolleys have limited loading capacities, so mass had to be kept to a minimum, but at the same time maximum strength of certain parts of the target was required. In order to define a mass parameter within which to work, a basic dummy target with various lead weights was constructed. The dummy target was used to check the loading on all the relevant equipment. A maximum design mass of 5,5 kg was determined.

Initially, two options were available for the general construction of the target. The first was a screwed-together construction with sealing rings, and the second an all-welded closed construction (see Fig. 14). The former makes inspection and servicing possible, whereas the latter has greater strength benefits.

The first approach in the development of the target was to investigate the screwed-together construction. An aluminium cone and end plates with maximum thickness and maximum size/number of screws clamping the sealing faces together was manufactured. This construction represented the inner vessel. Selecting a material with a higher density would have been unacceptable as far as the allowable mass is concerned.

Various hydrostatic tests were performed on the target and although the deflection of the rear end plate was minimal ($\sim 0,01$ mm), slow and sporadic leaks at $3000 - 6000$ kPa were encountered. The target's operating pressure was assumed to be 3000 kPa, and a safe testing pressure was therefore taken to be in the region of 8000 kPa.

Sealing was accomplished by means of two mating knife-edges with a soft aluminium sealing ring in-between (Aluminium Gr 1070A, annealed). Other more resilient aluminium grades were also experimented with but were found to give similar results.

The use of O-rings was impossible because of radiation damage considerations and replacement difficulties. A further possibility was to use a metallic cup seal, which would compensate for deflections and so provide a more effective seal at high pressures. This particular type of seal (High flex internal pressure E-seal) is available overseas, but unfortunately importing these items was found to be unsuccessful due to sanctions against South Africa. This construction, however, proved to be unreliable at the operating pressure, and to eliminate any risks the all-welded closed construction was thus investigated.

The all-welded construction finally developed (see Figs. 14, 15 and 16) comprises:

(1)   An inner vessel which consists of a longitudinally-welded cone and two circularly-welded dished end caps on either end.

(2)   A beam-stop and base housing, complete with cooling channels mounted behind the rear end cap.

(3)   A cooling-jacket cone welded onto the front face-plate which together screws onto the base housing.

(4)   Four struts which are bolted to the face-plate and base housing.

(5)   Yoke-guides which are mounted on the struts and also house the yoke-lock.

(6)   Coupling valves connected to piping which is welded to both the cooling jacket and inner vessel and terminating inside the inner vessel.

To arrive at this construction, each individual component was, of course, investigated in detail:

4.2.2.1   Inner Vessel

The first factor taken into consideration regarding this component, is the high operating pressure and the possibility that this would necessitate coding of it under pressure vessels. According to the design and manufacturing specifications ASME (American Society for Mechanical Engineering) VIIII DIV 1(c)(9), vessels having an inside diameter, width, height or cross-section diagonal not exceeding 152 mm are not considered to fall within this classification, independent of length or pressure. The inner vessel, having smaller dimensions, is thus exempt from coding.
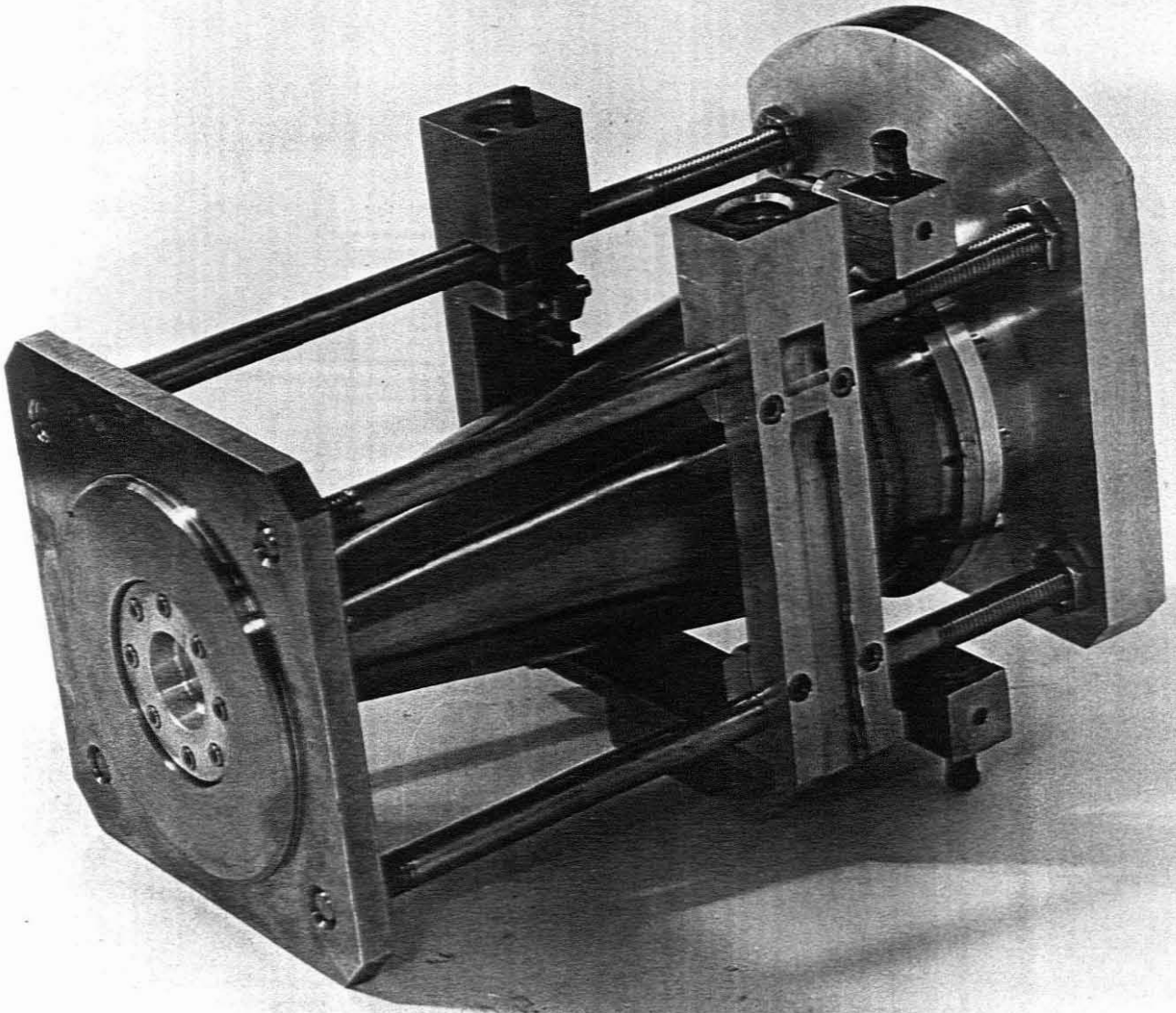
Fig. 15: *Production gas target construction – front view.*
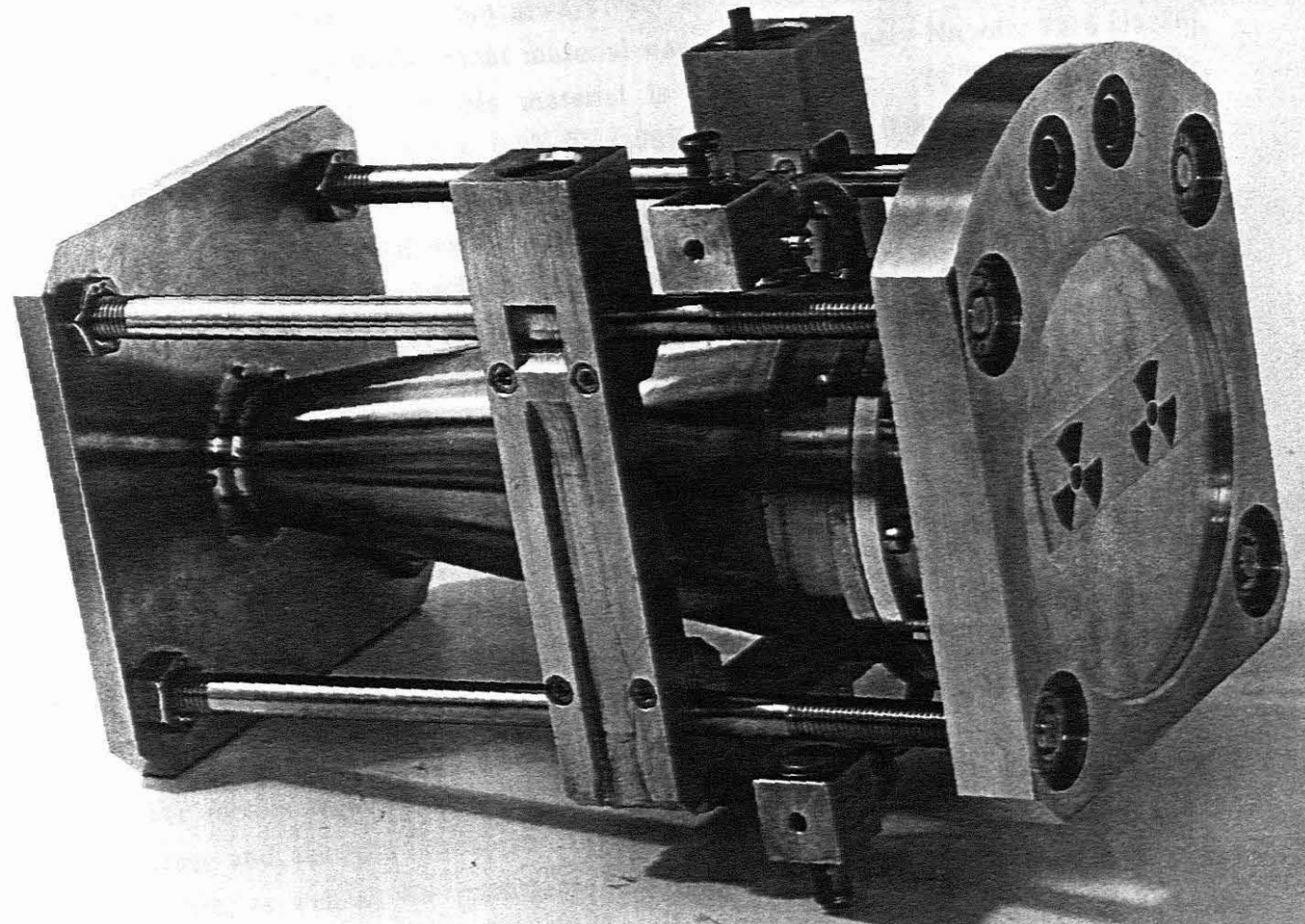
Fig. 16: *Production gas target construction — rear view.*

The second factor was material selection. According to overseas experience in krypton gas targetry, nickel seems to be a very stable material, chemically not very responsive to Rb [Wat86]. This is an important consideration for the inner vessel, because high radiation-doses and elevated temperatures will be experienced during bombardment. Polishing would further increase these qualities. A practical, light but strong material to use would be nickel-plated stainless steel sheeting, but nickel-plating (electroless process) on stainless steel is not always very successful [Sch90]. For these reasons a high strength, high nickel-content material was selected, namely Nicrofer 7216 [Jac86]. The alloy composition of this material is the following: 74,7% Ni, 15,85% Cr, 8,35% Fe, 0,26% Si, 0,24% Mn, 0,2% Ti, 0,06% C, 0,05% Cu, 0,007% P, 0,003% S.

Due to the high tooling costs for forming or spinning a 162 mm deep cone, local construction thereof was preferred, and hence sheeting of Nicrofer 7216 was cut, rolled and welded. A convenient shape of the end caps was determined and the drawing dies required to produce them were locally designed and manufactured (see par. 4.2.2.1.1). Before the cone and end caps were welded together, they were first rough polished with water paper and then electropolished.

The inner vessel has a 1 mm wide × 2 mm high rib welded along the periphery of the median plane, excluding the beam entrance area, so that the cooling water flows in along one hemisphere, past the beam entrance window and out along the other hemisphere (see Fig. 21).

Other factors which had to be considered are the longitudinal and circumferential stresses and also the lateral and diametral dimensional changes due to the internal pressure, as well as the maximum operating pressure rating and the total internal volume of the vessel. The following symbols and dimensions are of relevance to this discussion:

L = length = 162 mm
ΔL = change in length L
D = vessel diameter at large end = 80 mm
ΔD = change in diameter D
D_1 = vessel diameter at small end = 25 mm
V = vessel volume
h = length of tubular section of large end cap = 12 mm
h_1 = length of tubular section of small end cap = 2,5 mm
t = wall thickness = 1 mm

E = Young's modulus of elasticity = 210 GPa [Jac86]

ν = Poisson's ratio = 0,3

p = internal pressure = 3000 kPa

σ_U = ultimate tensile strength = 550 MPa [Jac86]

σ_Y = yield stress = 200 MPa [Jac86]

σ_H = circumferential stress

σ_L = longitudinal stress

ε_H = circumferential strain

ε_L = longitudinal strain

<u>Stresses and dimensional changes</u>:

To analyze the highest stress values and for ease of calculation, the conical vessel was treated as a cylindrical vessel with a diameter equal to the large diameter D of the cone. The ratio $\frac{t}{D} = \frac{1}{80} < \frac{1}{20}$, therefore thin cylinder formulae were used [Hea89].

Cylindrical body:

$$\sigma_H = \frac{pD}{2t}$$

$$= \frac{3 \times 80}{2 \times 1}$$

$$= 120 \text{ MPa}$$

$$\sigma_L = \frac{pD}{4t}$$

$$= \frac{3 \times 80}{4 \times 1}$$

$$= 60 \text{ MPa}$$

$$\varepsilon_H = \frac{pD}{4tE} [2 - \nu]$$

$$= \frac{3 \times 80}{4 \times 1 \times 210 \times 10^3} [2 - 0,3]$$

$$= 4,86 \times 10^{-4}$$

$$\Delta D = \varepsilon_H \times D$$

$$= 4{,}86 \times 10^{-4} \times 80$$

$$= 0{,}039 \text{ mm}$$

$$\varepsilon_L = \frac{pD}{4tE} [1 - 2\nu]$$

$$= \frac{3 \times 80}{4 \times 1 \times 210 \times 10^3} [1 - 2 \times 0{,}3]$$

$$= 1{,}14 \times 10^{-4}$$

$$\Delta L = \varepsilon_L \times L$$

$$= 1{,}14 \times 10^{-4} \times 162$$

$$= 0{,}019 \text{ mm}$$

Hemispherical end:

$$\sigma_H = \frac{pD}{4t}$$

$$= \frac{3 \times 80}{4 \times 1}$$

$$= 60 \text{ MPa}$$

$$\varepsilon_H = \frac{pD}{4tE} [1 - \nu]$$

$$= \frac{3 \times 80}{4 \times 1 \times 210 \times 10^3} [1 - 0{,}3]$$

$$= 2{,}0 \times 10^{-4}$$

$$\Delta D = \varepsilon_H \times D$$

$$= 2{,}0 \times 10^{-4} \times 80$$

$$= 0{,}016 \text{ mm}$$

Maximum operating pressure rating:

Factor of safety used: 1,5

Therefore, maximum allowed operating stress $\sigma_{max} = \frac{200}{1,5} = 133,33$ MPa

The maximum operating gas pressure thus is:

$$p_{max} = \frac{2t\sigma_{max}}{D}$$

$$= \frac{2 \times 1 \times 133,33}{80}$$

$$= 3333,3 \text{ kPa}$$

Internal volume:

Frustum of cone:

$$V_1 = \frac{\pi}{12} L (D^2 + DD_1 + D_1{}^2)$$

$$= \frac{\pi}{12} \times 162 (80^2 + 80 \times 25 \times 25^2)$$

$$= 382,764 \times 10^3 \text{ mm}^3$$

Tubular section of large end cap:

$$V_2 = \frac{\pi}{4} D^2 h$$

$$= \frac{\pi}{4} \times 80^2 \times 12$$

$$= 60,319 \times 10^3 \text{ mm}^3$$

Large end cap:

$V_3 = 51,072 \times 10^3$ mm^3 (Volume determined using computer program)

Tubular section of small end cap:

$$V_4 = \frac{\pi}{4} D_1^2 h_1$$

$$= \frac{\pi}{4} \times 25^2 \times 2,5$$

$$= 1,227 \times 10^3 \text{ mm}^3$$

Small end cap:

$$V_5 = 1,605 \times 10^3 \text{ mm}^3 \quad \text{(Volume determined using computer program)}$$

Total internal volume:

$$V = V_1 + V_2 + V_3 + V_4 + V_5$$

$$= 496,987 \times 10^3 \text{ mm}^3$$

$$\approx 0,50 \text{ dm}^3$$

$$= 0,50 \ \ell$$

4.2.2.1.1 *Manufacturing of End Caps*

The most practical way to manufacture the end caps was to form them, or more precisely to "shallow draw" them (no redraws), because the sidewalls are not very deep (see Fig. 17). The material used, as indicated in par. 4.2.2.1, was 1 mm thick Nicrofer 7216 and, according to the manufacturers, the formability is very good. The tooling for the shallow drawing was designed and manufactured at the NAC and the hardening was done at Bohler Steel, Cape Town. The material used was a K107 Bohler tool steel [Ver83] and both die sets were hardened to 62 Rockwell 'C'. All mating surfaces were ground and polished. The drawing was done on a hand-operated fly-press and the drawing compound used was Shell Tivena Compound A.

The designs for both the front and rear end cap dies were of the push-through type (see Fig. 18). All design formulae and approximations used were from [Ost67]:

Design dimensions for front end cap die (see Fig. 19):

(1) Die depth H ~ 9 to 13 mm.
    However, H = 19 mm with a slight increased taper to the bottom of the die block proved experimentally to be satisfactory.
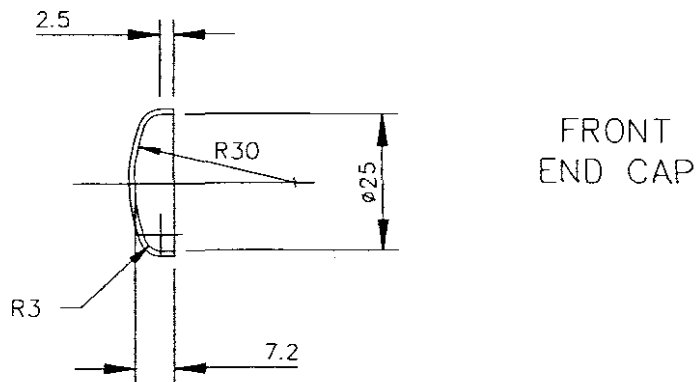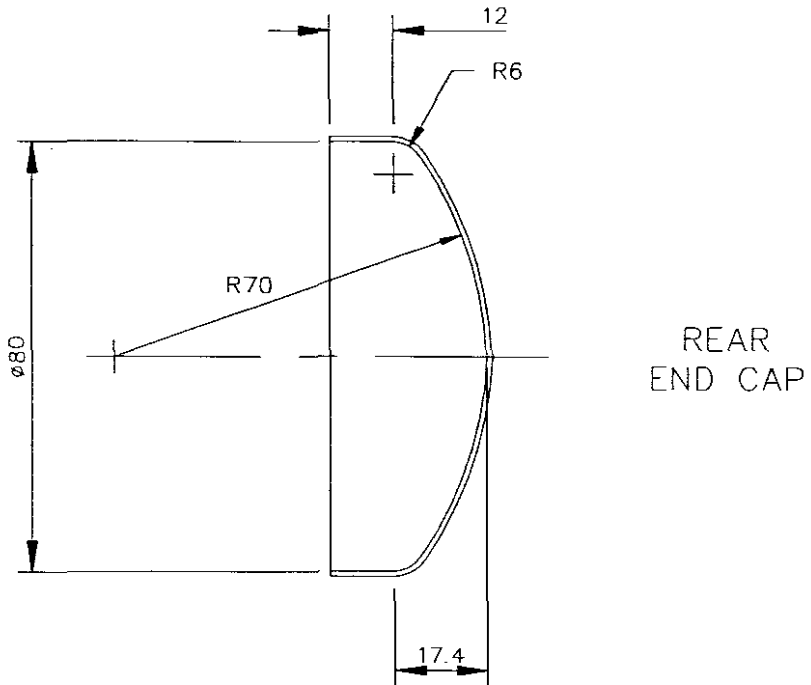
Fig. 17:   *Front and rear end caps.*
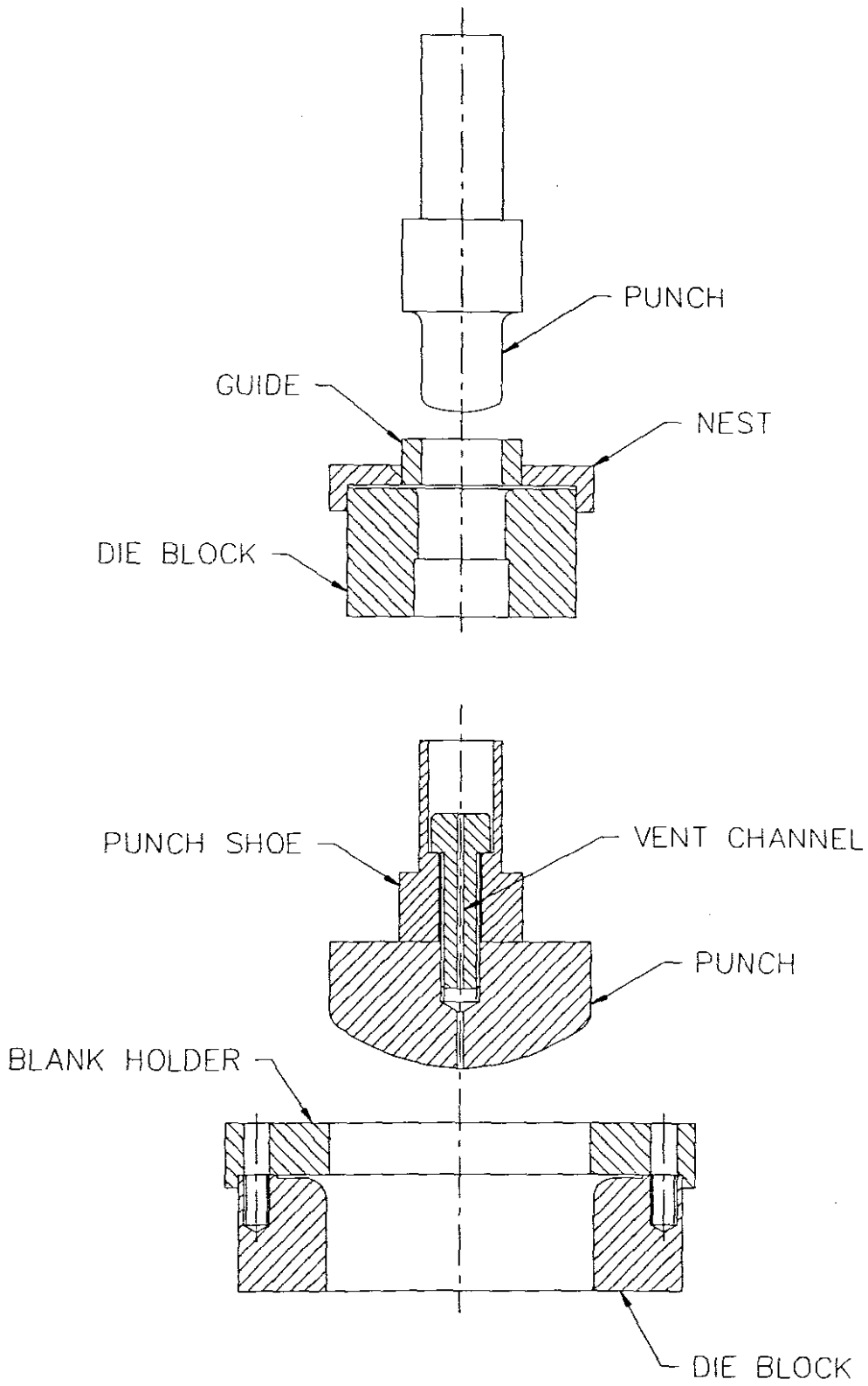
Fig. 18:   *Front and rear end cap dies.*
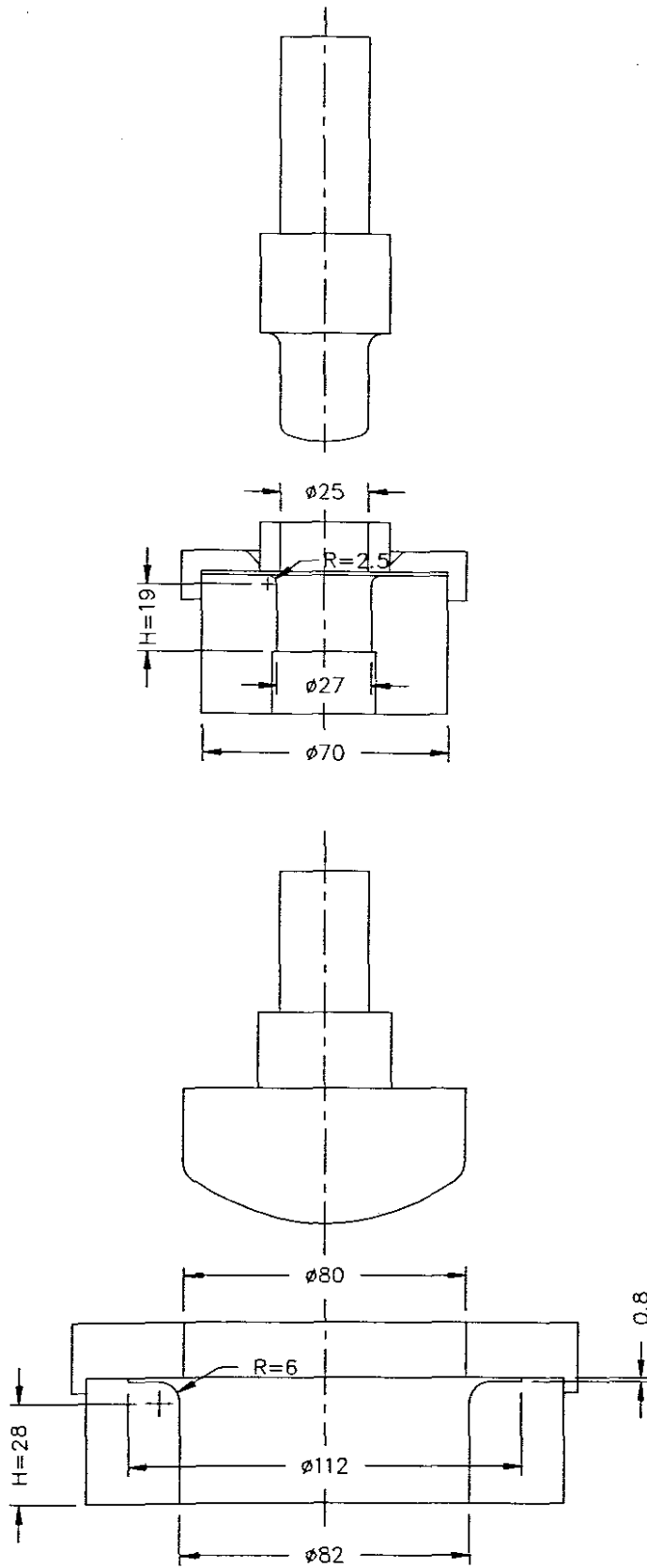
Fig. 19: *Die construction proportions.*

(2) Draw radius $R = 4 t$, where t is the material thickness (1 mm).

Therefore: $R = 4 \text{ mm}$

During machining of the draw radius, the drawing operation was tested at every 0,5 mm increase and at $R = 2,5$ mm the front end cap was successfully drawn.

(3) For no blank holder application, caps can be drawn to a depth d of 1/3 their mean diameter:

$$d = \frac{26}{3}$$

$$= 8,7 \text{ mm}$$

The required front end cap depth was 7,2 mm and therefore no blank holder application was necessary.

(4) Draw clearance $C \sim 8$ to 20% of blank thickness.

An 8% draw clearance was used:

$$C = 0,08 \times 1$$

$$= 0,08 \text{ mm}$$

(5) Blank diameter D_B is calculated as follows:

End cap depth: $h_C = \dfrac{(D_B^2 - d_M^2)}{4d}$, where d_M is the mean diameter of end cap.

Therefore: $7,2 = \dfrac{(D_B^2 - 26^2)}{4 \times 26}$

Thus: $D_B = 38 \text{ mm}$

A diameter of 45 mm was used to allow for machining the uneven rim after drawing.

Design dimensions for rear end cap die (see Fig. 19):

(1) Die depth $H \sim 9$ to 13 mm.

However, $H = 28$ mm with a slight increased taper towards the bottom of the die block also proved experimentally to be satisfactory.

(2) Draw Radius $R = 4 t$, where t is the material thickness (1 mm).

Therefore: $R = 4 \text{ mm}$

The same procedure during machining of the draw radius was followed as with the front end cap and the best results obtained were at $R = 6$ mm.

(3) Blank holder application was also checked:

$$d = \frac{81}{3}$$

$$= 27 \text{ mm}$$

The required depth of the rear end cap, however, is 29,4 mm, which is greater than d, and therefore a blank holder had to be incorporated. The blank holder was designed so that the torque applied on the blank holder bolts determines the force at which the blank is gripped. Experiments were carried out to ascertain the optimum force.

(4) A draw clearance C of 8% of blank thickness was also used:

$$C = 0,08 \text{mm}$$

(5) Blank diameter D_B is calculated as follows:

End cap depth: $h_C = \dfrac{(D_B^2 - d_M^2)}{4d}$, where d_M is the mean diameter of end cap.

Therefore: $29,4 = \dfrac{(D_B^2 - 81^2)}{4 \times 81}$

Thus: $D = 126,8 \text{ mm}$

By means of experimentation a convenient diameter of 112 mm, which allowed for machining after drawing, was established. An additional feature that was incorporated on the large end cap punch was a venting channel for easy work removal.

4.2.2.1.2 Electropolishing

The fact that the inner cone surface must be extremely smooth and free of abrasive particles, disqualifies many standard methods of polishing. A further limitation is the practical problem of polishing the profiles of the end caps and cone. For these reasons, it was decided to investigate the electropolishing method.

By definition, electropolishing is the improvement in the surface finish of a metal by making it anodic in a suitable solution. With the proper selection of current density, temperature and other conditions, the surface is smoothed and brightened by the

removal of the metal [Sch81]. Electropolishing thus can achieve a chemically clean, lustrous-to-mirrorbright surface. The process also tends to remove surface inclusions which have arisen from rolling and forming. Electropolishing is exceptionally useful for polishing complex and convoluted parts, because the solution is in contact with all surfaces to be polished. A further advantage of electropolishing is that the surface is more passive and decidedly more corrosion resistant.

The only company found in South Africa that uses the electropolishing process intensively is the Atomic Energy Corporation (AEC). After consulting both the AEC and existing literature, it was decided to build up a small facility at the NAC, as most of the components for the process were readily available. The facility was built up in a laboratory fume cupboard and is shown schematically in Fig. 20.

In electropolishing there are no fixed values, but only guidelines, regarding variables such as current, voltage, anode/cathode distance and electrolyte ratios, and for this reason the process is normally developed experimentally. A number of 40 × 30 mm samples pieces were therefore manufactured and various combinations of the variables were experimented with. The best combination was selected and the process was finally carried out as follows:

Pre-Treatment

(1) Clean sample in trichloroethylene solvent degreaser.

(2) Hot swill in water and dry.

Electropolishing

(1) Various solution or electrolyte ratios are given in the literature, but as a starting point average ratios for polishing nickel and nickel alloys were selected: Phosphoric acid − 254,8 g, sulfuric acid − 200,0 g, hydrochloric acid − 7,8 g, water − 37,4 g.

(2) Heat electrolyte to 60° C.

(3) Mount sample on anode, insert in electrolyte and line up at a distance of 30 mm from cathode.

(4) Turn on compressed air line for agitation.

EXTRACTION FAN

DC POWER SUPPLY

Cu ANODE/CATHODE

ELECTROLYTE

COVER

COMPRESSED AIR

WATER

TEMP.CONTROLLER

WORK

GLASS BEAKER

ST.STEEL TANK

HEATING ELEMENT
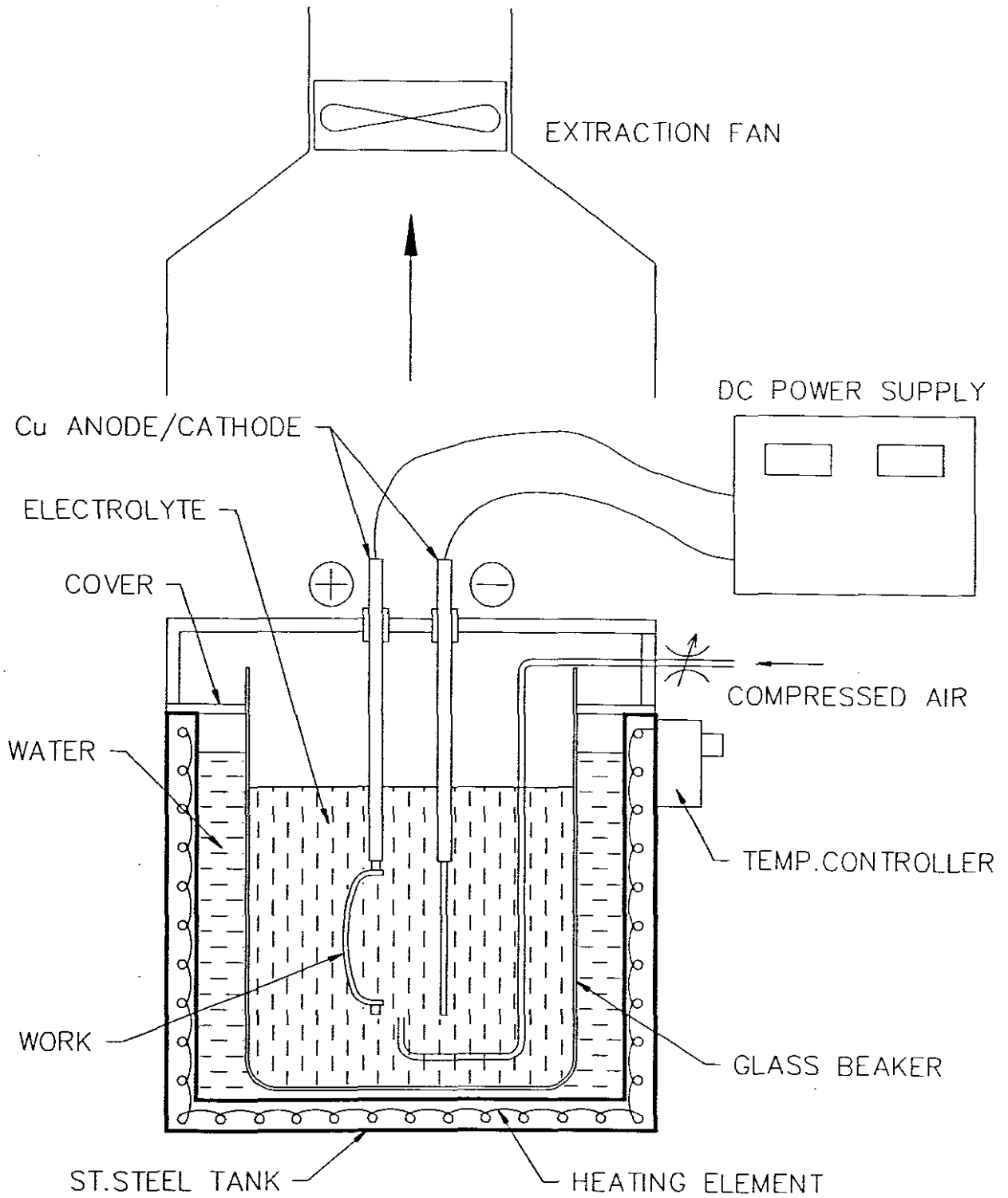
Fig. 20: *Electropolishing facility.*

(5)   Switch on current at 12 V, 21 A for 2 minutes.

(6)   Switch off current and remove work from electrolyte.

Post-Treatment

(1)   Passivate in a 5% sulfuric acid and 1% sodium dichromate solution at room temperature.

(2)   Hot swill in water and dry.

The target inner vessel components were electropolished before being welded together. The front end cap, rear end cap and cone had separate jigs/cathodes manufactured for them and were polished individually. The components were angled in such a manner that the gas bubbles formed could easily escape.

4.2.2.2   Cooling Jacket

The conical stainless steel cooling jacket design follows the inner vessel profile but is situated on the outside with a 2 mm water layer gap between the two. The inner vessel fits snugly into the cooling jacket so that contact between the vessel rib and the jacket inner surface forms an adequate seal for cooling water to flow in the one hemisphere, past the beam entrance window and out the other hemisphere. The advantage of this design is that a reduced cooling channel cross-sectional area causes high water velocities at the beam entrance area, where the heat build-up is the highest.

The cone of the cooling jacket was rolled from a pre-cut development and butt-welded along the length. The large end of the cooling jacket has a welded flange which bolts onto the target base and the small end is welded to the front face plate (see Fig 21).

4.2.2.2.1   *Cooling*

As previously mentioned, the most critical heat build-up due to beam bombardment is at the beam entrance area. Due to the complexities of accurate heat and cooling calculations, a few indicators were investigated to confirm adequate cooling.

Beam power losses in the various target components and the corresponding cooling power densities required (see Appendix A2), are given in Table 1.
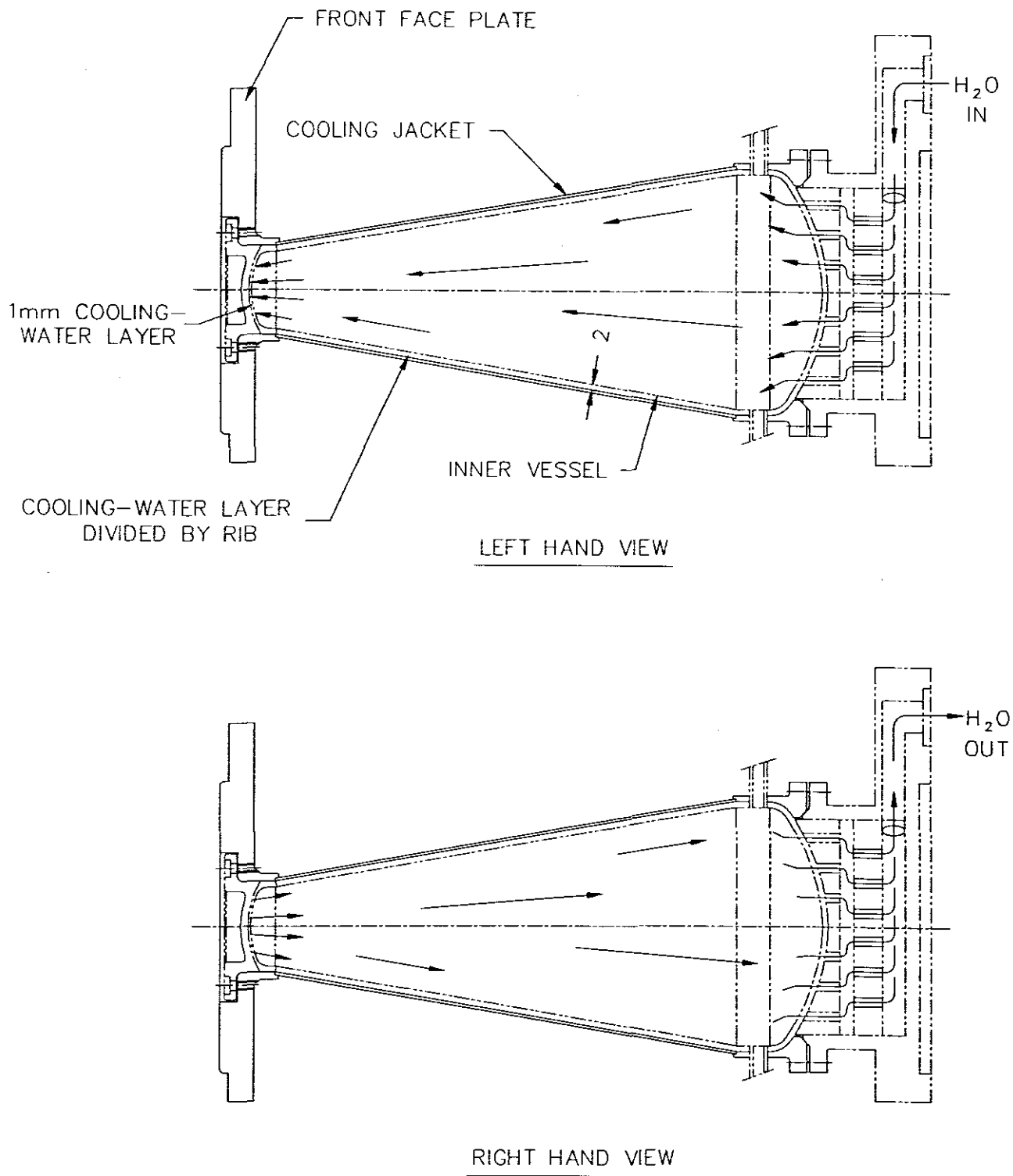
Fig. 21: *Cooling jacket.*

As previously investigated at the NAC [Mil89b], heat flux densities in excess of 1 kW/cm² can easily be achieved at the interfaces between the target and cooling-water layers with the existing water cooling system. At these high heat flux densities, effective cooling is provided by utilizing sub-cooled nucleate boiling at the heat transfer surfaces. In this process, the energy required to change the phase of the cooling water from liquid to steam, i.e. the latent heat of the cooling water, is utilized to transfer heat from the cooling interfaces. However, a catastrophic failure of the target material will occur if this local boiling should develop to the stage where a steam layer isolates the heated surfaces from the bulk of the cooling water.

Table 1: *Beam power losses in target components and the corresponding cooling power densities required.*

Component	Energy Values [Ste90] (Entry – Exit) (MeV)	Energy Loss (MeV)	Power[1] (W) (see app. A2)	Required cooling power density (W/cm²) (see app. A2)
H_2O–cooled front entrance area	65,72 – 52,50	13,22	793,2	505,2
Krypton gas @ 1500 kPa (abs.)	52,50 – 44,48	8,02	481,2	1,2
Beam–stop	44,48 – 0	44,48	2668,8	136,2
TOTAL			3942	

[1] For a beam current of 60 μA.

In order to shift this critical point of departure from the sub-cooled nucleate boiling regime to above the required heat flux densities, one or more of the following techniques may be employed at the heat transfer surfaces:

(1)   High water flow rate.
(2)   Promotion of turbulence in the cooling water.
(3)   High static pressure of the cooling water.

A high flow rate ensures that the steam bubbles are transported away from the cooling interfaces at a sufficient rate.

Turbulence is required to mix these steam bubbles as fast as possible with the bulk of the cooling water, preventing them from combining with one another to form a layer, and to aid in their effective removal from the heat transfer surfaces. The individual steam bubbles eventually implode and disappear when the steam condenses back to the liquid phase.

The higher the static pressure of the cooling water, the higher the boiling point of the water layer against the heated surface becomes, resulting in an increased critical heat flux density. The use of an operating water pressure of 1000 kPa on the existing water cooling system results in an increase in the boiling point to 180° C [Crc87].

In the sub-cooled nucleate boiling regime, the heat transfer is determined by the so-called film properties of the cooling water (ie. the thin sub-layers of water in direct contact with the heat transfer surfaces) and not by the bulk properties of the cooling water. The overall increase in the bulk temperature may be very small while local boiling takes place in the film sub-layers (hence the term sub-cooled nucleate boiling). The bulk temperature increase may be calculated as follows:

By definition, 1 Calorie (4,2 J) increases 1 cm³ water by 1° C at 20° C [Hol82]. At 1000 kPa the pump produces a flow of 25 ℓ/min or 417 cm³/s. For a total heat transfer of 3942 W (Table 1) the increase in bulk temperature ΔT is therefore given by:

$$\Delta T = \frac{3942}{417 \times 4,2}$$

$$= 2,25°\,C$$

The required cooling power density at the entrance window (as given in Table 1) is ~ 0,5 kW/cm². For the sake of safety, however, cooling conditions are provided that should easily accommodate heat fluxes in excess of 1 kW/cm². As mentioned, the target is cooled at a bulk cooling water pressure of 1000 kPa and at a flow rate of 25 ℓ/min. The water is forced through a 1 mm thick channel, across the heat transfer surfaces of the window area, resulting in a linear flow velocity of ~ 13 m/s. The water layer is thus replaced at a rate of 520 per second and the flow regime is highly turbulent, as can be shown by calculating the Reynolds number Re, which is a measure of the nature of the flow of a fluid:

$$Re = \frac{\rho v d}{\mu}$$

where ρ = density of cooling medium (water) = 1000 kg/m³

v = average linear velocity of medium = 13 m/s

μ = dynamic viscosity of medium = 1,12 × 10⁻³ kg/m.s

d = hydraulic diameter

The hydraulic diameter d is given by:

$$d = \frac{4A}{p}$$

where A = cross-sectional area of flow passage

p = wetted circumference of flow passage

Therefore:

$$d = \frac{4 \times 37 \times 1}{76} \text{ mm}$$

$$= 1{,}95 \times 10^{-3} \text{ m}$$

Thus:

$$Re = \frac{1000 \times 13 \times 1{,}95 \times 10^{-3}}{1{,}12 \times 10^{-3}}$$

$$= 22634$$

The transition from laminar to turbulent flow for water is in the region $2000 \leq Re \leq 4000$. Below 2000 the flow is laminar and above 4000 the flow is turbulent.

At all the other heat transfer surfaces in the gas target the heat flux is much smaller than 1 kW/cm², and the cooling is more than adequate (see Table 1).

4.2.2.3 Beam-Stop

The beam-stop's function is to absorb and dissipate the residual energy which has passed through the target. A minimum thickness of material is required to stop a certain proton energy and attention must be given to the fact that the cooling channels in the beam-stop must not reduce the effective thickness to below the required thickness. For mass reduction, aluminium was chosen. The beam-stop has to absorb

2669 Watts (see par. 4.2.2.2.1) and aluminium requires a minimum thickness of 15 mm
to absorb the remaining proton energy [Ste90].

For ease of assembly and manufacturing, the beam-stop was designed as a separate
cooled unit which fits into the target base (see Figs. 22 and 23). The beam-stop unit
basically consists of two isolated halves, each consisting of a series of offset cooling
channels with an intermediate chamber. The one half channels the cooling-water inlet,
while the other half channels the cooling-water outlet. The target base front section,
with the beam-stop in position, screws onto the cooling jacket and seals by means of
two mating chamfers. The target base rear section couples with the target pusher
when the target is pushed up against the beamline. The cooling ports between the
target base and pusher are sealed by means of O-rings.

4.2.2.4   Window

The design of the aluminium beam entrance window is such that it bolts directly onto
the front face plate and seals by means of two mating chamfers at the neck of the
window flange (see Fig. 24). For strength and minimal deflection reasons, the window
was manufactured in a convex shape. A further reason was that the cooling water flow
is not restricted with this shape. For the correct beam degradation, the window
thickness was calculated to be 2,7 mm [Ste90], and for constant thickness in the
horizontal direction, the inner and outer surface radii of 31 mm each therefore had to
be offset by this amount.

4.2.2.5   Yoke Guides

The function of the yoke guides is to enable the handling of the target and its securing
during transportation.

The yoke guides basically consist of two aluminium columns which are clamped onto
the struts and a connecting bridge which makes provision for an electrical connection
which would be used for target identification purposes (see Fig. 25). The columns each
contain machined grooves on the outer edges for guiding in the rotary target magazine
and transport trolley yokes, while also containing locating recesses on the upper ends
for handling by the robot arm and hot-cell hoist. An additional feature on the one
column is a yoke lock.

SEALING CHAMFER

COOLING PORTS

TARGET BASE

INTERMEDIATE CHAMBER

COOLING-WATER
OUTLET

COOLING CHANNELS

COOLING-WATER
INLET
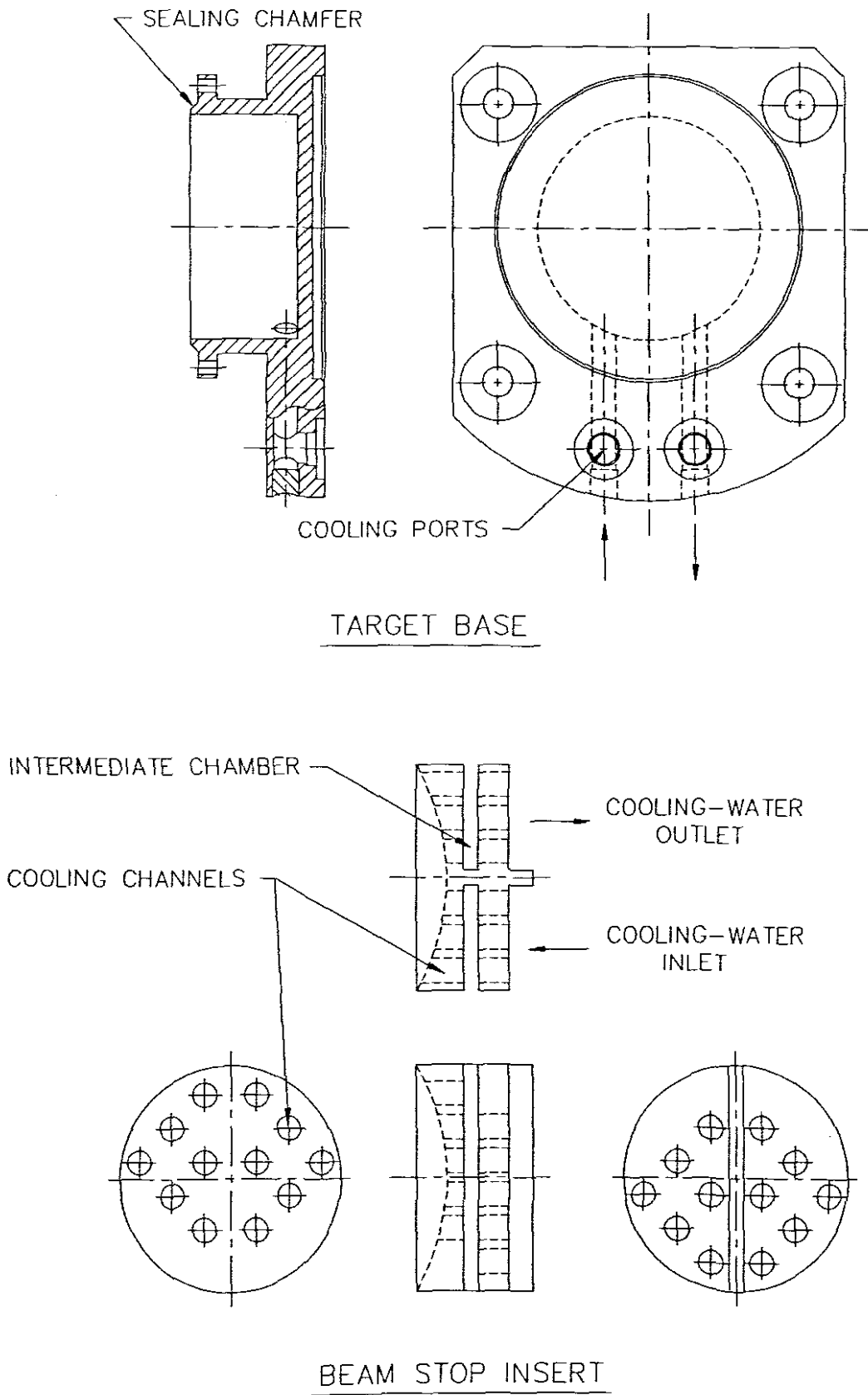
BEAM STOP INSERT

Fig. 22: *Target base and beam-stop insert details.*
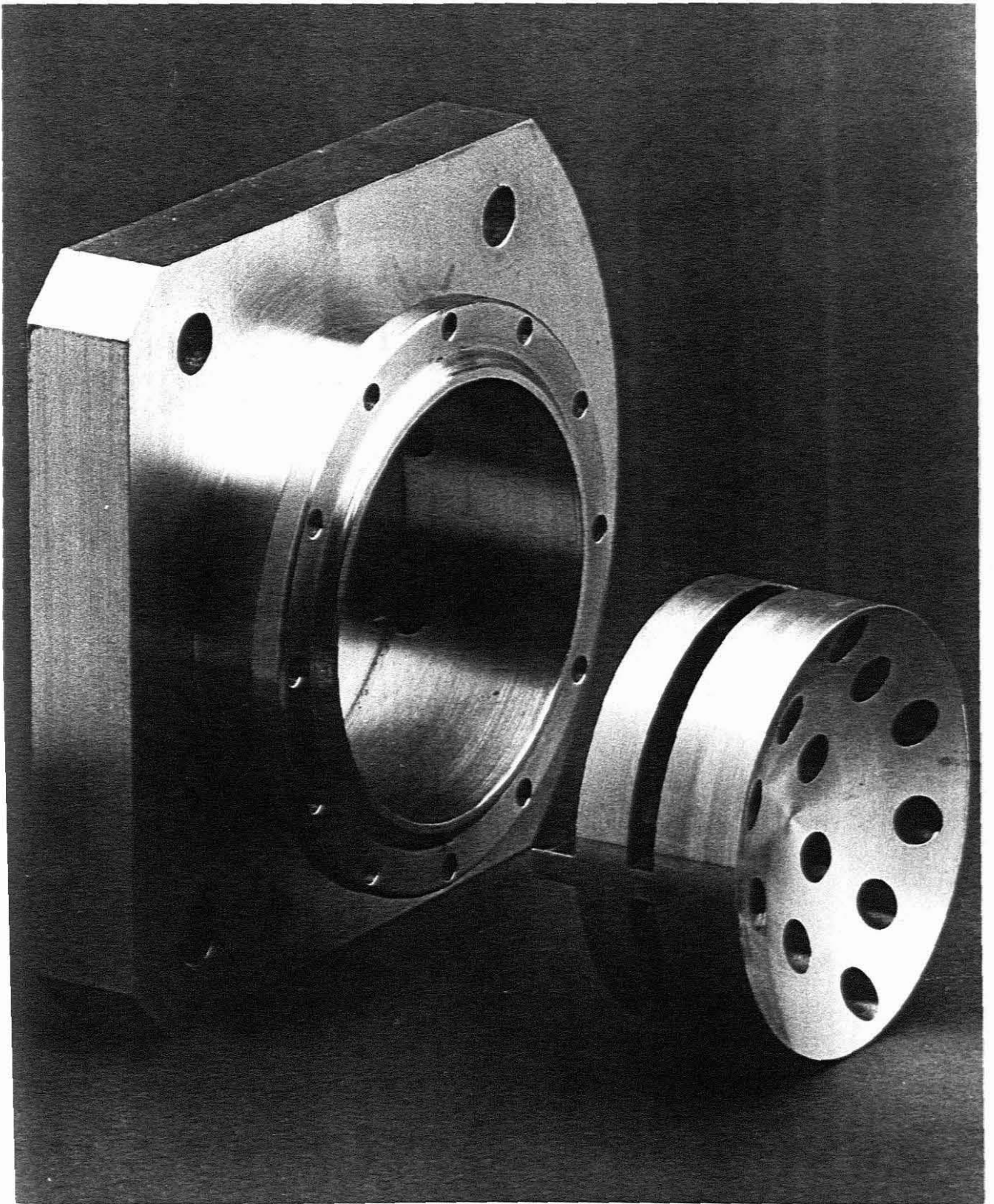
Fig. 23: *Target base and beam-stop insert.*
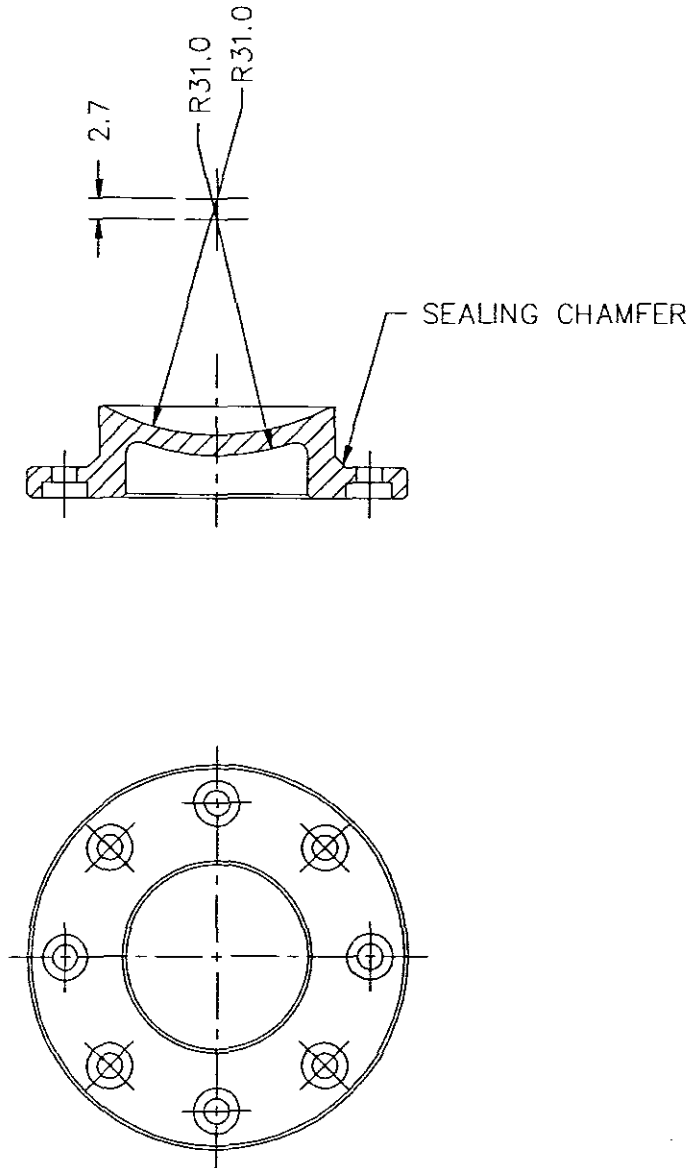
Fig. 24: *Beam entrance window.*
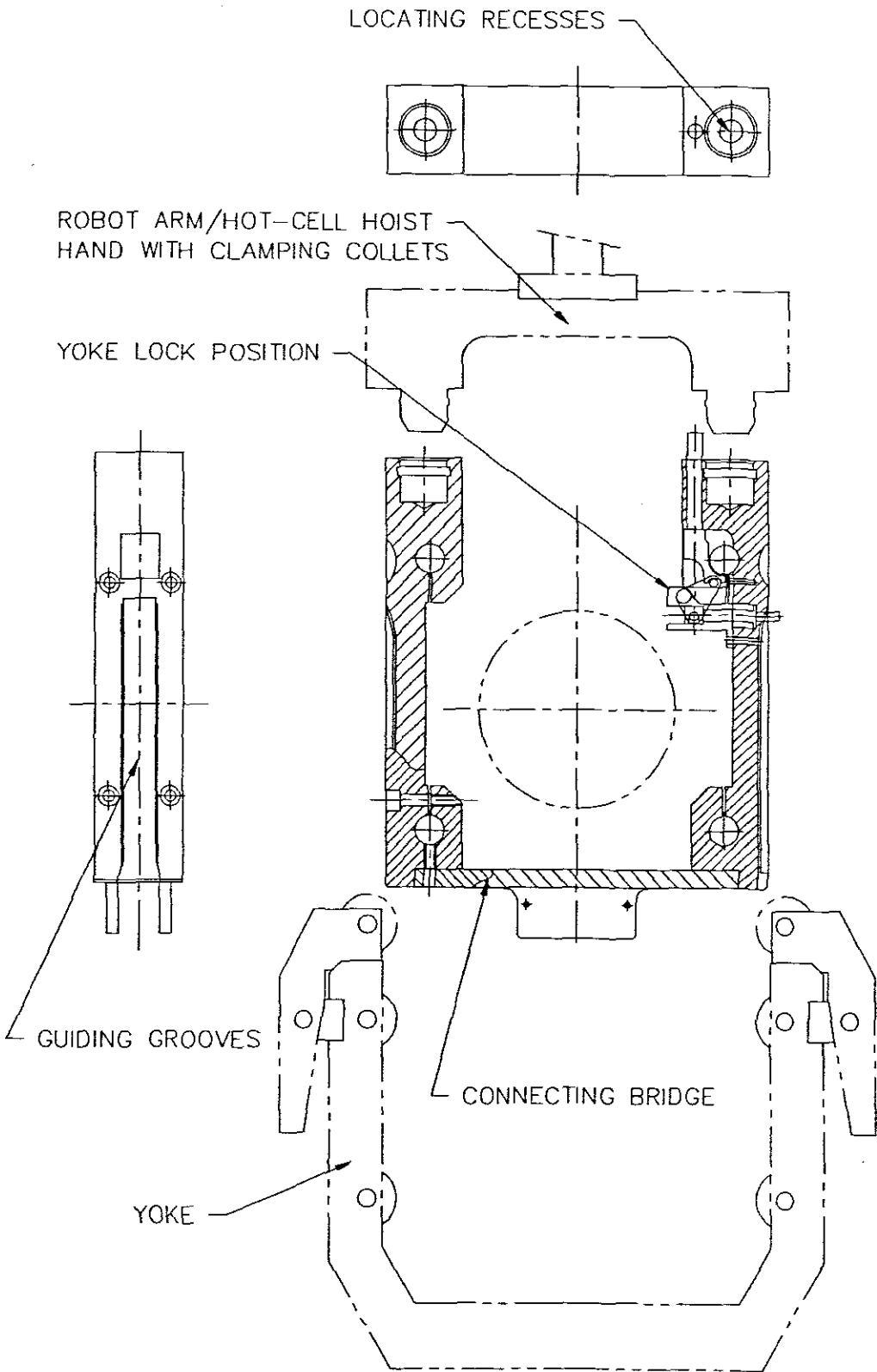
Fig. 25: *Yoke guides.*

4.2.2.5.1   *Yoke Lock*

Once the target is positioned in one of the yokes, spring loaded rollers on the yoke arms are located in semi-circular recesses on the guide columns. The spring loaded rollers keep the target in position whilst in motion, but when the target is in an inverted position and is exposed to excessive vibration, there is the danger of it being released from the rollers and dropping out of the yoke. For this reason a yoke lock was designed (see Fig. 26). It functions in such a manner that when the target is in position in the yoke, a spring loaded locking pin locks the target to the yoke arms. When the robot arm or hoist is coupled to the target, a release pin releases the locking pin from the yoke arm, thus enabling the extraction of the target from the yoke.

4.2.2.6   Valves

The target valves which form part of the coupling valves (see par. 4.2.7) are mounted on 1/4" stainless steel inlet and outlet tubes which curve down towards the top and bottom half of the target respectively. These tubes are welded into the cooling jacket and inner vessel and then open into the spray nozzles and drain respectively.

The target valves are subjected to a sealing load of 110 N (see par. 4.2.7) and a simple loading test on the curved tubes indicated that their strength was more than adequate to carry the load.

4.2.2.7   Struts

Factors to consider due to pusher arm loading on the struts are the buckling load, stress induced and axial deformation. The following symbols and values are of relevance to this discussion:

Target pusher arm force $=$ 5 800 N
Number of struts $=$ 4
Material: Stainless steel, Gr 316

F = force on each strut $=$ 1 450 N
A = strut cross sectional area
L = length of strut $=$ 202 mm
ΔL = axial deformation
D = diameter of strut $=$ 10 mm

RELEASE PIN

CAM

SLIDING MECHANISM

COIL SPRING

LOCKING PIN
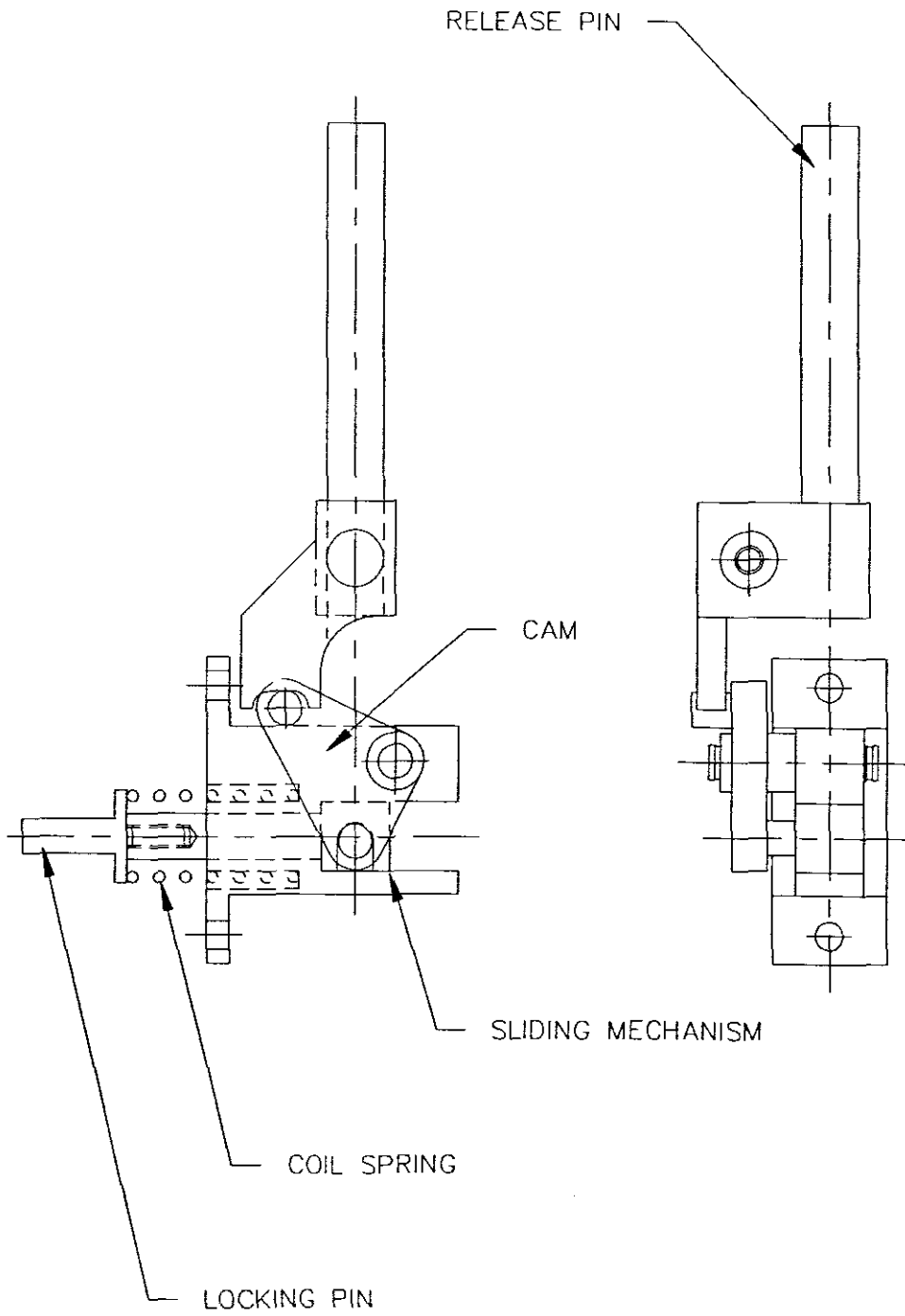
Fig. 26:   *Yoke lock.*

I   = moment of inertia

P   = buckling load

k   = radius of gyration

L_E = equivalent length of strut

E   = Young's modulus = 195 GPa [Jac86]

σ_U = ultimate tensile strength = 580 MPa [Jac86]

σ_y = yield stress = 310 MPa [Jac86]

S   = slenderness ratio

ϵ = strain

σ = stress

Buckling of struts [Hea89]:

In order to calculate the buckling load, the following values first need to be calculated:

Moment of inertia:

$$
\begin{aligned}
I \quad &= \frac{\pi}{64} D^4 \\
&= \frac{\pi \times 10^4}{64} \\
&= 490{,}87 \text{ mm}^4
\end{aligned}
$$

Cross-sectional area of strut:

$$
\begin{aligned}
A \quad &= \frac{\pi}{4} D^2 \\
&= \frac{\pi}{4} 10^2 \\
&= 78{,}54 \text{ mm}^2
\end{aligned}
$$

Equivalent length of strut:

$$
\begin{aligned}
L_E \quad &= \frac{L}{2} \text{ (both ends fixed)} \\
&= \frac{202}{2} \\
&= 101 \text{ mm}
\end{aligned}
$$

Radius of gyration:

$$k = \sqrt{\frac{I}{A}}$$

$$= \sqrt{\frac{490,87}{78,54}}$$

$$= 2,499 \text{ mm}$$

Slenderness ratio of strut:

$$S = \frac{L_E}{k}$$

$$= \frac{101}{2,499}$$

$$= 40,416$$

As $\dfrac{L_E}{k} < 120$ the strut is intermediate, therefore the Rankine formula is used:

$$P = \frac{\sigma_U A}{1 + a\left[\dfrac{L_E}{k}\right]^2}$$

where a is a numerical constant, given by:

$$a = \frac{\sigma_U}{\pi^2 E}$$

$$= \frac{580}{\pi^2 \times 195 \times 10^3}$$

$$= 3,014 \times 10^{-4}$$

Thus the buckling load is given by:

$$P = \frac{580 \times 78,54}{1 + 3,01 \times 10^{-4} \times 40,416^2}$$

$$= 30538,4 \text{ N}$$

Stress induced:

Normal stress due to loading:

$$\sigma \quad = \frac{F}{A}$$

$$= \frac{1450}{78,54}$$

$$= 18,46 \ N/mm^2$$

Axial deformation:

$$\varepsilon \quad = \frac{\sigma}{E}$$

$$= \frac{18,46}{195 \times 10^3}$$

$$= 9,467 \times 10^{-5}$$

$$\Delta L \quad = L \times \varepsilon$$

$$= 202 \times 9,467 \times 10^{-5}$$

$$= 0,019 \ mm$$

4.2.3   Spray System

From previous similar krypton gas target experiments overseas it was found that after bombardment the Rb was deposited on the vessel inner surface, but that a percentage was also still in suspension in the gas for at least two hours [Wat86].

Rubidium, being an alkali metal, oxidizes when coming in contact with water and the rubidium-oxide is readily dissolvable in water [Bjo84]. The most simple method to solve the problem of retrieving the Rb isotopes therefore seemed to be the use of an effective water jet spray system inside the vessel.

Before the investigations into the design began, certain factors had to be considered:

(1) The spray system should not intercept any part of the beam during bombardment.

(2) The spray system should be sufficiently water cooled due to heat build-up of the gas inside the vessel during bombardment.

(3) The spray should cover the maximum possible internal area/volume of the vessel for maximum Rb retrieval.

(4) The spray should have sufficient force to remove the Rb isotopes from the vessel inner surface.

Taking all these factors into consideration, a design making use of small spray nozzles was deemed the best solution (see Fig. 27). Various combinations of nozzles were experimented with and eventually the most effective one was selected: Two solid cone spray nozzles at the side quadrants covered the sides and centre and, partially, the top and bottom areas of the vessel. A flat spray nozzle at the top quadrant covered the top and front areas of the vessel. Another flat spray nozzle at the top quadrant covered the rear area of the vessel.

All the nozzles were linked by a specially profiled pipe which made good physical contact with the vessel inner surface for cooling purposes. The whole structure was fully welded together.

In order to test the effect of the spray nozzles under working conditions, a perspex model was manufactured so that it could be monitored visually. This originally enabled the positions and angles of spray to be determined experimentally in order to achieve maximum spray coverage. The process was further assisted by adding a red liquid dye to the water to make it more visible.

To clarify the rinsing cycle, let us look at the relevant steps in the process:

(1) After bombardment the gas is released to the reservoir via the stainless steel mesh filter, cryopump and coalescing filter. Radioisotopes in the gas should be trapped on the mesh filter and inner surfaces of the target and the pipe leading up to the filter.

INLET PORT

SOLID CONE NOZZLES

OUTLET PORT

INNER VESSEL
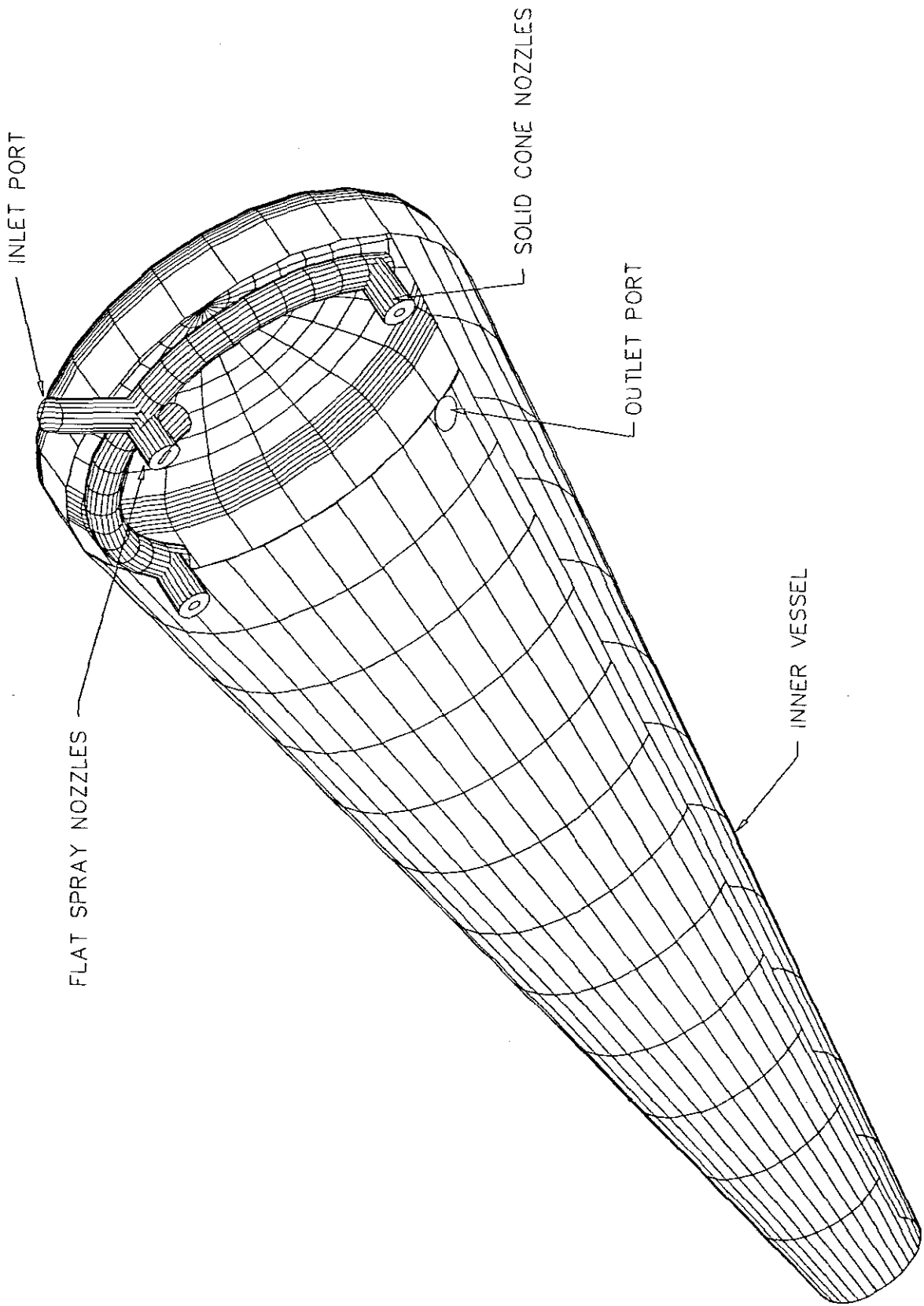
FLAT SPRAY NOZZLES

Fig. 27: *Spray nozzle arrangement.*

(2) The relevant valves are operated and 100 m*l* of distilled water is extracted into the circulating pump.

(3) When the pump advances, water flows via the cryopump, through the mesh filter, through the nozzles, onto the inner surfaces and finally settles on the bottom half of the vessel.

(4) When the pump retracts, water flows through the outlet port of the vessel and accumulates in the pump again.

(5) This cycle is repeated numerous times until all radioisotopes are satisfactorily removed from the mesh filter and inner surfaces.

(6) The product can then be drained.

Originally, suitable spray nozzles were difficult to obtain and, considering their complex design, were also difficult to manufacture. Eventually the problem was solved by importing spray nozzles and locally modifying their housings to suit. The solid cone spray nozzles selected produced 60° solid angles at 600 kPa. The flat spray nozzles selected produced standard spray angles of 90°.

The circulating pump delivers a pressure of approximately 600 kPa to the inlet of the spray nozzles and this pressure can be monitored on the compound gauge between the cryopump and coupling valves. If the pumping pressure increases to an abnormally high value, it would mean that either the coupling valves are closed (which can easily be checked) or that the nozzles have become blocked. This is unlikely, as the rubidium is in molecular suspension and should not change the fluid viscosity or adhere to the nozzle orifice (the high flow rate should prevent this occurrence). Dirt or impurities may, however, enter from the distilled water vessel outlet if the mesh filter is ineffective and possibly cause a blockage. To remove the blockage, high pressure water may be introduced alternatively to the inlet and outlet target coupling valves.

If the pumping pressure drops, it could mean that either insufficient water was extracted or that the pump has not primed properly. The extraction volume can be checked by monitoring the distilled water extracted from the graduated supply vessel. The pump should be allowed to operate through a few cycles before priming itself.

4.2.4   Circulating Pump

A water pressure of at least 500 kPa is required for the effective operation of the spray nozzles. Generally, standard pumps delivering this pressure are of a bulky construction and are costly. A further investigation indicated that continuous flow pumps would be unsuitable, because only 100 m*l* water is required in the system (a convenient volume to pump through the peristaltic pump and divide between the generators) and this low volume would result in water accumulation in the vessel and hence a large drop in pressure. Contamination of the Rb must also be avoided and therefore the pump's wetted parts should be manufactured from stainless steel or a similar material. The simplest solution to these problems was to design and manufacture a piston pump to the exact specifications.

The general design of the circulating pump consists of a pneumatic cylinder which operates a plunger in a barrel, with check valves controlling flow direction at the inlet and outlet ports (see Fig. 28). A barrel volume of 100 m*l* was chosen for the previously mentioned convenience of subsequent processing of the fluid. The barrel was manufactured from Gr 316 stainless steel and the plunger used was a standard Festo cylinder seal made from Perbunan. The check valves used were standard Nupro stainless steel check valves which have cracking pressures of 1/3 PSI (2,3 kPa). The plunger seal and check valve O-rings, although being relatively radiation resistant, are in direct contact with the radioactive product and do experience radiation damage. Their total radiation dose therefore has to be monitored, and they should be replaced before the recommended maximum dose for the materials are exceeded.

The product fluid in contact with the Perbunan seal will have an activity of ~ 1 Rad/hr [Ste90]. The safe dose for Perbunan = 2×10^6 Rad (see Table 2).

The maximum exposure period therefore = 2×10^6 hrs.

From this figure, it can be seen that the radiation damage is negligible.

Two aluminium side plates brace the barrel to the pneumatic cylinder and a nylon guide on the cylinder shaft activates two pneumatic limit switches on the one side plate which make provision for automatic pumping. A mounting bracket is also connected to one side plate for mounting the pump onto the hot-cell rear panel.

PNEUMATIC CYLINDER

ALUMINIUM SIDE PLATES

LIMIT SWITCHES

MOUNTING BRACKET

NYLON GUIDE

ST.STEEL BARREL

CHECK VALVES

PLUNGER

BARREL BASE
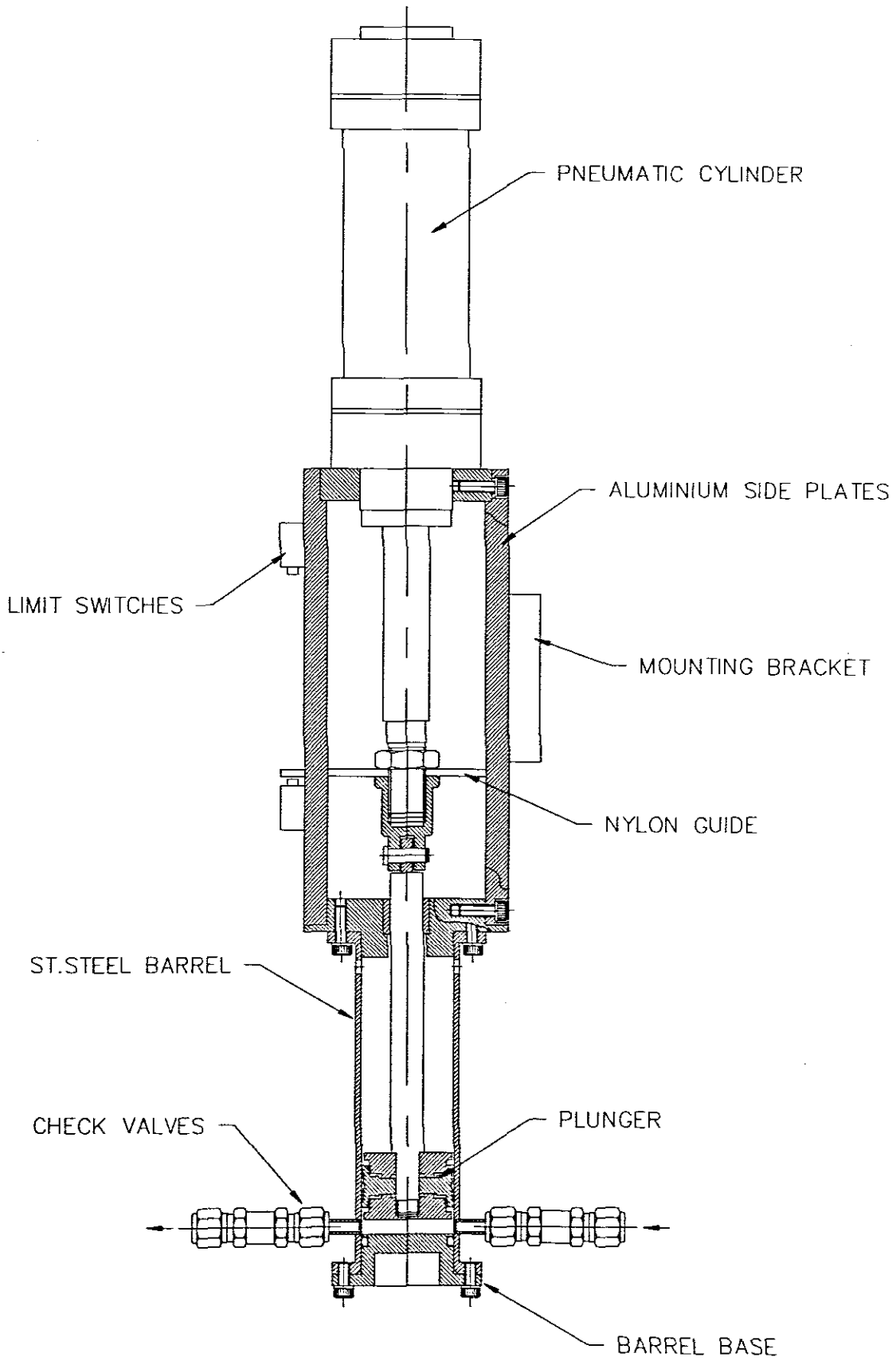
Fig. 28: *Circulating pump.*

A vacuum and internal hydrostatic pressure test of 1000 kPa was carried out successfully on the assembled barrel.

Calculation of pneumatic cylinder size:

A pressure of 600 kPa is required at the nozzles, therefore it was assumed that a static pressure of 800 kPa at the barrel outlet was a reasonable estimate. The 40 mm diameter plunger would therefore be subjected to this static pressure. Furthermore, the friction on Perbunan seals at 40 mm diameter is approximately 4% [Fes90].

Thus, pump advance force F required:

$$F = P \times A \times (1 + 0.04) \qquad (\text{where } P = \text{pressure, } A = \text{area})$$
$$= 0.8 \times \frac{\pi}{4} \times 40^2 \times 1.04$$
$$= 1050.7 \text{ N}$$

A Festo cylinder DN-50-80 PPV, having an advance force of 1130 N at 600 kPa, was therefore used.

The construction of the pump is such that the cylinder, together with the plunger and shaft, can easily be removed for maintenance and servicing.

4.2.5 Cryogenic Pump

In order to pump all the krypton gas from the reservoir into the target vessel at 1400 kPa, expensive and sophisticated standard gas pumps could be purchased. A reliable alternative method would be to use a cryogenic pump. However, standard cryogenic pumps are also too sophisticated, large and costly, and therefore a decision was made rather to use the basic cryogenic principle to design and develop a suitable pump for this specific application.

The system finally developed merely operates in such a way that the krypton from the gas reservoir is frozen onto the internal walls of the cryopump (which is a tube or vessel inserted in liquid nitrogen). Directional valves are then actuated and the gas is heated and released to the smaller volume of the target. A higher pressure due to the smaller volume can thus be achieved in the target. The cryopump must have sufficient internal volume to accommodate the frozen gas. A prototype cryopump

tube was manufactured in order to investigate this principle and the results are documented in par. 5.2.1. The transferring of the gas back to the reservoir follows the same pumping principle, but in reverse. However, there will be a small volume of gas contained in the line between the gas reservoir and cryopump which cannot be further pumped and must be accepted as a loss. This volume is eventually mixed with the distilled water during the rinsing cycle.

An additional feature to increase the heating rate of the cryopump, was to include a compressed air heater. It simply consisted of a 1/4" stainless steel tube mounted next to and following the same U-shaped profile as the cryopump. The tube has a series of 1 mm holes drilled along its length which are all directed at the cryopump. Compressed air blowing through these holes results in total vaporization of the krypton gas in ~ 4 minutes.

When the cryopump is inserted into the liquid nitrogen dewar, a vast amount of splashing occurs due to the LN_2 immediately boiling as a result of the rapid heat exchange. To prevent this splashing, a Tufnol dewar cover was manufactured and clamped onto the cryopump. A vent pipe was mounted on the dewar cover to serve as a pressure relief.

Another item that was necessary to incorporate, was a LN_2 filling baffle. When the dewar is filled from the main supply dewar, the LN_2 enters at a high flow rate also causing excessive splashing. The baffle reduces this flow considerably and allows the operator to fill the dewar up to the required brim level. The baffle was mounted onto the hot-cell panel and insulated with Thermaflex insulation. All pipes linking the main supply dewar to the cryopump dewar were also insulated with Thermaflex insulation.

For the cryopump design, the volume, gas pressure, stresses, maximum operating pressure rating and characteristics at sub-zero temperatures needed to be investigated:

<u>Volume</u>:

Stainless steel (Gr 304) seamless tubing with dimensions 12,7 mm OD × 10,7 mm ID was selected for the cryopump (see Fig. 29). A larger inner diameter, compared to the 6,35 mm OD × 4,8 mm ID tubing for the rest of the system, provides a larger surface area so as to facilitate the freezing of the gas on the inner walls. A U-shaped in-line
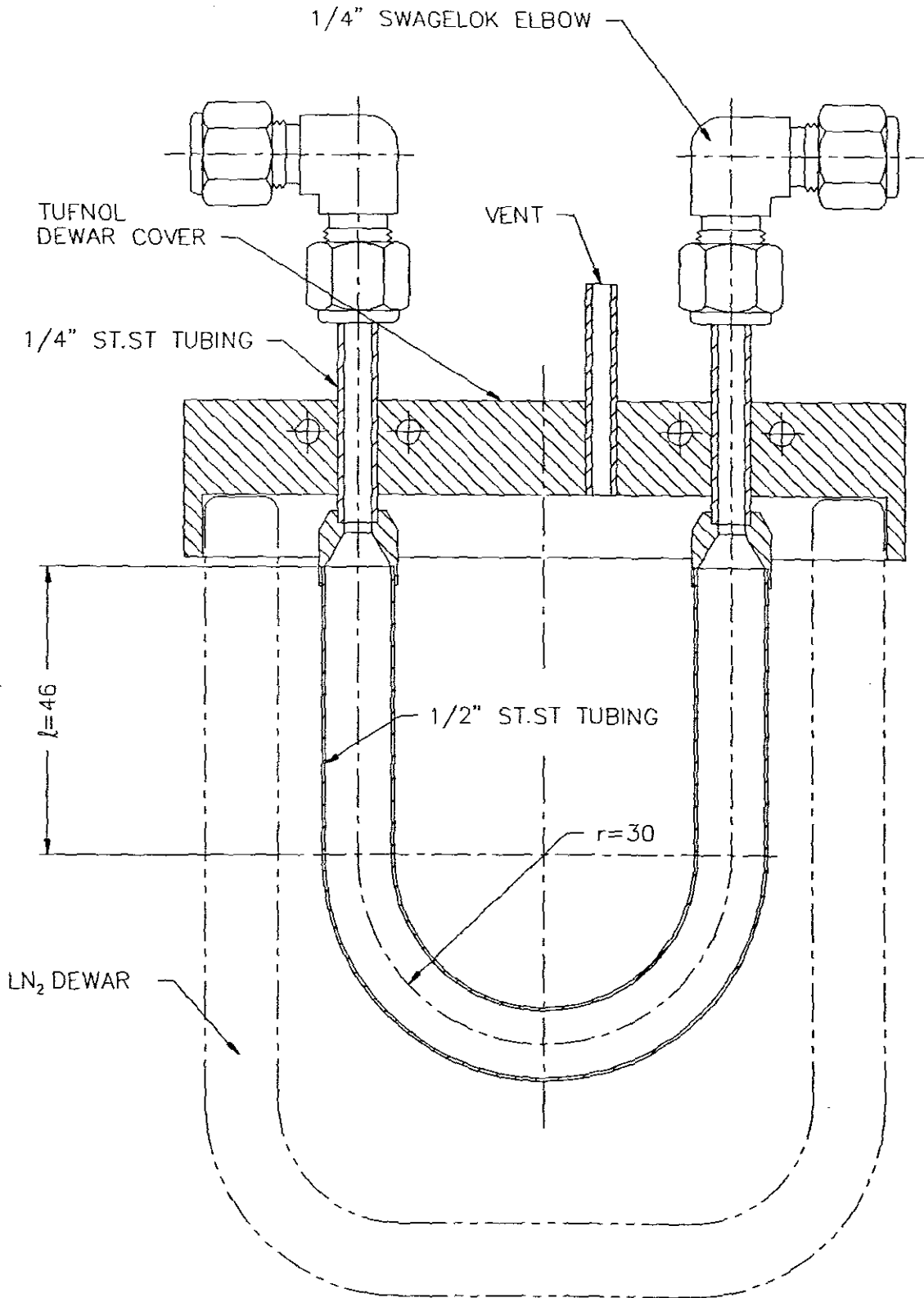
Fig. 29:   *Cryogenic pump.*

configuration was chosen, so that during the rinsing cycle all surfaces are efficiently rinsed. Convenient dimensions of the U-tube leg ($l = 46$ mm) and bend radius ($r = 30$ mm) were selected in order to provide sufficient clearance inside the liquid nitrogen dewar.

Thus, total length of tube:

$$L = l \times 2 + r\theta$$

$$= 46 \times 2 + 30 \times \pi$$

$$= 186,3 \text{ mm}$$

Therefore, cryopump volume:

$$V_C = \frac{\pi}{4} \times 10,7^2 \times 186,3$$

$$= 0,01675 \text{ dm}^3$$

$$= 16,75 \text{ m}l$$

In order to ensure that the volume V_C of the cryopump will accommodate the krypton, the volume V_k of the frozen krypton gas had to be calculated:

Krypton density @ $0°$C $= 3,733$ g/l [Crc87]

Krypton density @ $20°$C $= \dfrac{3,733 \times 273}{273 + 20}$

$$= 3,478 \text{ g}/l$$

Krypton density @ $-152,9°$C $= 2155$ g/l [Crc87]

Mass of gaseous state $=$ Mass of non-gaseous state

$$3,478 \times 7 = 2155 \times V_k$$

Therefore:

$$V_k = 0,0113 \text{ } l$$

$$= 11,3 \text{ m}l$$

Thus:

$$V_C > V_k$$

Gas pressure:

In the final system, 7 l of krypton gas is cryopumped from the gas reservoir, at 100 kPa (abs), to the gas target of inner volume 0,5 l. To calculate the exact pressure P_2 with the target fully filled with gas, the cryopump and tubing volumes have to be added to the target volume, because they are also in the system line and subjected to the same pressure.

Thus:

$$P_1V_1 \text{ (reservoir)} = P_2V_2 \text{ (target, cryopump and tubing)}$$
$$100 \times 7 = P_2 \times (0,5 + 0,0168 + \tfrac{\pi}{4} \times 0,048^2 \times 8) \qquad (1 \text{ dm}^3 = 1 \, l)$$

Therefore:

$$P_2 = 1317,6 \text{ KPa (abs)}$$

A higher pressure in the target can easily be obtained by filling the gas reservoir to a pressure above 100 kPa (abs). For example, with an initial pressure of 113,8 kPa (abs) in the gas reservoir, the target is filled to the required 1400 kPa (see par. 4.1) gauge pressure.

Stresses:

It was decided to machine the cryopump tube outside diameter down by 1 mm for two reasons:

(1)   For ease of bending, because a tight bend radius is called for.

(2)   To facilitate better heat transfer through the material, as stainless steel has a low thermal conductivity of 15,7 W/m· C [Jac86].

The thin wall thus demanded an investigation into the strength of the tube:

d   = tube diameter = 10,7 mm

p   = gas pressure = 1318 kPa

t   = wall thickness = 0,5 mm

σ_u = ultimate tensile strength = 600 MPa [Jac86]

σ_y = yield stress = 310 MPa [Jac86]

Circumferential stress:

$$\sigma_H = \frac{pd}{2t}$$

$$= \frac{1,318 \times 10,7}{2 \times 0,5}$$

$$= 14,1 \text{ MPa}$$

Thus:

$$\sigma_H \ll \sigma_y$$

Maximum operating pressure rating:

Factor of safety used: 1,5

Therefore, maximum allowed operating stress $\sigma_{max} = \frac{310}{1,5} = 206,7$ MPa

The maximum operating gas pressure thus is:

$$p_{max} = \frac{2t\sigma_{max}}{d}$$

$$= \frac{2 \times 0,5 \times 206,7}{10,7}$$

$$= 19318 \text{ kPa}$$

Sub-zero temperature characteristics:

Since the stainless steel will be in direct contact with liquid nitrogen (LN_2), during gas freezing, the material properties at sub-zero temperatures also had to be investigated:

LN$_2$ boiling point: 77,4 K (–195,6 °C) @ 101,3 kPa [Crc87]

LN$_2$ freezing point: 63,2 K (–209,8 °C) @ 101,3 kPa [Crc87]

The stainless steel will therefore be exposed to a temperature of ~ 70 K, and if the temperature/yield stress graph in Fig. 30 is examined, it can be seen that the yield stress at this temperature increases to ~ 1350 MPa.

On examining the temperature/thermal conductivity graph in Fig. 31, it can be seen that the thermal conductivity of the material at ~ 70 K decreases to ~ 7 W/m°K (7 W/m°C). The thermal conductivity of stainless steel (Gr 304) at 25°C is 15,7 W/m°C [Jac 86].

4.2.6   Gas Reservoir

The design of the gas reservoir makes use of a stainless steel tube (Gr 316) of standard dimensions 129 mm OD × 2 mm thick (see Fig. 32). Both ends are closed by means of stainless steel blank flanges and sealed with Viton O-rings. Access for cleaning and inspection is therefore easily achieved.

The advantage of using a large volume reservoir (7 ℓ) is that storage at a low pressure is possible and that the gas loss during pumping is therefore minimal. The gas loss referred to here is the gas remaining in the tube and cryopump when the gas is transferred back to the reservoir (see par. 4.2.5). At 100 kPa pressure (abs), this loss is very small (~ 0,36%) and the gas in the reservoir will therefore only have to be replenished from the krypton gas bottle when a noticeable drop in the reservoir pressure is observed. The gas depletion rate during bombardment is negligible. For a 30 minute irradiation at 60 μA beam current, it is calculated to be only 7,206 × 10^{-6}% of the total gas volume [Ste90].

The 7 ℓ of gas which needs to be frozen onto the cryopump (see par. 4.2.5), would be contained both in the reservoir and in the reservoir pipes and fittings up to the isolating valve. The volumes in the pipes, fittings and reservoir therefore needed to be calculated in order to determine the reservoir length L:

Volume in pipes and fittings:

$$V_p = \frac{\pi}{4} \times 0,048^2 \times 6,28 \qquad (1 \text{ dm}^3 = 1 \text{ } \ell)$$

$$= 0,011 \text{ } \ell$$

2000

1800

1600

1400

1200

1000

800

600

400

200

O

Yield stress, MPa

(5)

(4)

(3)

(2)

(7,9)

(6)

(1)

(8)

0   50   100   150   200   250   300   350

Temperature, K
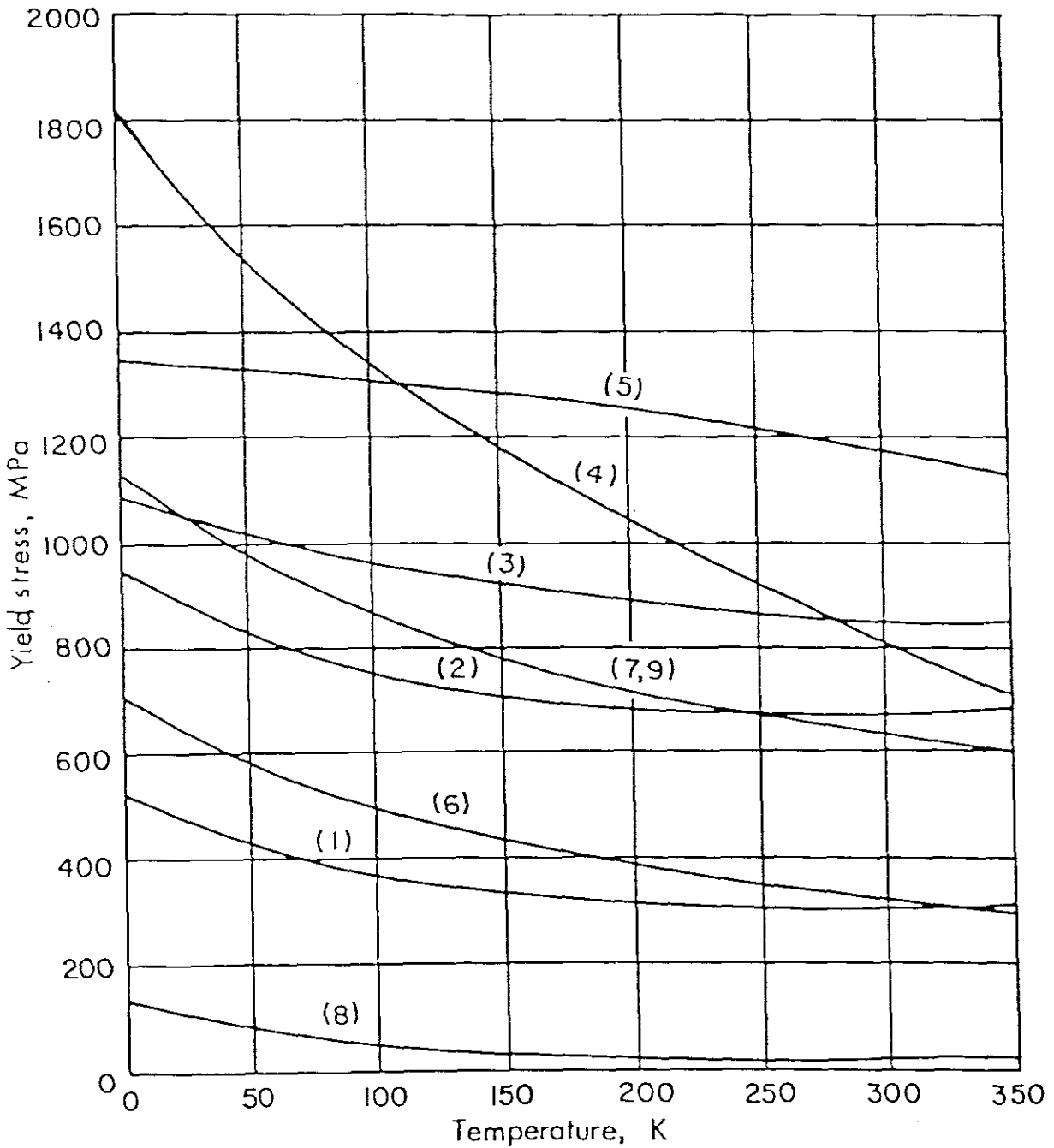
Fig. 30:   *Yield strength for several engineering materials [Bar85]:   (1) 2024-T4 aluminium,   (2) beryllium copper,   (3) K Monel,   (4) titanium   (5) 304 stainless steel,   (6) C1020 carbon steel,   (7) 9 percent Ni steel,   (8) Teflon, (9) Invar-36.*
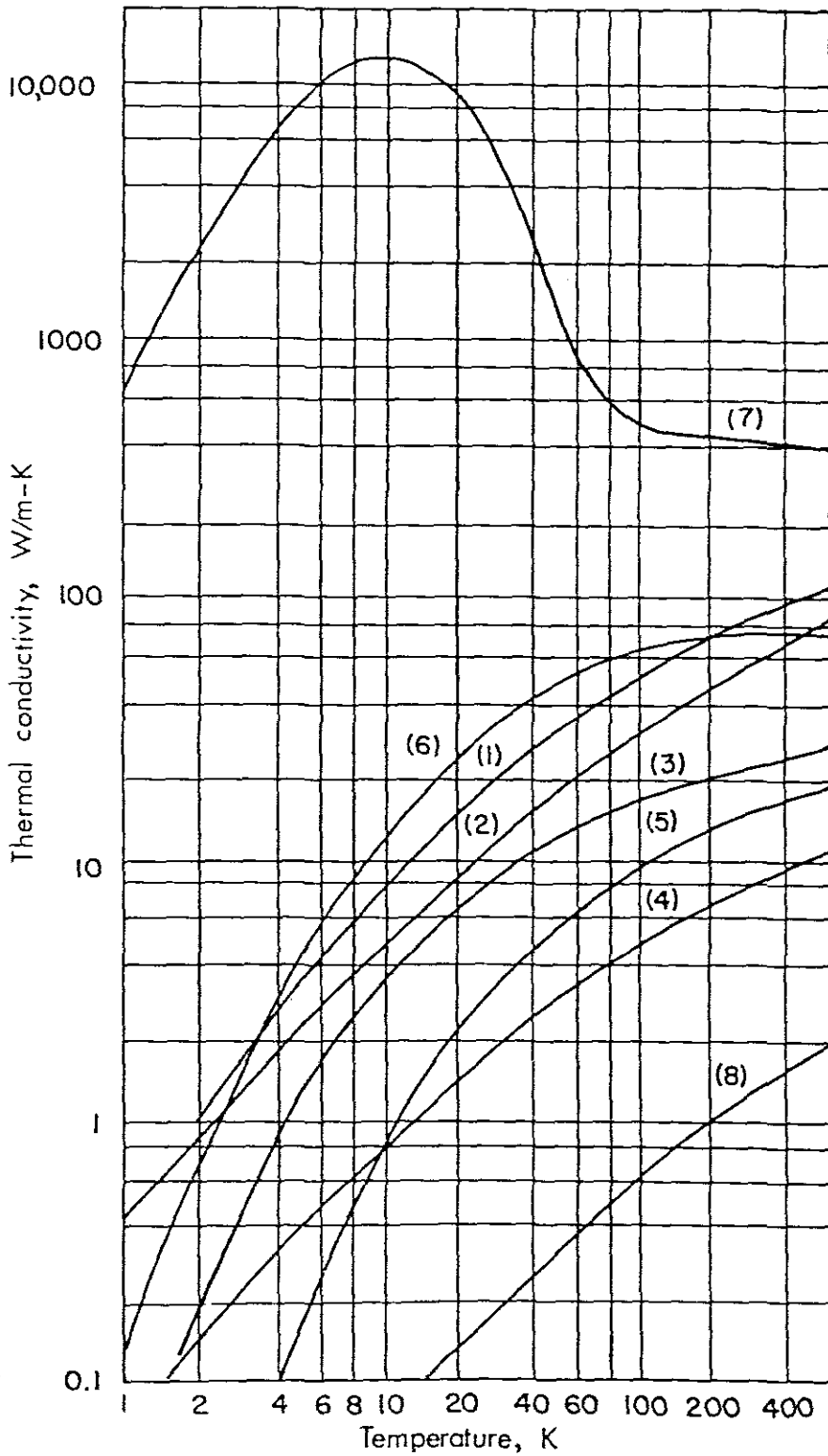
Fig. 31: *Thermal conductivity of materials at low temperatures [Bar85]: (1) 2024-T4 aluminium, (2) beryllium copper, (3) K Monel, (4) titanium, (5) 304 stainless steel, (6) C1020 carbon steel, (7) pure copper, (8) Teflon.*

PRESS.SWITCH

COMPOUND GAUGE

MOUNTING BRACKET

PRESS.RELIEF VALVE

GAS BOTTLE PORT

CRYOPUMP PORT
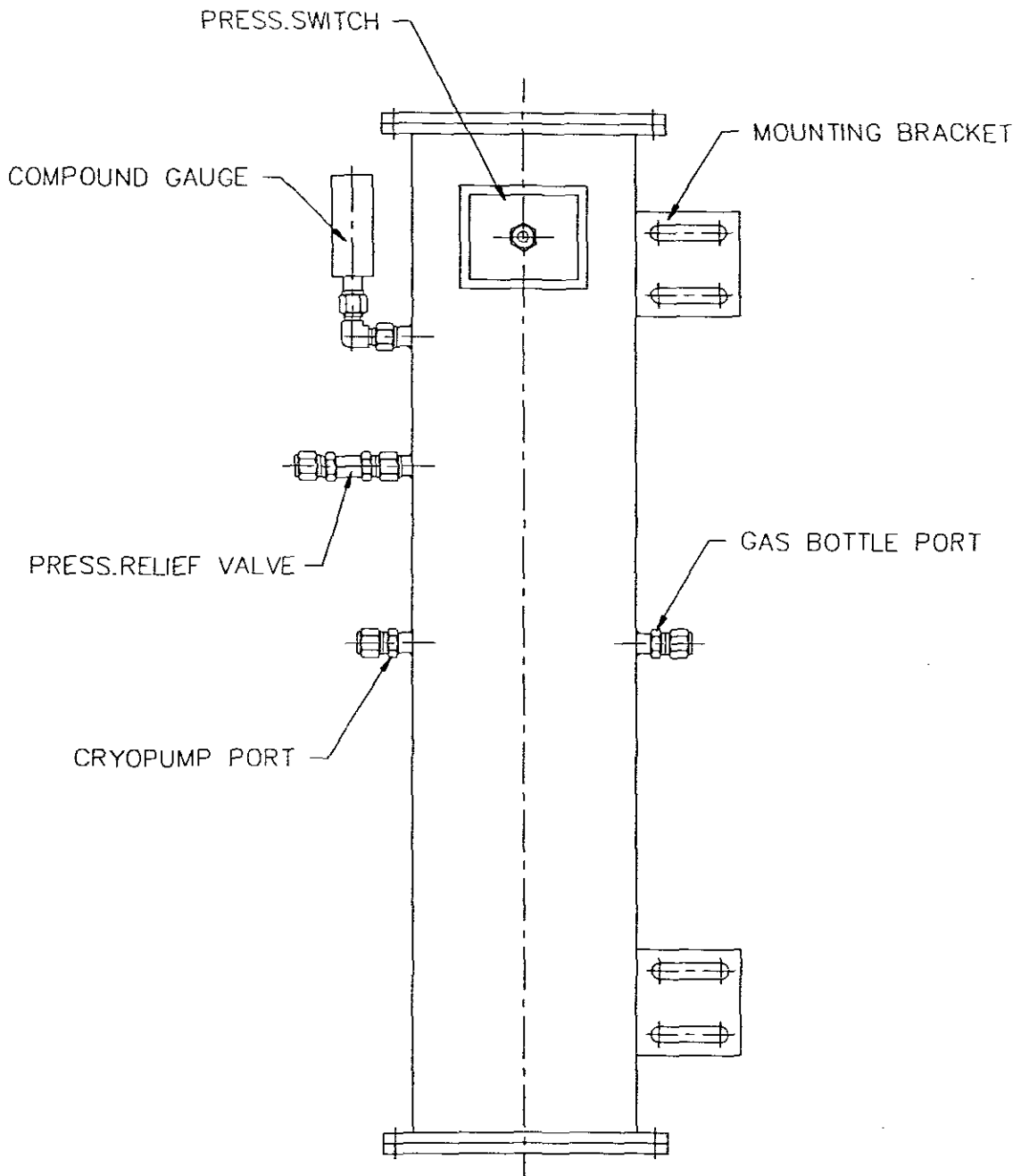
Fig. 32: *Gas reservoir.*

Therefore, volume in reservoir:

$$V_r = 7 - 0,011$$
$$= 6,99 \; \ell$$

Reservoir length L can thus be calculated:

$$V_r = A \times L \qquad \text{(where A = area)}$$
$$6,99 = \frac{\pi}{4} \times 1,25^2 \times L$$
$$L = 569,6 \; mm$$

The port fittings selected were standard fittings, namely 1/4" Swagelok weld ends [Swa88]. The inlet and outlet ports are connected to the gas supply line and cryopump line respectively. A compound pressure gauge (Wika: -100 to +300 kPa) is mounted on one mounting port, a pressure switch (Asco: -100 to +100 kPa) on another and a pressure relief valve (Nupro) on the third.

Under normal operating conditions, the gas reservoir is filled to a pressure slightly above 100 kPa (abs) (see par. 4.2.5) to achieve an operating pressure of 1400 kPa in the target. In principle, the gas reservoir can be used with pressures up to 200 kPa, should higher pressures in future targets be required.

4.2.7   Coupling Valves

The most practical method of coupling the target to the rest of the processing system is to have one set of valves on the target itself and one set of valves on the processing system. The system valves can then be advanced or retracted in order to couple or de-couple with the target valves. High-pressure flexible lines between the system coupling valves and the processing system can be incorporated in order to compensate for this movement.

The acquisition of standard commercial valves for this purpose proved problematic, as they are generally very complicated in design and operation, expensive and too large for the design under consideration. Small, robust Nupro plug valves were finally selected. They had to be modified and adapted, however, in order that they could remotely be coupled to one another (see Fig. 33). One face of each valve set was machined down, and the system valve face additionally housed an O-ring to seal the two faces when coupled.

PNEUMATIC ROTARY ACTUATORS

ROTARY COUPLING

VALVE PLUG

TARGET VALVE

MACHINED FACES

SYSTEM VALVE
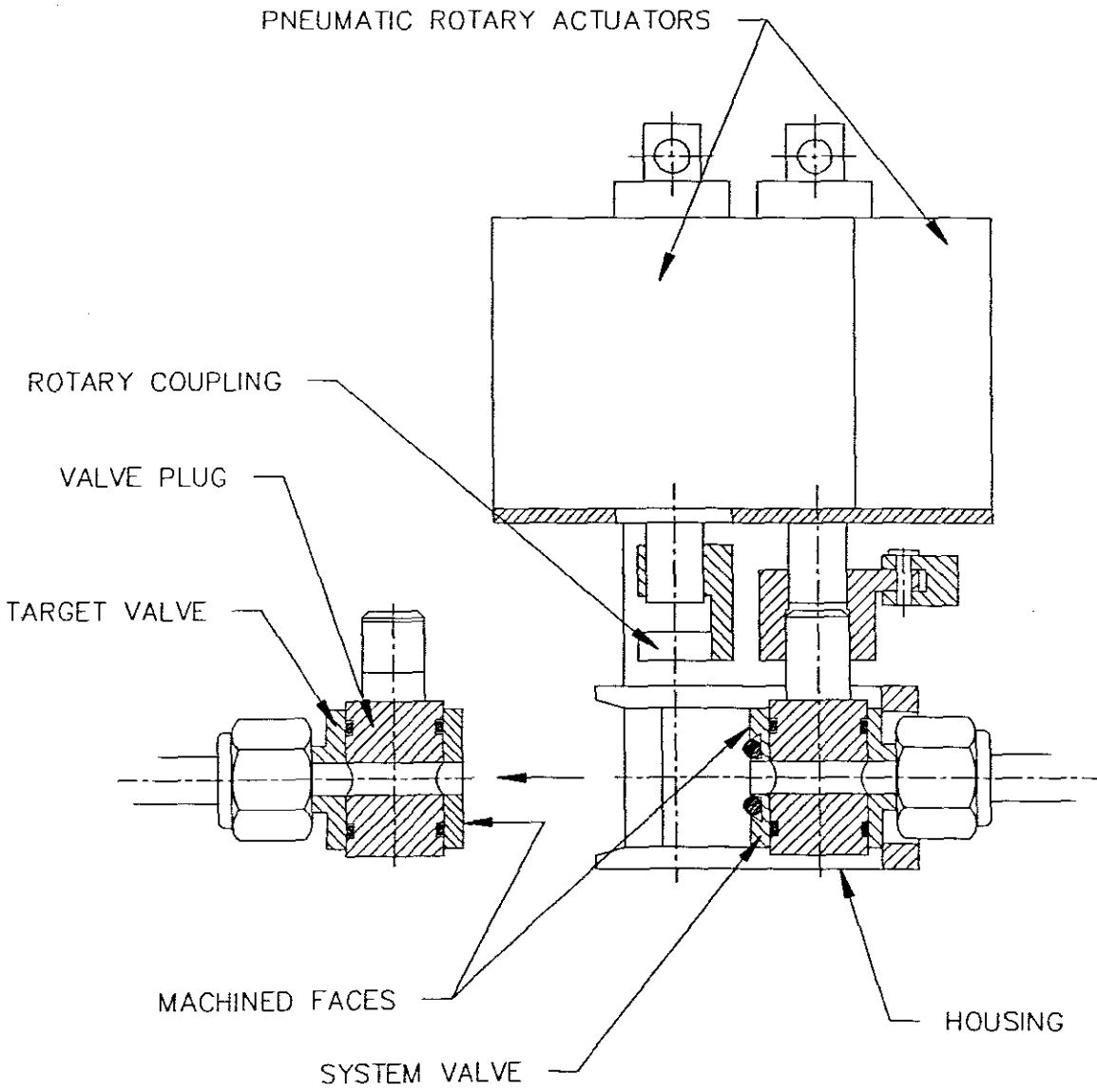
HOUSING

Fig. 33: *Coupling valves.*

The system valve is mounted in a housing which aligns itself onto the target valve. The housing also consists of two pneumatic rotary actuators which actuate both valves independently when coupled. Festo pneumatic actuators were utilized because of their reliability and compactness.

The flexible line selected was a standard Festo 1/4" polyamid tubing which has a maximum operating pressure rating of 2700 kPa. In order to check the durability and flexibility of the tubing, a simple operating test jig was manufactured. The tubing was operated through 3000 cycles and a pressure test of 2500 kPa was performed.

The coupling and de-coupling of each system valve is operated by means of two pneumatic cylinders (see par. 4.2.8).

4.2.8 Pneumatic System

All the gas control valves in the krypton gas system are operated by means of Festo pneumatic rotary actuators, which are in turn controlled by solenoid operated pneumatic control valves (see Fig. 34). This is a very positive and reliable actuating system with the added advantage that the actuators can be manually overridden in case of a power failure. The gas control valves selected were standard 1/4" Nupro plug valves.

The up and down actuation of the liquid nitrogen dewar of the cryopump is controlled by means of a twin-rod cylinder in order to prevent rotation without having to manufacture a special guiding system for this purpose. Flow control valves were included to retard the cylinder movement in order to prevent LN_2 spillage. The circulating pump's operating cylinder is controlled manually or automatically, and these operations are also carried out with pneumatic circuitry as indicated in Fig. 34. The cryopump heater (see par. 4.2.5) is operated by means of a simple pneumatic control valve on/off actuation.

The coupling and de-coupling of the system coupling valves, as previously mentioned, are both operated by means of a pair of pneumatic cylinders. These particular cylinders were selected for their compactness and their ability to seal the coupling valves under the system operating pressure of 1400 kPa.

85
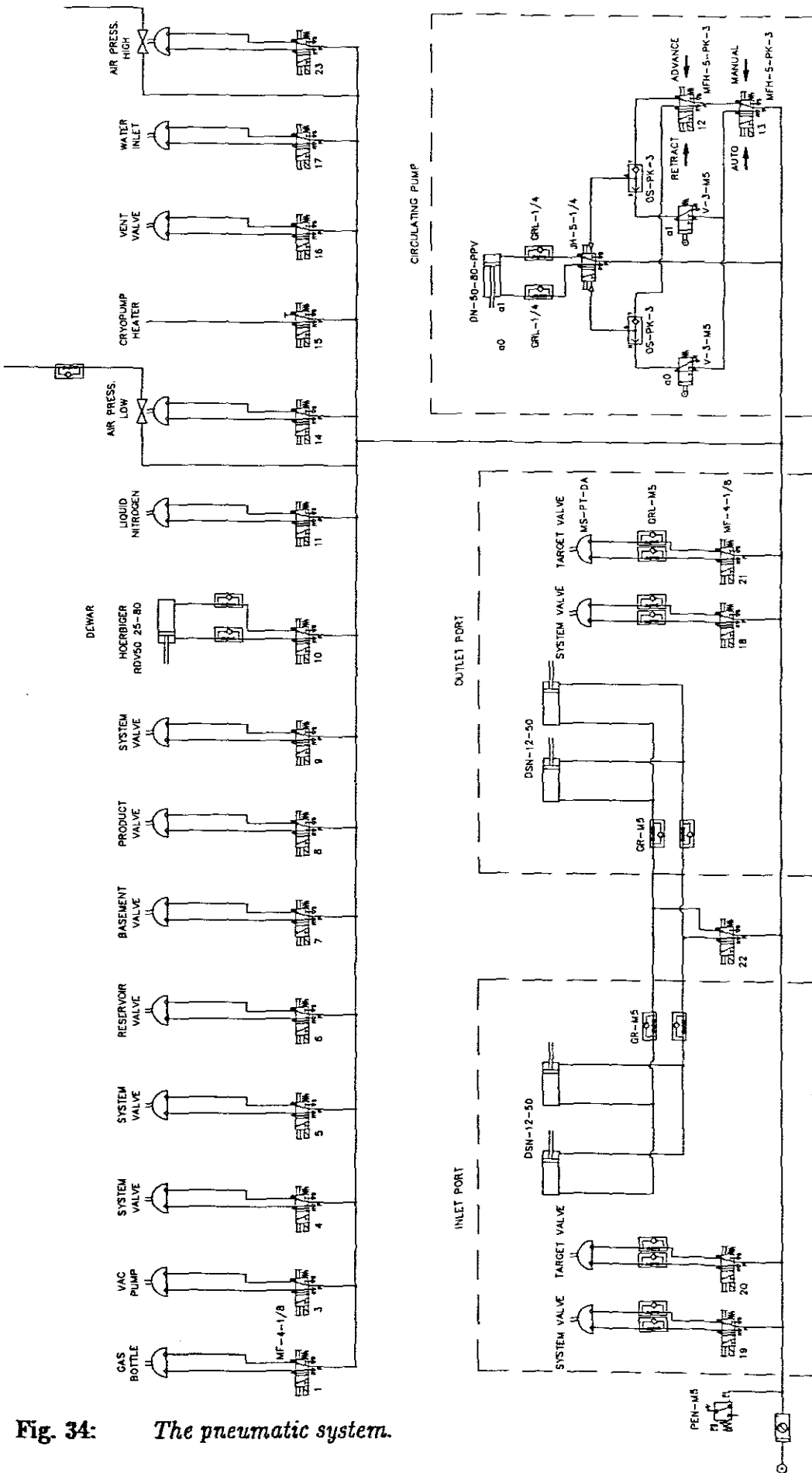
Fig. 34:   *The pneumatic system.*

The cylinder selection had to be investigated:

Valve face O-ring: Parker 2-107: 5,23 ID × 2,62 dia (mean dia = 7,8 mm)
System operating pressure: 1400 kPa
System design pressure: 2200 kPa

Force F on O-ring face due to internal gas design pressure:

$$F = P \times A \qquad \text{(where P = pressure,\ \ A = area)}$$

$$= 2{,}2 \times \frac{\pi}{4} \times 7{,}8^2$$

$$= 105{,}1 \text{ N}$$

Therefore, cylinder selected: Festo DSN 12-50-P (55N advance force @ 600 kPa)

Thus total cylinder force on O-ring = 55 × 2
$$= 110 \text{ N}$$

The minimum pressure on these cylinders is critical and therefore a pressure switch was incorporated in the compressed air supply line. A pressure drop below the switch setting will send an electrical signal to the control system, which in turn will send a signal to close the coupling valves in order to avoid gas leakage.

The minimum supply pressure P_m to the cylinders therefore had to be calculated:

Cylinder diameter = 12 mm
Force on O-ring face due to internal gas design pressure = 105,1 N
Number of cylinders = 2

$$P_m = \frac{F_c}{A_c} \qquad \text{(where } F_c \text{ = force on cylinder, } A_c \text{ = area)}$$

$$= \frac{\frac{105{,}1}{2}}{\frac{\pi}{4} \times 12^2}$$

$$= 0{,}465 \text{ N/mm}^2$$

$$= 465 \text{ kPa}$$

Pneumatic flow control valves were included in the coupling/de-coupling and open/close actions of the coupling valves in order to facilitate smooth operations.

Maximum fluctuations from the compressed air supply line vary between 550 kPa and 600 kPa, depending on the demand from the rest of the radioisotope production group. In addition to the aforementioned pressure switch, a pressure gauge on the air supply line was installed for monitoring by the operator.

For ease of servicing, space saving and problem tracing, all pneumatic control valves were mounted on the rear side of the hot-cell panel (see Fig. 35). A quick-coupling connector was included on the pneumatic supply line to facilitate panel removal.

4.2.9   Control System

For the testing of the individual electrically-operated solenoids/components and operation of the system as a whole during the development stage, a preliminary simple control panel had to be constructed by means of which the valves, circulating pump, cryopump, coupling valves, vacuum pump and cryopump heater were all operated individually with electrical toggle switches. Using this control system, the following items were checked and perfected both outside and inside the hot-cell:

(1)   The circulating pump pressure and speed were set to give the required water spray coverage.

(2)   The cryopump freezing and heating cycles at different pressures and time intervals were checked.

(3)   The adjustment and lining up of the coupling valves was effected.

(4)   The correct operation of all the system valves was checked.

(5)   The operation of the vacuum pump and the leak-tight condition of the system was checked.

Further mechanical additions to the control system were:

(1)   A compound pressure/vacuum gauge (−100 to 2400 kPa) between the cryopump and target for visual monitoring during gas pumping, water circulating and vacuum pumping.

(2)   A pressure relief valve (set at 2500 kPa) on the gas filling line between the cryopump and reservoir isolating valve.

(3)   A compound pressure/vacuum gauge (−100 to 300 kPa), mounted on the reservoir for visual monitoring during gas filling from the bottle, vacuum pumping and gas pumping.
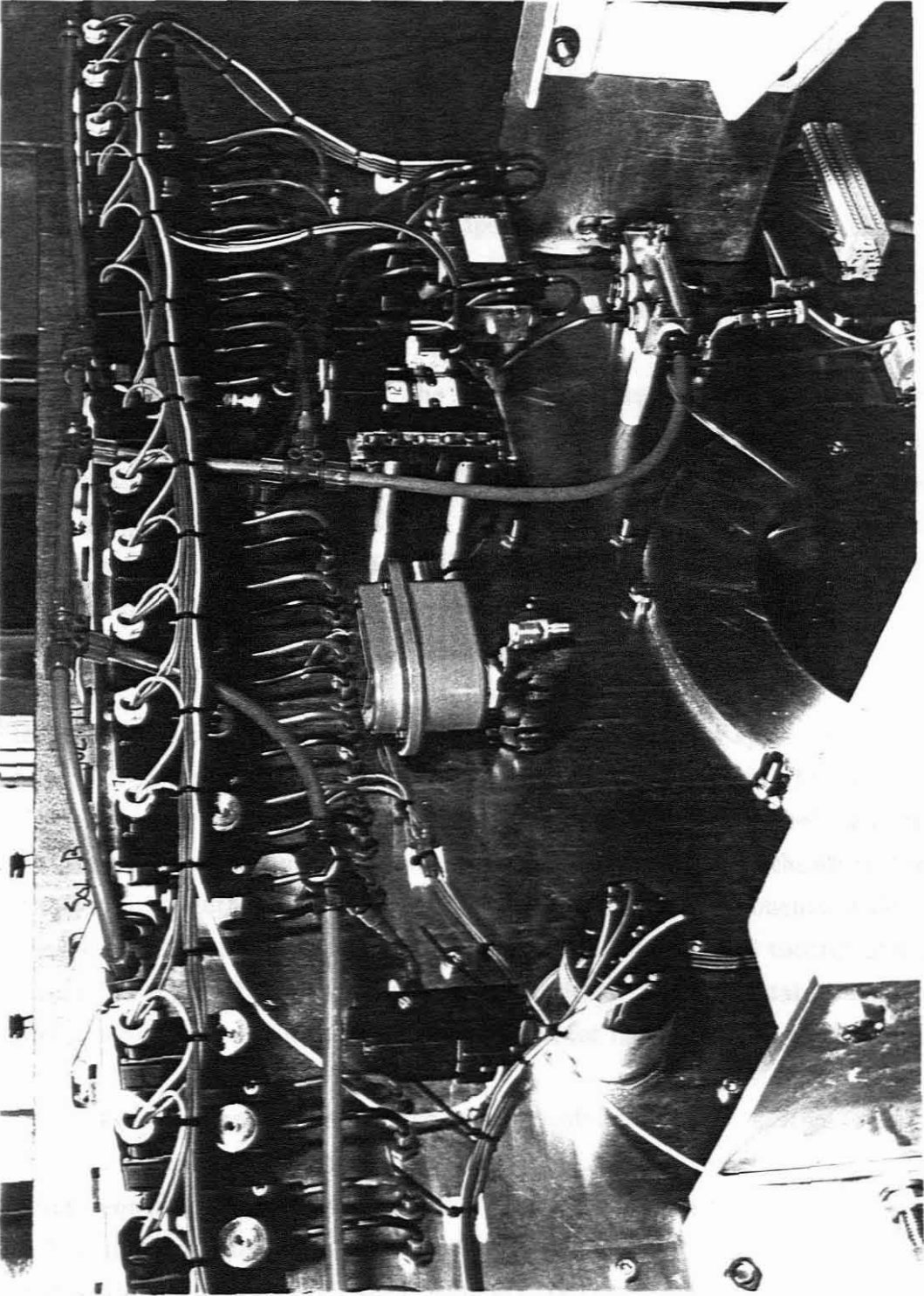
Fig. 35   *Pneumatic control valves.*

(4) A pressure relief valve (set at 500 kPa) mounted on the reservoir.

(5) A pressure switch mounted on the reservoir which is responsible for closing the gas inlet valve from the cylinder when the required pressure is reached. The gas pressure in the reservoir determines what the final pressure in the target will be after gas transfer.

(6) A coalescing filter with a drain and disposable borosilitate glass microfibre filter element which is mounted at the reservoir entrance for the purpose of preventing moisture or residual radioisotopes from entering the clean reservoir.

After all the tests were completed, the entire operating procedure was repeated numerous times until satisfactory and consistent results were obtained. A switching sequence diagram was then drawn up (see Fig. 36). However, although the diagram is an accurate guide for the operator, it does not prevent accidental incorrect switching, which may have disastrous consequences. Also, if large time periods have lapsed between operations, the operator may forget at which stage of the sequence the system is.

These factors led to the building up of a microcomputer control system which works through a SABUS relay interface. The relay interface section of the project was handled by electronic personnel of the NAC, and will therefore not be dealt with in this thesis. A schematic lay-out of the microcomputer control system is shown in Fig. 37, while the system, together with all the krypton processing components which have been removed from the hot–cell, are shown in Fig. 38. The original control panel was used, but LED's replaced the toggle switches for visual ON/OFF status monitoring. This panel was mounted at the front of the hot–cell, for monitoring by the operator.

The programming language used for the control software of the system was Turbo Pascal (version 5) and the program structure was written in such a way that changes in switching sequences and delays could easily be made during the development stage [Ste92]. The program provided for three levels of operation. The first level enables the operator to switch each of the 23 relays manually, the second level allows the selection of 32 operations while the third level allows a selection of 6 condensed operations.

4.2.10 Hot–cell Lay–out

The relatively small internal volume of the hot-cell (1180 mm wide × 740 mm deep × 850 mm high) meant that the lay-out of components inside it had to be as compact as

PROCEDURE	RELAY SWITCHES																						
	1	2	3	4	5	6	7	8	9	10	11	12	13	14	15	16	17	18	19	20	21	22	23
1 INITIAL STATUS			ON																				
2 GAS SUPPLY ON	ON																						
3 GAS SUPPLY OFF																							
4 EVACUATE		ON		ON	ON				ON									ON	ON	ON	ON		
5 PREP.GAS FREEZING FROM RESERVOIR			ON		ON																		
6 LN ON					ON						ON												
7 GAS FREEZING					ON	ON			ON														
8 PREP.GAS HEATING TO TARGET									ON										ON	ON			
9 GAS HEATING ON														ON					ON	ON			
10 GAS HEATING OFF																			ON	ON			
11 PREPARE FOR TARGET TRANSPORT																							
12 UNCOUPLE SYSTEM																						ON	
13 COUPLE SYSTEM																							
14 PREP.GAS FREEZING FROM TARGET																			ON	ON			
15 LN ON 2											ON								ON	ON			
16 GAS FREEZING 2										ON									ON	ON			
17 PREP.GAS HEATING TO RESERVOIR										ON													
18 GAS HEATING ON 2					ON	ON									ON								
19 GAS HEATING OFF 2																							
20 RELEASE PRESSURE																			ON	ON			
21 VENT TARGET																ON OFF			ON	ON			
22 INSERT WATER												ON					ON OFF		ON	ON	ON		
23 PREPARE TO CIRCULATE									ON			ON						ON	ON	ON	ON		
24 CIRCULATE ON									ON			ON	ON					ON	ON	ON	ON		
25 CIRCULATE OFF									ON									ON	ON	ON	ON		
26 EXIT PRODUCT								ON						ON OFF				ON	ON	ON	ON		ON OFF
27 PREPARE TO WASH SYSTEM																			ON	ON	ON		
28 INSERT WATER 2												ON					ON OFF		ON	ON	ON		
29 PREPARE TO CIRCULATE 2									ON			ON						ON	ON	ON	ON		
30 CIRCULATE ON 2									ON			ON	ON					ON	ON	ON	ON		
31 CIRCULATE OFF 2									ON									ON	ON	ON	ON		
32 EXIT WASTE							ON		OFF ON									ON OFF	ON	ON	ON		ON OFF
33 COMPRESSED AIR ON							ON											ON	ON	ON	ON		ON
	1	2	3	4	5	6	7	8	9	10	11	12	13	14	15	16	17	18	19	20	21	22	23

ALL BLANK SPACES = "OFF" STATUS

Fig. 36: *Switching sequence diagram.*
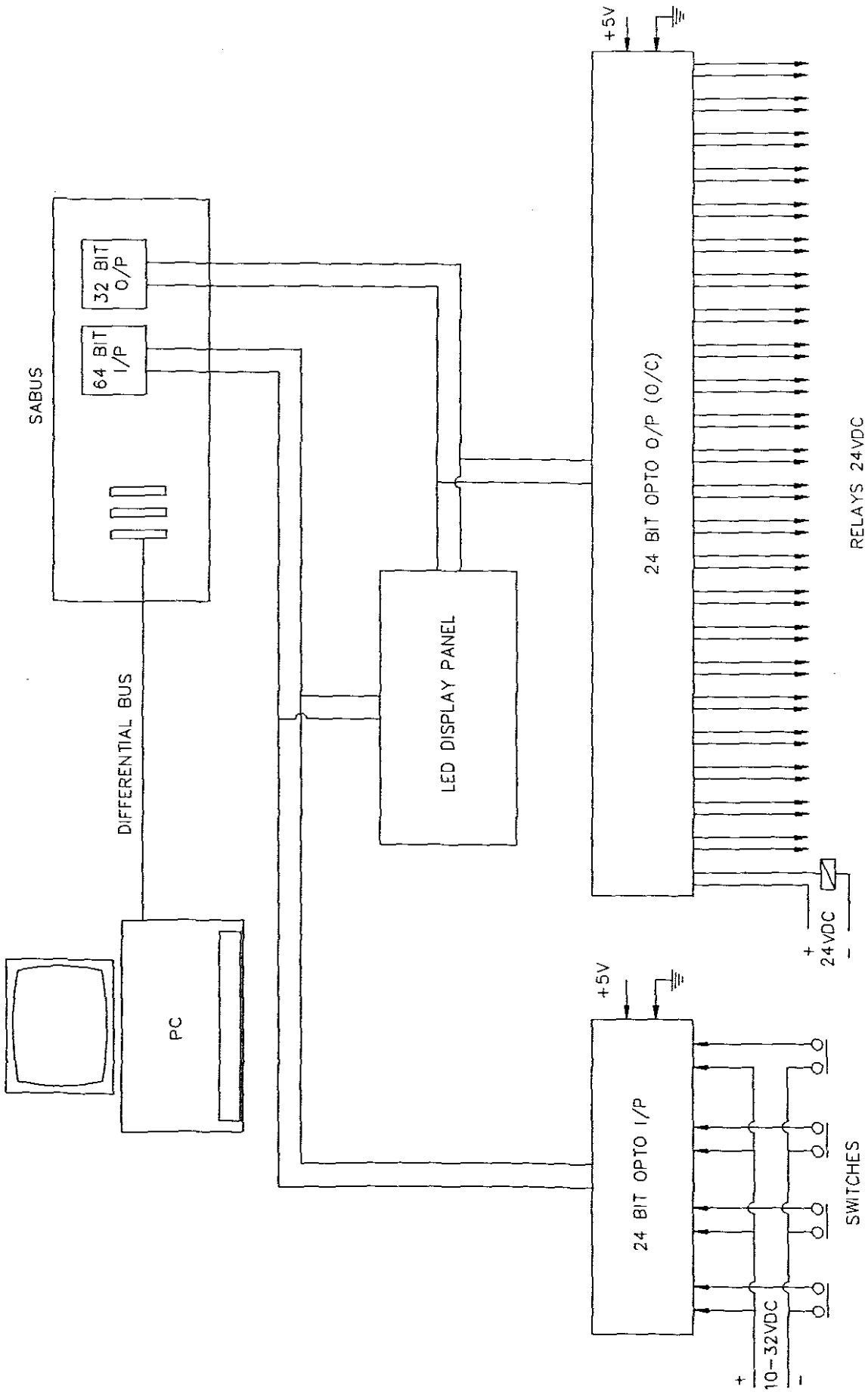
Fig. 37: *Microcomputer control system.*
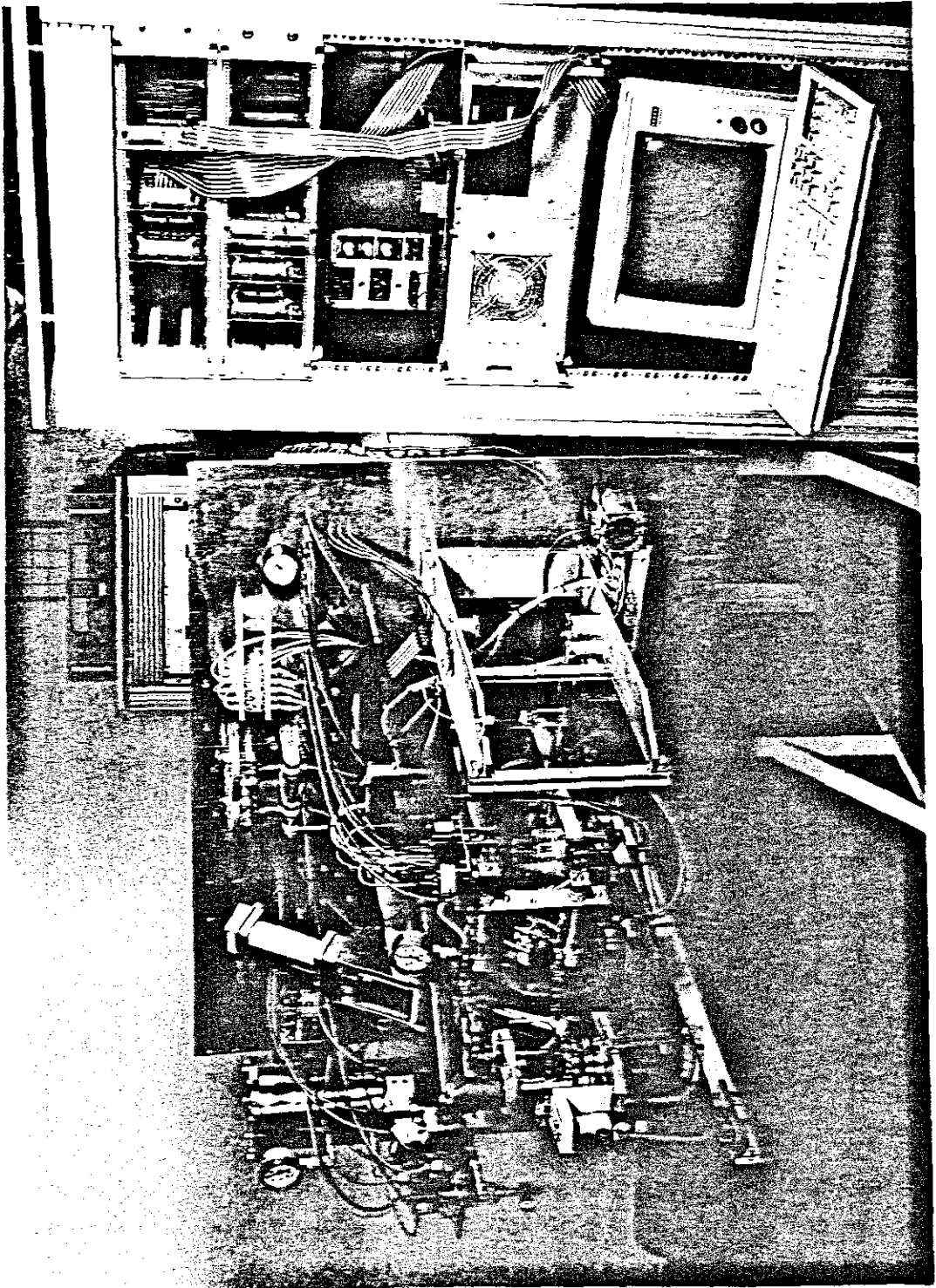
Fig. 38:   *Microcomputer control with processing components.*

possible. Furthermore, it had to be efficient, dead volumes in the system tubes minimized and adequate drainage provided. Various system configurations were therefore considered, and eventually the most suitable one was selected (see Figs. 39, 40 and 41).

The gas target is lifted into the hot-cell from the transport trolley (which passes underneath the hot-cell) by means of an electrically-driven hoist (see Fig. 42). The target is coupled to the hoist by means of a pneumatically-operated hand. The hoist moves up into the hot-cell and activates a limit switch which stops the hoist motor when the target reaches a position which lines up with the coupling valves. The target is guided into the hot-cell by means of a support rail which also serves to brace it when the coupling valves are engaged. When entering the hot-cell, however, the target is aligned parallel to the coupling valves due to the orientation of the entry hatch. Another limit switch was therefore incorporated to activate 90° target rotation before entering the support rail so that the coupling valves would line up.

For ease of maintenance and fault-finding, all pneumatic control valves were mounted on the rear side of the panel, and can thus be accessed without panel removal. A 1 ℓ and 60 mℓ glass vessel mounted inside the hot-cell, both contain the distilled water which is used for target rinsing and generator loading respectively. All gas, electrical, vacuum and pneumatic service lines are also connected to the rear side of the panel by means of quick-coupling connectors to make panel removal relatively easy.

The vacuum pump is stationed below the hot-cell, with the exhaust line coupled to the air ventilation outlet duct.

The liquid nitrogen service line terminates at the front of the hot-cell so that connection of the portable liquid nitrogen supply dewar can easily be accomplished.

4.2.11   Generator Loading System

The generator loading system design that was used on the RbCl system worked successfully and was therefore also used on the krypton gas target system. A few modifications were made however, in order to facilitate the remote control thereof. The system basically consists of a product vessel (which is filled from the krypton processing system), a peristaltic pump which can pump multiple lines from the product vessel to the drain via the generators and glass drippers, and a drain vessel (see Fig. 43). A 60 mℓ distilled water vessel is included for rinsing the system after loading the generators and also a sample line for analysing small quantities of the product. A
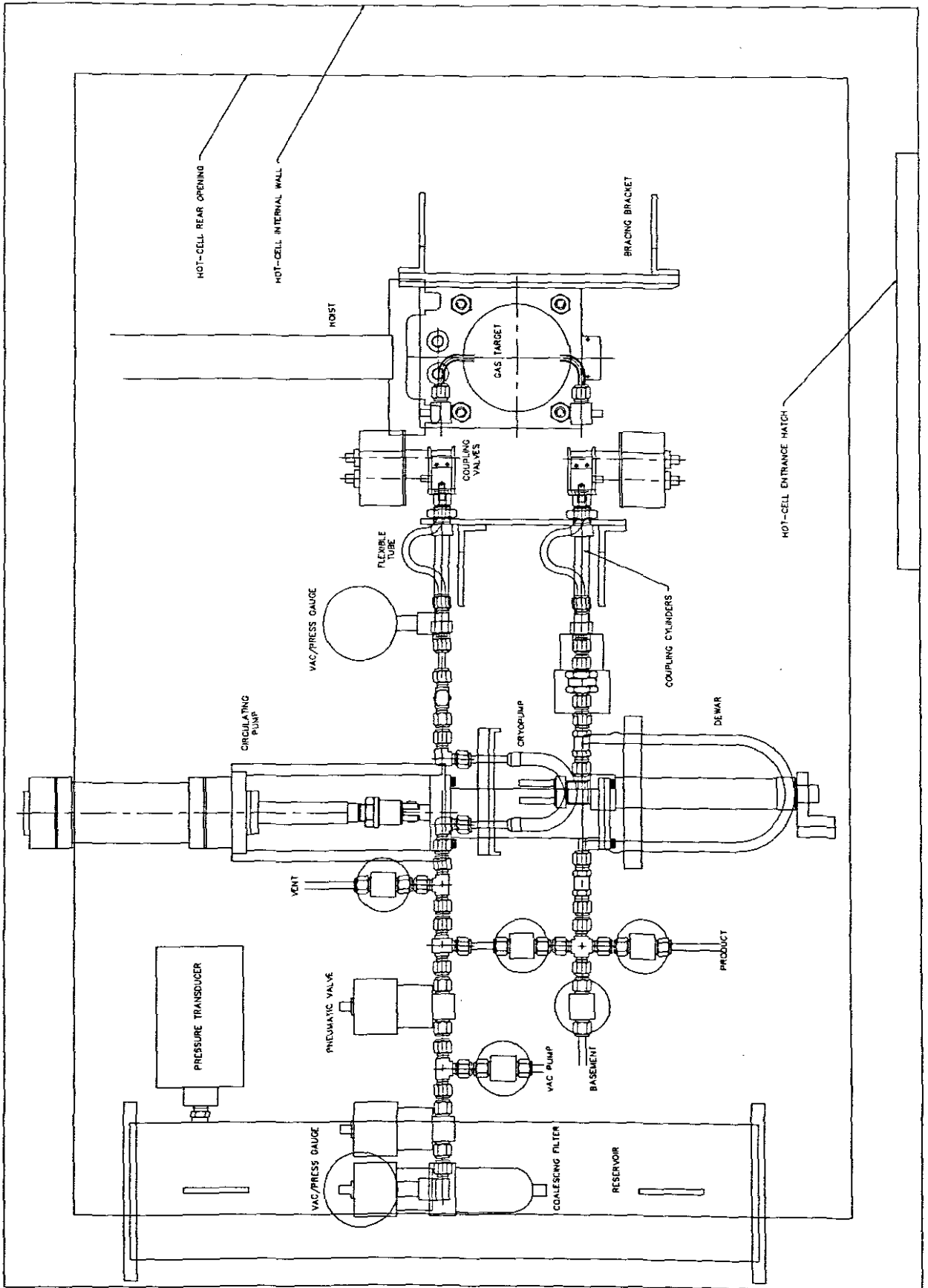
Fig. 39: *Hot-cell lay-out — side elevation.*
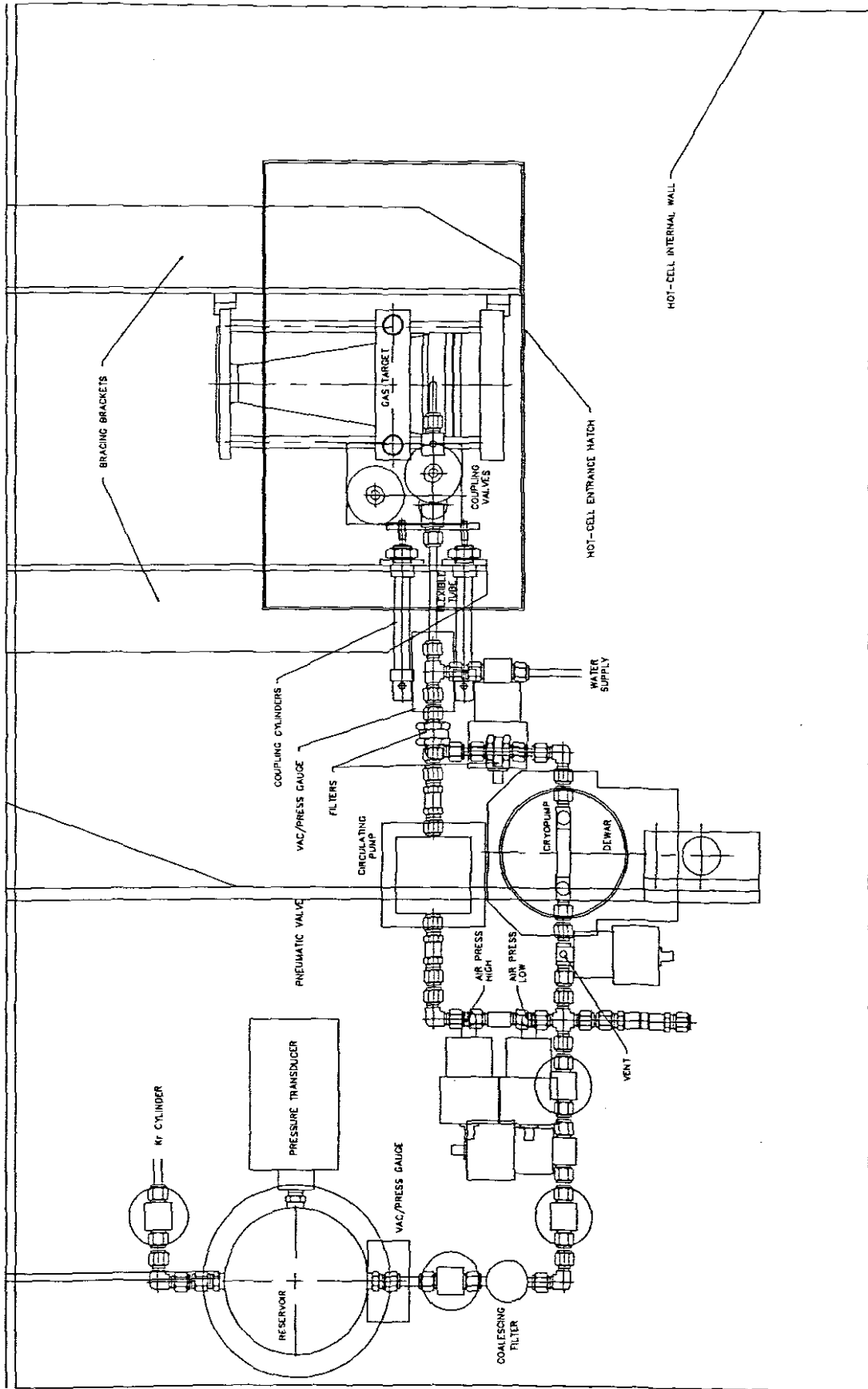
Fig. 40: *Hot-cell lay-out — plan.*
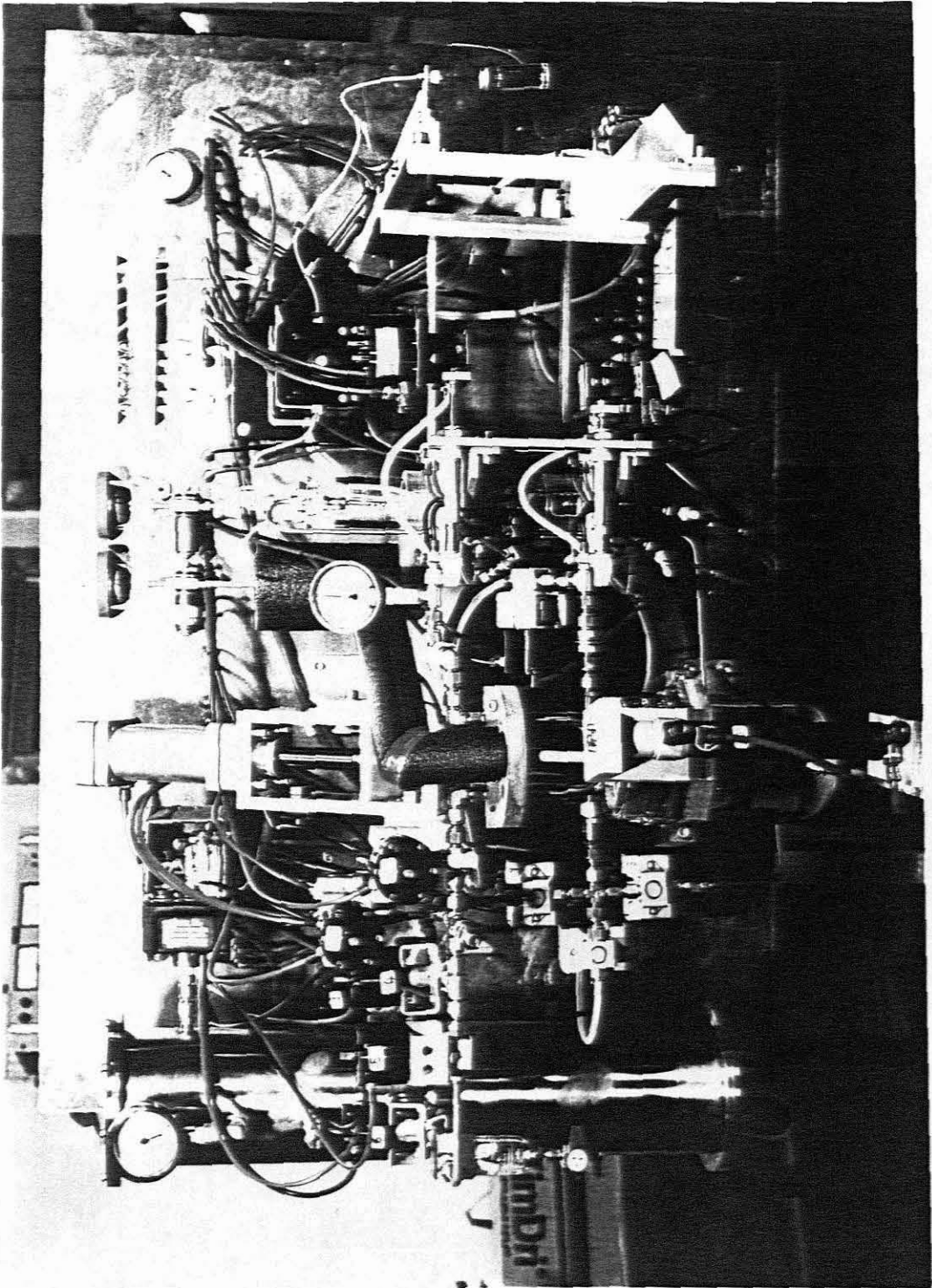
Fig. 41:   *Hot-cell lay-out – panel removed.*
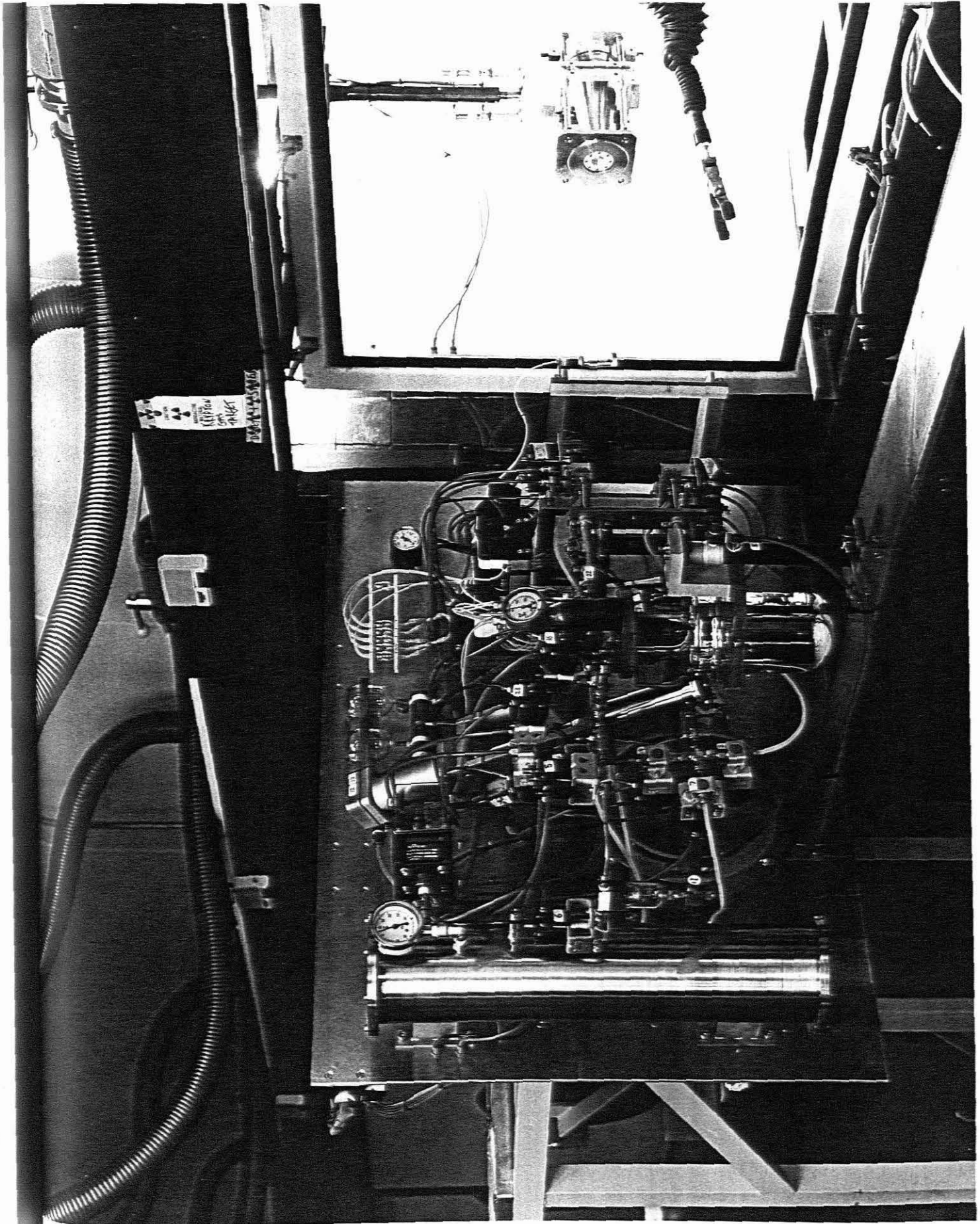
Fig. 42: *Hot—cell — rear view.*

Fig. 43: Generator loading system.

DISTILLED WATER

PERISTALTIC PUMP

GENERATORS

PRODUCT LINE

SAMPLE

PRODUCT VESSEL

GLASS DRIPPERS

DRAIN VESSEL

DRAIN
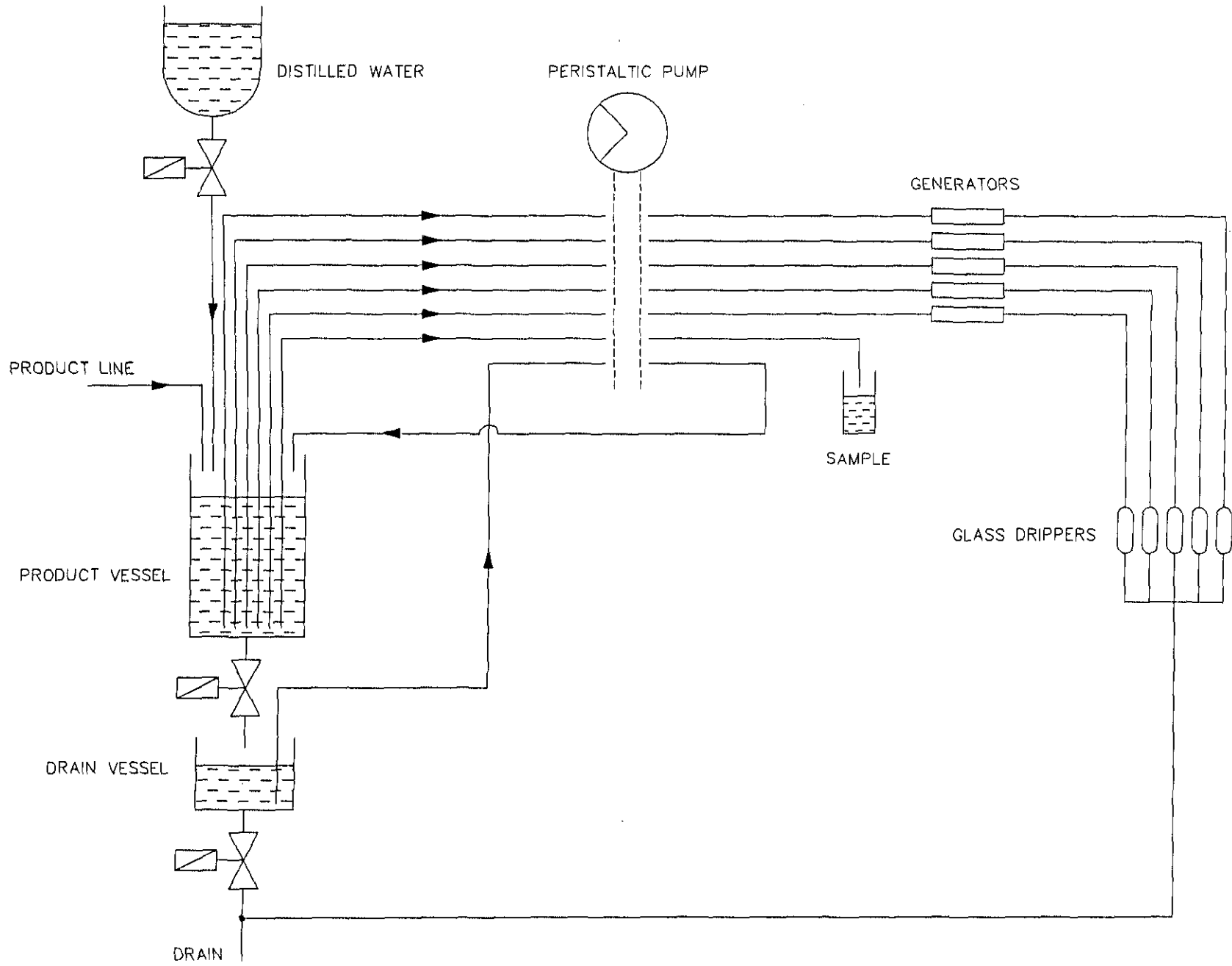
remote-controlled solenoid valve is mounted below each of the three vessels in order to control fluid transfer.

The system is set up for loading five generators simultaneously, although provision has been made for loading ten to cater for future demands. Additional to the sample line, another auxiliary line is provided for pumping the drained product back into the product vessel. All the lines used are soft transparent silicone tubing which enables visual monitoring of fluid flow and compressibility between the peristaltic pump rollers. Any line can be selected by means of remotely activating a small pneumatic cylinder which couples the relevant peristaltic pump cassette rollers to the tubing.

The operation of the generator loading system is carried out as follows:

(1)   The 100 ml product is expelled from the krypton processing system into the product vessel by means of compressed air.

(2)   The lines supplying the selected generators are remotely coupled to the relevant peristaltic pump cassette rollers.

(3)   The peristaltic pump is then switched on and the product is slowly pumped from the product vessel at a rate of 0,9 mℓ/min along the selected lines, through the generators which trap the Rb onto resin columns (see Fig. 44), through the glass drippers (used for visual flow monitoring) and finally to the drain which terminates at the radioactive waste storage tanks. Typically 15 to 20 mℓ of product solution is passed through each generator.

(4)   The remainder of the product that has not been used, is released into the drain vessel by activating a solenoid valve mounted on the base of the product vessel.

(5)   Approximately 40 mℓ distilled water is now released into the product vessel also by means of a solenoid valve.

(6)   The peristaltic pump is again switched on and all the used lines and components are rinsed with the distilled water which is discharged to the drain. When all the distilled water has been pumped through the system, the pump continues pumping air for ~ 10 minutes in order to dry the generators.

(7)   The generators which are mounted in a tray on the rear of the hot-cell panel, are now de-coupled from the system by means of a pneumatically operated coupling bulkhead. The operator can now remove the generators from the back of the hot-cell which are now ready for packaging before being dispatched.

ST.ST.NEEDLE WITH
PVC MOUNTING DISC

LEAD SHIELDING

RUBBER PLUG

1mm I/D PE TUBING

CRIMPED END CAP

COTTON WOOL

GLASS TUBE

CATION
EXCHANGE RESIN

LEAD BALLS

SINTERED GLASS

Ø50.0
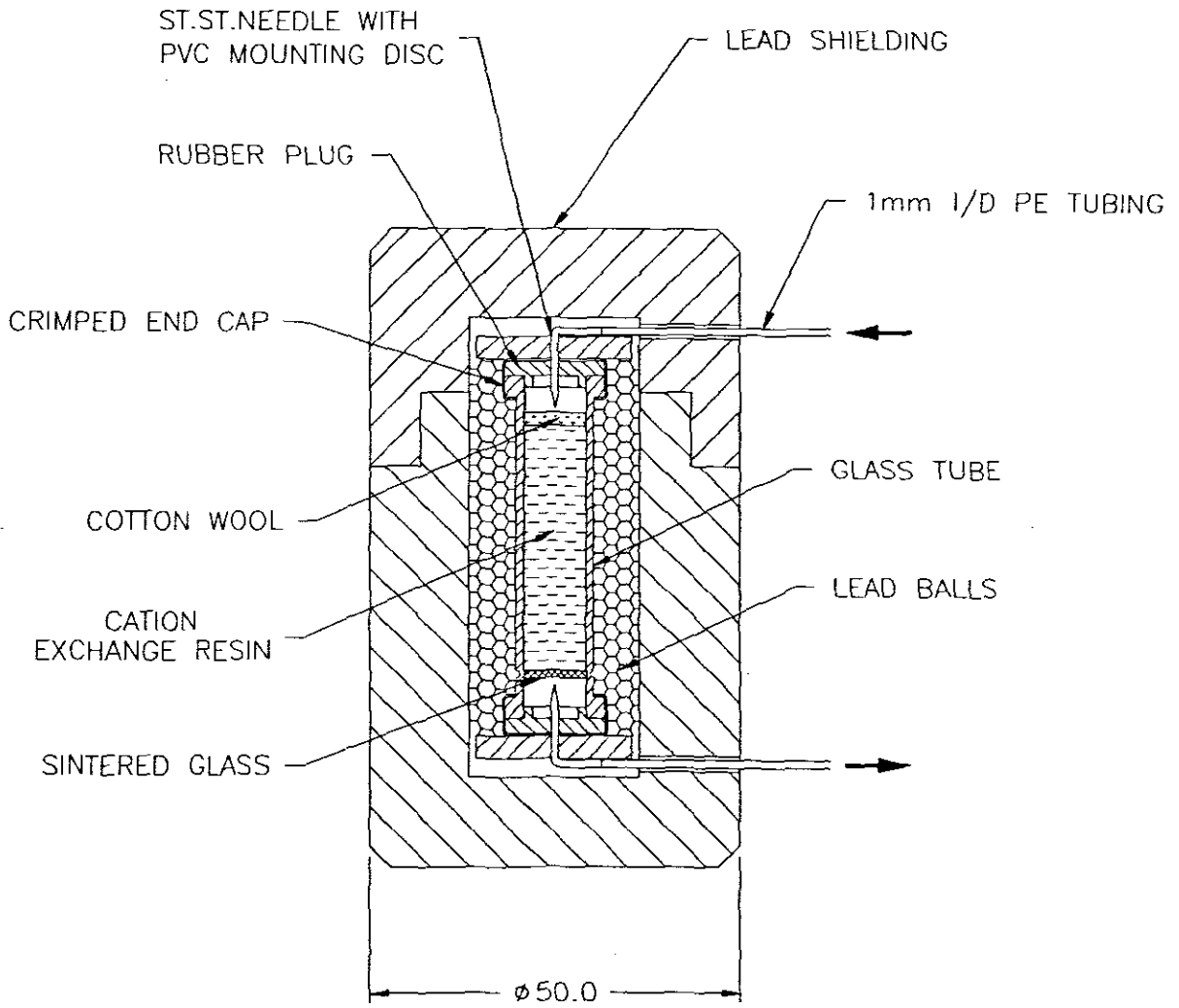
Fig. 44: *Cross-sectional view of generator.*

(8)   If no further generators need to be loaded or the yield checked, the product from the drain vessel can be released to the drain by means of activating a solenoid valve.

The generator loading system is now ready for the next production run.

4.3   ROUTINE MAINTENANCE AND BREAKDOWN PROCEDURES

4.3.1   Test Target

The test target is not a component that would be used on a routine basis, but if further tests are required or if another gas is to be experimented with, it is advisable to:

(1)   Carry out an internal hydrostatic pressure test to check that the chain clamp has not expanded and that the vacuum and gas valve O-rings have not collapsed or perished from non-use.

(2)   Carry out a hydrostatic pressure test on the front and rear cooling jackets in order to check that the O-rings have not collapsed or perished.

4.3.2   Production Gas Target

Production runs on the gas target will be carried out twice per week and during each run the target will be exposed to elevated temperatures, high pressures and radiation damage. These factors produce cyclical stresses on the material and weld seams and could produce cracks over a period of time. It is therefore important to perform a pressure test on the inner vessel on a routine basis.

The components that would experience the highest destruction due to radiation damage would be the O-rings in the valves and cooling ports. The total bombardment time on the Viton O-rings therefore has to be monitored so that they can be replaced before destruction. The measured radiation dose figures during bombardment are 5×10^4 Gray/hr at 100 μA beam current [Ste90].

The gas target however, will be bombarded at a beam current of 30 μA, therefore:

$$\text{Dose} = \frac{30 \times 5 \times 10^4}{100}$$

$$= 1{,}5 \times 10^4 \text{ Gray/hr}$$

$$= 1{,}5 \times 10^{6} \text{ Rad/hr} \qquad (1 \text{ Gy} = 100 \text{ Rad}).$$

The safe dose for Viton $= 5 \times 10^6$ Rad (see Table 2)

The maximum exposure period therefore $= 3{,}33$ hrs.

Initially each bombardment period will be 30 minutes long, thus to be safe the O—rings should be replaced after every 6 bombardments.

Bombardment tests however, were carried out on the O—rings and it was found that only after 30 hours of irradiation, noticeable destruction of the material occurred.

Another aspect to consider is the loosening of bolts and nuts on the target assembly due to cyclical stresses.

The only moving mechanical part besides the valve plugs, is the yoke lock. The reliable functioning of this component is of vital importance and servicing thereof should not be neglected.

4.3.3   Spray System

The spray system and specifically the spray nozzles, is maintenance free and no attention is further demanded. If however, in the unlikely event, the nozzles should become blocked or an excessive loss of water occurs, a water pressure increase or decrease on the compound gauge will be observed during pumping. The nature of the problem can thus be monitored and corrective action taken as described in par. 4.2.3.

4.3.4   Circulating Pump

From par. 4.2.4 it was seen that the plunger seal and check valve O—rings are exposed to relatively low radiation doses and would not require routine replacement. The check valve operation should however, be monitored by observing pressure fluctuations during pumping as described in par. 4.2.3

A routine pressure test on the circulating pump needs to be performed in order to ensure a leak-tight condition.

Table 2: *Radioactive persistancy of various elastomers.*

NATURAL RUBBER				
STYROL−BUTADENE−RUBBER				
PERBUNAN−N				
NEOPRENE				
BUTYL−RUBBER				
ETHYLENE−PROPYLENE−RUBBER				
HYPALON				
SILICON				
VITON				
VULKOLLAN				

$10^4 \qquad 10^5 \qquad 10^6 \qquad 10^7 \qquad 10^8$

DOSE IN RAD

USABLE

ALREADY DAMAGED

NOT USABLE
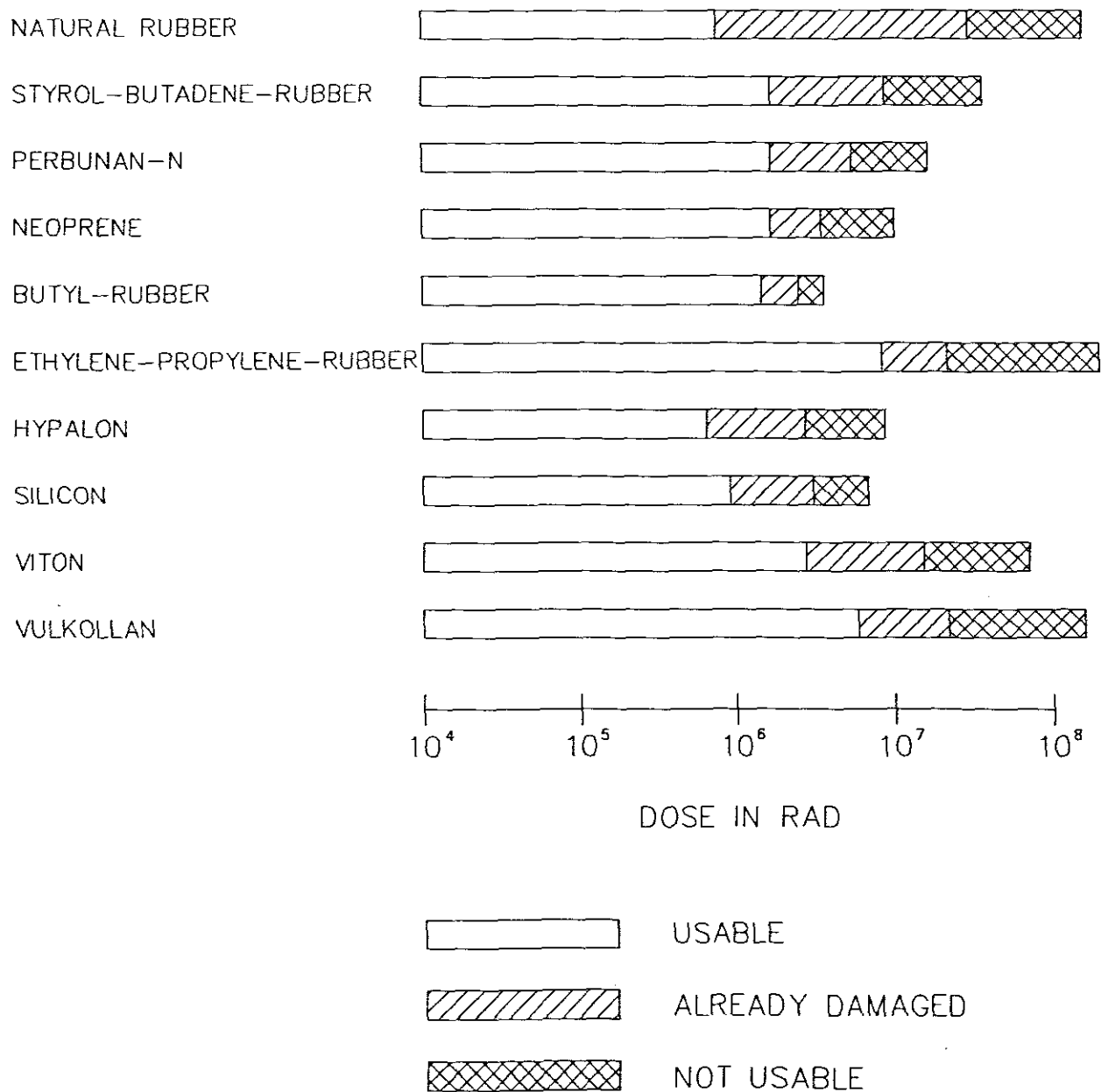
The table shows the application limits of different Elastomers in relation to the absorbed doses of gamma rays [Ang67].

4.3.5   Cryogenic Pump

The cryogenic pump is a maintenance free unit with no moving parts. The material and welded areas are, however, exposed to severe thermal shocks and a pressure test on the component on a regular basis would be a safe practice.

4.3.6   Gas Reservoir

The gas reservoir is a static unit requiring low maintenance. Radiation levels affecting the flange seals are very low, but a routine pressure test may be carried out to check the sealing of all ports and the accurate operation of the pressure switch.

4.3.7   Coupling Valves

As previously mentioned, reliable operation and sealing of the coupling valves is vitally important. Proper alignment procedures must therefore be carried out each time the panel is fitted to the hot-cell, to ensure accurate alignment of the mating coupling valves. The coupling valve engagement and open/close actuation should always be checked before final operation.

The coupling valves are the closest system components to the radioactive gas target and are thus exposed to a high dose rate. Additional mechanical wear on the valve face O-rings is caused by the repeated coupling and de-coupling of the valves. The sealing O-rings therefore need to be checked and replaced on a routine basis. The O-rings in the rotary actuators, valve plugs and coupling cylinders receive the same dose and should also be checked.

The condition of the flexible tubing should be inspected regularly as it is subjected to continued cyclical stresses.

4.3.8   Pneumatic System

Previous experience with the pneumatic components selected has shown very little or no maintenance is necessary. Radiation damage to the pneumatic system should be negligible.

4.3.9   Control System

All the mechanical and electro-mechanical control units in the system are maintenance-free and need no further attention.

The coalescing filter initially requires radiation monitoring after each operation to check for fluctuations in radioisotope collection efficiency (for general recording purposes). Replacement of the element should not be necessary, but regular inspections may be carried out.

The microcomputer control system should not require any routine maintenance, but occasional inspections by the relevant electronic personnel should be arranged.

4.3.10   Hot–cell Lay–out

All components mounted on the rear panel of the hot-cell need no maintenance, but sporadic checks may be carried out on the flexible service lines between the panel bulkheads and quick couplings. These lines could be subjected to excessive flexing while coupling and de-coupling them during panel removal, causing possible cracks after long-term usage.

Another component of which reliable service is demanded, is the hoist. The motor, limit switches, lead screw and hoist-hand collets should be checked and serviced on a routine basis.

The rotary vane vacuum pump will accumulate water in the oil due to pumping moisture from the krypton system. The moisture levels must be monitored and servicing done on a regular basis.

Finally, special attention should be given to the re-mounting of the hot-cell rear panel after removal, so that the target and coupling valves line up accurately.

4.3.11   Generator Loading System

The uninterrupted operation of the peristaltic pump and its integral components needs to be effected. Further attention should be given to the generator bulkhead-connector, solenoid valves and the leak-tight condition of the tubes and connectors. The reliable operation of these components is of vital importance because they are all used in the loading process of the highly radioactive final product onto the generators.

CHAPTER 5

RESULTS

5.1 GENERAL LAYOUT AND PROCEDURES

Once all the individual components were manufactured and successfully tested, the system operation as a whole was tested. Initially the electrical components and pneumatic system were operated by means of the manual control system. This allowed for checking the sequence of operations as well as the time intervals between operations. The proposed operation sequence proved to be adequate.

5.2 INDIVIDUAL COMPONENTS AND SYSTEMS

5.2.1   Test Target

Once the test target was accurately lined up on the beam-line with a theodolite, the various service lines could be connected. The krypton and vacuum lines were connected to the gas cylinder and vacuum pump respectively, and the water-cooling lines were connected to the front and rear cooling jackets. A vacuum gauge (0 to −100 kPa) and a pressure gauge (0 to 2400 kPa) were connected to the gauge ports for vacuum and pressure monitoring. The coupling valves were assembled on the test target mounting cradle and the pneumatics connected.

The first experiment required bombardment of the test target under vacuum. The coupling valves to the vacuum pump were coupled and opened, and a vacuum of −100 kPa was achieved. The coupling valves were then closed and left in this condition for 1 hour to check for leaks. The coupling valves sealed satisfactorily.

Thereafter the target was bombarded at 100 nA for a period of 30 minutes. The results, after counting the activity over the span of each copper wire, showed that the beam profile has a solid conical shape, tapering approximately linearly from 8,0 mm diameter at the first wire to 69,1 mm diameter at the last wire (see Table 3). This experiment specifically indicated the scattering effect the windows and water layer have on the beam.

The second experiment required bombardment of krypton gas under pressure. This experiment however, also provided the opportunity for testing the prototype cryopump's operation:

In this experiment the prototype cryopump (see par. 4.2.5) was connected between the gas cylinder and the coupling valves. With the vacuum coupling valves coupled, a vacuum was initially pumped in order to prevent any air from contaminating the krypton gas. The vacuum coupling valves were then closed and the gas coupling valves opened. Gas was subsequently released from the cylinder into the test target, up to a pressure of 1400 kPa. The gas coupling valves were closed and left in this condition for an hour to check for leaks. No leaks were found and the target was again bombarded at 100 nA for 30 minutes.

On completion, the gas coupling valves were opened and the prototype cryopump was inserted in liquid nitrogen. The gas froze onto the inner surface of the cryopump, leaving a vacuum in the target. The gas coupling valves were then closed, the gas cylinder opened and the liquid nitrogen removed. As the frozen gas started heating, it would return to the cylinder.

The target was vented and the copper wires removed for activity counting [Ste90]. The beam profile was found to taper from 8,3 mm at the first wire to 85,96 mm at the last wire (see Table 3). These final results could now be used for the design of the gas target.

Table 3:   *Test target beam profile measurements*

Distance from front entrance window (mm)	Target under vacuum Beam diameter* (mm)	Target under 1400 kPa krypton Beam diameter* (mm)
28	8,0	8,3
82,4	18,7	20,4
136,8	31,4	34,9
191,9	42,2	51,5
245,6	56,3	65,8
300,0	69,1	85,9

*The activity measured over each copper wire is typically a Gauss distribution and the effective diameter selected is 6x the std. deviation of the distribution [Ste90].

5.2.1.1   Construction

The construction of the test target was satisfactory as far as size to accommodate the beam profile and strength was concerned. The rear chain clamp however, needed excessive initial tightening before a leak-tight condition was achieved. The ratio of the flange diameter to chain link sizes was slightly excessive.

The front flange, cooling jackets and wire mounting cage operated successfully.

5.2.1.2   Window Deflection

The finite element analysis assisted greatly in the window and front flange investigations.

Studying the figures in Fig. 12 (0,385 mm deflection at 4500 kPa internal pressure) and assuming that the deflection is linearly proportional to the internal pressure, it was seen that a deflection of 0,119 mm at the operating pressure of 1400 kPa could be used for the beam degradation calculations.

Further, the Von Mises Stress contours in Fig. 13 indicated a maximum internal stress of 4687 kPa at the outer central region of the window and a maximum internal stress of 3462 kPa at the inner edge of the window. These figures show acceptable induced stresses when compared to the yield stress of 310 MPa for stainless steel (Gr 304) and thus safe window conditions are ensured.

5.2.2   Production Gas Target

On completion, the gas target was tested for compatibility with the target bombardment station, robot arm, transport trolleys and hot-cell hoist. The results were satisfactory, and the only modifications that had to be carried out to existing equipment were:

(1)   Increasing the roller clamp tension on the transport trolleys and rotary target magazine yokes, in order to accommodate the additional mass.

(2)   Reducing the hot-cell hoist hand width to avoid interference with the processing system.

Table 4: *Target pressure measurements during bombardment.*

66 MeV − 5 min irradiations	
Beam current (μA)	Gas Pressure (gauge) kPa
2	14,5
5	15,2
10	17,0
15	17,9
20	19,0
25	19,7
30	20,2
35	20,7
40	21,5
45	21,8
50	22,2
55	22,6
60	23,2
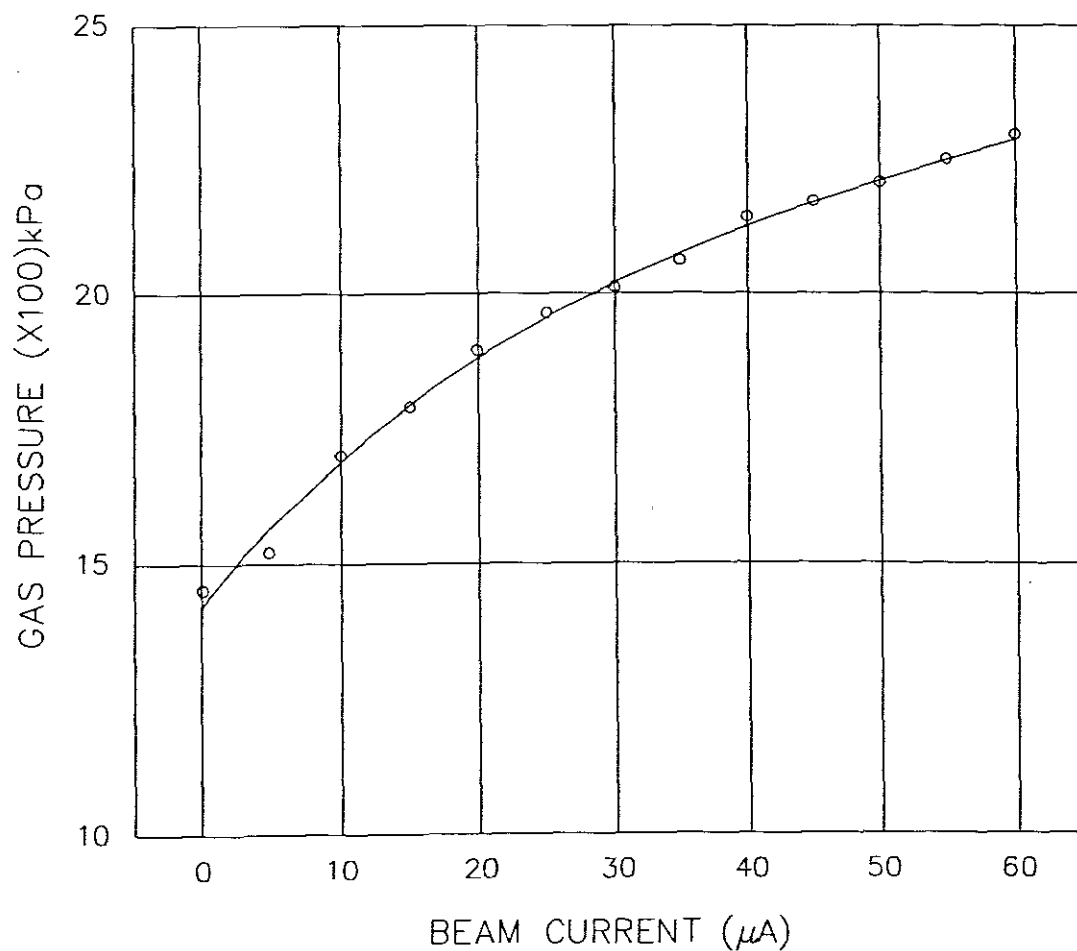
Fig. 45: *Graph showing gas pressure versus beam current.*

The final target was now ready for the first test bombardment. After gas insertion at 1400 kPa, the target was coupled to one of the rotary target magazine yokes with a 1/8" copper tube linking the target with a pressure gauge on the exterior of the shielding. A remote camera was focused on the gauge to monitor pressure rises during bombardment.

The target was bombarded at various beam currents and the corresponding pressure rises were recorded. The values were incorporated in a graph for future reference (see Table 4 and Fig. 45). As can be seen from the table, the gas pressure rise at the required operational beam current falls within the design figures.

The second bombardment experiment was carried out under normal production conditions, involving the operation of the system as a whole. The 1400 kPa filled target was bombarded for 1 min at 30 μA and returned to the hot-cell where the gas was returned to the reservoir. The target was flushed out four times and the yield of each sample measured. The results are given in Table 5.

Table 5:   *Yield figures for product at different flushing stages.*

Flush no.	Yield (mCi/μAh)
1	23,7
2	4,08
3	1,23
4	0,44
TOTAL	29,45

The expected yield according to excitation curves was 33 $\pm$ 2.6 mCi/μAh [Ste91].

5.2.2.1   Inner Vessel

After rolling, forming and electropolishing of the cone and end caps, TIG butt-welding was used to join the individual components. Initially stainless steel filler material was used in the welding process, but a very rough and porous weld bead was deposited. Further research in the welding of Nicrofer 7216 resulted in the use of Nicrofer 7020 filler material and an argon purge inside the vessel. The vessel was hydrostatically tested at 8000 kPa and held for 24 hours at this pressure. The vessel was found to be

leak tight. Additional information recorded was that at this pressure the longitudinal deflection was 0,1 mm and the diametrical deflection was 0,2 mm.

5.2.2.1.1 *Manufacturing of end caps*

The drawing of the small end caps provided no problems. The finished product neatly followed the profile of the punch and the normal waviness at the rim was machined square. The drawing of the large end cap initially resulted in crinkling at the cylindrical section, but tighter adjustment on the blank holder solved the problem. The finished product also neatly followed the punch profile and the rim waviness had to be machined square.

5.2.2.1.2 *Electropolishing*

The electropolishing process required a systematic experimental approach. Results showed that electropolishing for periods over 2 minutes at the recommended 12V and 21A as indicated in 4.2.2.1.2, produced excessive polishing and rounding of outer edges. Polishing for longer periods does however produce a general higher surface finish. Increasing the anode/cathode distance reduces the surface finish, leaving a finely pitted appearance.

Reducing the voltage/current and increasing the anode/cathode distance produces similar results to the recommended specifications, but the polishing time needs to be increased.

Stainless steel cathodes were also used, but very little difference in results were observed.

Further, it was noted that agitation did not provide any noticeable improvements. The ideal combination is to first remove visible roughness with sand paper and then to buff the material before electropolishing. A typical surface finish of 0,4 μm can be achieved, which is adequate for our purposes.

5.2.2.2 Cooling Jacket

In order to test for leak-tight welds, the target base and beam entrance window were assembled to the cooling jacket to produce a sealed unit. The operating pressure of the cooling water is in the region of 1000 kPa and for adequate safety the cooling jacket

was hydrostatically tested at 5000 kPa. At the same time the sealing of the mating chamfers on the beam entrance window and target base was checked. All the tests produced satisfactory results.

As can be seen from the cooling investigations and calculations, all prerequisites for effective cooling have been met, namely high water flow rate, high static pressure and high turbulence.

5.2.2.3   Beam-Stop

The aluminium beam-stop was produced so that it could be assembled into the target base by means of a push fit for future removal. Because the beam-stop directs the cooling water to the inner vessel's one hemisphere and out the other, it is important that the orientation of the beam-stop remains fixed. High water pressure surges could possibly reorientate the beam-stop and for this reason a locating pin was included between the beam-stop and target base.

5.2.2.4   Window

When the window was hydrostatically tested with the cooling jacket, deflection measurements were taken at the centre. At 1000 kPa, no significant deflections were observed on the dial gauge. Because accurate horizontal dimensions could not easily be achieved when the inner vessel was wedged into the cooling jacket, the window flange thickness had to be machined afterwards, so that a water layer channel of 1 mm between the window inner surface and small end cap outer surface could be achieved.

5.2.2.5   Yoke Guides

Once the yoke guides were clamped onto the struts, the target was tested for accurate positioning in both the rotatory target magazine and hot-cell hoist and fine adjustments were made.

During the continued transportation testing of the target, it was noted that excessive wear occurred on the guide grooves due to contact with the hard steel rollers of the yoke. A second set of hard anodized aluminium yoke guides was therefore manufactured for use under routine production conditions.

The functioning of the yoke lock is adequate, although care must be taken when manually removing the target from the yoke. The release pin at the top of the guide must be depressed before manually removing the target, otherwise the locking pin can be bent when excessive force is applied. Increasing the locking pin diameter is not possible due to space restrictions, but as an increased strength feature, the pin material was replaced with a half-hardened K105 Bohler tool steel, which pushed up the strength to 820 N/mm² and the hardness to ~ 47 Rockwell 'C'.

5.2.2.6   Valves

Once the target valve faces were machined, they were further polished with water paper to ensure positive sealing with the mating system valve O-rings. The target valves were mounted on the target inlet and outlet tubes and squared up before tightening the Swagelok fittings. It was also found that lightly oiling the rotary couplings on the system valve housings and thus reducing the friction, facilitated the open/close actions.

5.2.2.7   Struts

The calculations in par. 4.2.2.7 indicate that the buckling load of the struts is vastly greater than the operating load and the stress induced is much less than the yield stress of the material. An operating load of 5800 N was applied on the struts in a test rig and the results showed negligible deflections. In the final assembly of the target, the struts needed to be adjusted in order to achieve parallelity between the front face and the target base so that equal forces are distributed on all four struts.

5.2.3   Spray System

The perspex model of the inner vessel produced valuable results. The model was connected to the circulating pump with the same length of tubing and restrictions as with the final system.

During the advance stroke of the circulating pump, the gauge on the target inlet line indicated a water pressure of ~ 600 kPa, which produced a powerful spray force through the small aperture nozzles. At this pressure the spray coverage inside the vessel was estimated to be 95%, which is adequate for our purposes.

The pneumatic advance flow control valve on the circulating pump cylinder was fully open so as to produce maximum force. The pneumatic return flow control valve however, was throttled sufficiently so as to allow for all water to settle at the bottom of the vessel and thus to avoid air extraction during the return stroke.

5.2.4   Circulating Pump

The general operation of the circulating pump was successful and the pneumatic cylinder flow control valves were adjusted during the perspex model test (see par. 4.2.3). The 1000 kPa internal pressure test was held for 30 minutes and no leaks were detected. A vacuum test was also performed because the pump would be subjected to vacuum conditions during the evacuation stage in the process. Again no leaks were detected.

One aspect of concern, was that during the perspex model test, a particle of dirt was lodged between the inlet flow control valve seats, which resulted in pumping in both directions. During this test however there was no filter at the inlet valve. On the final arrangement however, an inlet filter was included and further tests indicated no recurrence of the blockage.

5.2.5   Cryogenic Pump

The use of this pump as explained in par. 3.2.5 has great advantages in that there are no movable or rotating parts and hence no maintenance is required. It is also reliable and safe under pressure, vacuum, and sub-zero temperature conditions. A further advantage is the compact size, which is ideal for the system requirements.

The initial development work on the cryopump was carried out during the test target experiment (see par. 5.2.1). The prototype cryopump consisted simply of a 34 mm dia. × 204 mm long stainless steel vessel, the required volume of which was calculated on the same basis as the final cryopump (see par. 4.2.5). The cryopump vessel was welded closed on the one end and a 1/4" tube was welded onto the other end which in turn was coupled into test target/gas cylinder line.

The final cryopump was tested on the completed target system, but not all the gas in the reservoir could be pumped out. After analyzing the construction of the cryopump, it was assumed that the frozen gas at the inlet section prevented further freezing to occur on the outlet section. This problem was partially solved by linking the inlet and

outlet elbows with a 1/8" stainless steel tube. Once the inlet tube was blocked, the gas had free passage to bypass the blocked tube and enter into the outlet tube. Increasing the overall cryopump tube diameter would not have been a viable solution as this would increase the system volume, thus reducing the gas pressure and spray pressure. A small 1/8" linking tube was selected in this case, so that during the rinsing cycle the bulk of the water is forced through the cryopump.

Whilst continuing experimenting with the gas freezing, it was found that a small volume of gas was still not being frozen. From further analysis it was assumed that the coalescing filter retarded gas flow and also that both inlet and outlet sections were blocked and no further gas access was possible to the curved section at the bottom of the cryopump. This problem was solved by initially inserting gas into the reservoir at 150 kPa (abs). The increased 50 kPa pressure was sufficient to force the gas through the filter and the blocked sections of the cryopump. Heating the cryopump now produced the required 1400 kPa pressure in the target.

Another factor that had to be borne in mind was that if air in the system is present during cryopumping, efficient freezing of the gas would be affected. It is therefore important that a good vacuum is achieved in the system before cryopumping commences.

As far as the results of strength and thermal conductivity properties at sub-zero conditions are concerned (see par. 4.2.5) , it is clear that the strength is vastly increased while the thermal conductivity is only marginally decreased.

5.2.6   Gas Reservoir

The gas reservoir manufacturing and installation processes were performed successfully. Once the reservoir was installed and the compound gauge, pressure switch and pressure relief valve connected, a vacuum test was carried out. The reservoir and all its components were found to be leak-tight. The pressure relief valve was finally adjusted to a safe blow off pressure of 300 kPa.

5.2.7   Coupling Valves

The testing of the coupling valves was initially performed, during the test target experiment and repeated on the final system. Once aligned, the coupling and de-coupling, and open/close actions operated smoothly. A vacuum test was carried out on

the valves in the coupled position and after 24 hours no leaks were detected. A pressure test was also completed under operating conditions (600 kPa coupling cylinder pressure, 1400 kPa internal system pressure) and again no leaks were detected.

After the cyclical flexing test on the polyamid tubing was finished, a visual and a 2500 kPa pressure test indicated positive results. No kinking of the tube occurred and no cracks were formed.

On both sets of coupling cylinders and coupling valve rotary actuators, flow control valves were included and adjusted to facilitate smooth operations.

5.2.8   Pneumatic System

The individual pneumatic actuating components were tested and adjusted for correct and smooth operation. The pressure switch was set at a safe minimum operating pressure of 500 kPa. The switching was tested numerous times and consistent results were achieved. In order to test the maximum holding pressure of the coupling valve cylinders, the cylinder pressure was set at 500 kPa and the internal system pressure slowly increased. The coupling valves parted and started leaking at ~ 2400 kPa. The results were as expected and repeating the tests produced the same results.

For general neatness and problem tracing all valves and actuators were numbered according to the pneumatic system diagram (see Fig. 34) and all pneumatic supply/return line pairs were colour coded. The system valve rotary actuators were all connected in such a way that in the event of a power failure, they would all close in order to produce a safe condition. The coupling valve actuating cylinders would also move forward in order to keep the coupling valves coupled during a power failure.

5.2.9   Control System

The testing of all the operations from the control panel was carried out successfully and no further adjustments or alterations needed to be performed. The pressure relief valves were over-pressured, in order to check that the cracking pressures were set correctly. The reservoir pressure switch was set at 150 kPa (abs) and the gas inlet valve consistently closed when this pressure was reached. The standard coalescing filter drain under vacuum conditions, produced a fairly large leak, but this was modified by manufacturing a screw-on flange with an O-ring, which is coupled to a shut-off valve (Nupro 1/8" plug valve).

The wiring from all the solenoids on the rear of the panel was grouped in a neat bunch and terminated at a multiple connector plug for quick and easy disconnection during panel removed.

The switching sequence diagram was used to test operations and determine time intervals between certain operations and all final adjustments made.

The microcomputer and the interface cards/relays were then connected to the krypton system via the LED display panel. The manual section (Level 1) of the program could now be used to check the operation of the individual components and the working of the display panel. All units operated successfully. The sequence operations (Level 2) with the relevant time delays were tested thereafter and finally the semi-automatic operations (Level 3) were tested under full production conditions.

5.2.10   Hot-cell Lay-out

It is noted in Fig. 41, that the components are densely packed inside the hot-cell. The hot-cell lay-out was designed such that the reservoir ports, coalescing filter, cryopump, filter and target inlet port are all on the same upper level and the circulating pump, mesh filter and target outlet port are all on the same lower level. This lay-out was selected not only to fit all components into the hot-cell, but also to maintain minimum system tube volumes and to utilize gravity for drainage. Another factor that influenced the lay-out, was that the hoist is part of the existing equipment and is mounted in a fixed position above the hot-cell entrance hatch.

All components were mounted on the hot-cell panel and the majority of them being manufactured from stainless steel, resulted in to a great mass disadvantage ($\sim$ 100 kg). Standard panel mounting/removal trolleys at the Radioisotope Production Group are available for routine servicing. The incorporation of a counter-balance on a trolley, and skillful maneuvering of the panel when mounting onto the hot-cell, solved the mass problem.

On completion of the system assembly on the hot-cell rear panel, a vacuum leak test and a 2000 kPa pressure test were carried out. Leaks occurred, but adjustments and replacements to various fittings eventually resulted in a gas tight system.

The system on the rear panel was then fitted and lined up inside the hot-cell, in order to check the target loading and coupling operations. Fine adjustments were

successfully made and the alignment marks were scribed onto the panel and panel support brackets.

5.2.11   Generator Loading System

After numerous tests the general operation of the generator loading system proved to function successfully.   The pneumatic cassette—coupling cylinders needed fine adjustments made to their stroke lengths in order to achieve the correct roller pressure on the silicone tubing.

All the original solenoid valves had a tendency to become blocked due to the construction of their small apertures, but this problem was solved by replacing them with larger valves (Asco 1/8" sub—miniature valves).

5.3   ROUTINE MAINTENANCE AND BREAKDOWN PROCEDURES

5.3.1   Test Target

(1)   A hydrostatic internal pressure test is to be carried out on the vessel at 3000 kPa before experimentation and held for 2 hours whilst checking for leaks at the chain clamp and valves.

Component details:

Chain clamp: Evac 6 link (2 off joined)
                      Supplier: Evac AG, Switzerland

Copper seal: CF150
                      Supplier: Krisch Eng.

Valves: Nupro plug valves, SS4P4T
                      Supplier: Johannesburg Valve and Fitting Co.

(2)   A hydrostatic internal pressure test is to be carried out on the front and rear cooling jackets at 1000 kPa while running the cooling water pump.

<u>Component details</u>:

Front jacket O-ring: Parker 2–157
Rear jacket O-ring: Parker 2–163
          Supplier: Parker Hannifin.

5.3.2 <u>Production Gas Target</u>

(1) A hydrostatic internal pressure test is to be carried out on the vessel at 8000 kPa and held for 24 hours to check for small leaks. The test should be carried out once a year.

(2) Replace coupling valve and cooling port O-rings after every 26 hours of irradiation (currently for ~45 min. irradiation and 30 μA beam current). Therefore replace after every 34 production runs.

<u>Component details</u>:

Coupling valve O-rings: Parker 2-009
          Parker 2-012
          Supplier: Parker Hannifin.

Cooling port O-rings: Parker 2-205
          Supplier: Parker Hannifin.

(3) Torque all bolts and nuts every six months.

(4) Check for smooth yoke lock operation and lubricate moving parts every six months.

<u>Component details</u>:

Yoke lock spring: Coil spring − 6 mm ID × 0,6 mm thk, 18 mm free length, 5 active coils
          Supplier: Capewell Springs.

5.3.3   Spray System

No routine maintenance needs to be carried out on the spray nozzles, but corrective action procedures may be followed as described in par. 4.2.3 if operational problems occur.

Component details:

Solid cone spray nozzles:	Delevan BNM6 1/8", stainless steel
Flat spray nozzles:	Delevan CAC2.0, stainless steel
	Supplier: Spray Nozzle (Pty) Ltd, Hanna Instruments, Cape Town.

5.3.4   Circulating Pump

(1)   Despite the low radiation dose received by the plunger seal, a 1000 kPa hydrostatic pressure test should be performed on the barrel once per year for general routine maintenance.

Component details:

Plunger seal:	Perbunan PRT No.: 104163 – 40 mm dia; Cylinder DN-40-PPV.
	Supplier: Festo
Barrel base seal:	Parker 2-220, Viton
	Supplier: Parker Hannifin

(2)   The check valves contain Viton O-rings which are superior to Perbunan as regards radiation resistance, but they too must be checked by means of performing a 1000 kPa pressure test once per year for ensuring reliable operation.

Component details:

Check valves:	Nupro-stainless steel SS-4C-1/3
	Supplier: Jhb Valve and Fitting Co.

(3)   If operational problems between the manual and automatic mode during normal operation occur, the operator may consult the relevant section on the pneumatic circuit diagram (see Fig. 34).

5.3.5   Cryogenic Pump

The cryogenic pump should be hydrostatically tested at 3000 kPa once per year and held at this pressure for five hours to check for small leaks on the weld seams and fittings. The Tufnol cover must also be checked for cracks which may have formed due to prolonged exposure to cryogenic temperatures.

5.3.6   Gas Reservoir

The O-rings will be exposed to the same negligible dose as with the circulating pump, but a 300 kPa gas pressure test must be done once per year to check the O-rings and all port fittings.

Component details:

O-rings: Parker 2-160
             Supplier: Parker Hannifin

5.3.7   Coupling Valves

Each time the panel is fitted, the alignment marks on the panel and panel support brackets have to be accurately aligned so that the coupling valves line up properly. This should be finally checked by actuating all coupling valve operations before a production run is carried out.

The radiation damage on the target coupling valves has already been discussed in par. 4.3.2 and the damage to the system coupling valves would be slightly greater than that of the circulating pump. Even if the dose is a factor 100 higher, it can be seen from the circulating pump calculations (see par. 4.2.4) that the damage to the system coupling valves O-rings would still be negligible. As previously mentioned however, the valve face O-rings will also be subjected to mechanical wear during coupling and de-coupling and therefore replacement has to be carried out once per year. The valve plug O-rings need also only be pressure tested once per year as with the rest of the valves in the system. The flexible tubing and fittings must be pressure tested at

2500 kPa every six months but visual checks should be done every time the panel is removed.

Component details:

Valve face O-rings: Parker 2-107, Viton
                             Supplier: Parker Hannifin

Valve plug O-rings: Nupro replacement subassembly: SS-P4T-K9, Viton
                             Supplier: Jhb Valve and Fitting Co.

Flexible tubing: 1/4" Polyamid, PP-4
                             Supplier: Festo

5.3.8   Pneumatic System

As mentioned in par. 3.2.11.8 the system needs no maintenance, but brief visual and audible checks may be done on the pneumatic components each time the panel is exposed or removed. If a breakdown occurs, the problem may be approached by consulting the relevant circuit on the pneumatic system diagram (see Fig. 34).

5.3.9   Control System

As mentioned in par. 4.3.9, the mechanical and electro-mechanical control units need no maintenance. The operator must however familiarize himself with the normal operation of the control units so that abnormalities and problems can easily be detected. Faulty control units should always be repaired by the original suppliers.

Component details:

Pressure/Vacuum Gauge: −100 to +300 kPa, st.st, 1/4" NPT rear entry,
                             No. 23X63 R
                             Supplier: Wika Instrumentation

Pressure/Vacuum Gauge: −100 to +2400 kPa, st.st, 1/4" NPT bottom entry,
                             Gly. filled, No. 233-63-Q
                             Supplier: Wika Instrumentation

Pressure Relief Valve: Nupro SS-4CA-350-NE, setpoint 300 kPa
                                        Supplier: Jhb Valve and Fitting Co.

Pressure Relief Valve: Nupro SS-4CA-350-NE, setpoint 2000 kPa
                                        Supplier: Jhb Valve and Fitting Co.

Pressure Switch: −100 to +100 kPa, N/C, Asco No. 27ARV24A32
                                        Supplier: Ascoreg

Coalescing Filter: Headline 210 − 1/4" NPT, element: Borosilicate
                                        glass microfibre, Gr. 12-32-50C
                                        Supplier: David Rice and Co.

Microcomputer control: PC − 8MHz, 640kb, 20Mb HDD, 360kb FDD
                                        PC Interface − SABUS, 24 bit OPTO input card,
                                                        24 bit OPTO output card
                                        Supplier: NAC Control Group

Cryogenic Valve: Asco 1/4" 24 VDC, No. WP 8263205 LT
                                        Supplier: Ascoreg

Mesh filter: Nupro SS-4TF-140
                                        SS-4F-K4-40 (Strainer element)
                                        Supplier: Jhb Valve and Fitting Co.

5.3.10   Hot−cell Lay−out

All components mounted on the rear of the hot-cell panel should be visually checked each time the panel is exposed or removed. Special attention must be paid to the flexible connections.

The hoist lead-screw and hand collets need to be lightly lubricated every six months and the pneumatic/electrical components settings checked at the same time.

The moisture level in the vacuum pump oil may be checked once per week. Excessive moisture is present if the oil turns a milky colour. This can be observed through the oil level window on the side of the pump (pump must be running). In order to remove the moisture from the oil, the following sequence should be followed:

(1) Let pump run for 20 min. to warm up

(2) Close inlet valve

(3) Open gas ballast (large round knob on side of pump)

(4) Let run until oil is clear

(5) Close gas ballast

Component details:

Vacuum Pump: Alcatel-rotary vane-2 stage, No: 786725.

5.3.11   Generator Loading System

The correct operation of the peristaltic pump, the pneumatic cassette-coupling cylinders, the generator bulkhead connector and the solenoid valves can best be monitored under normal production conditions and should require no maintenance. A pumping speed of ~ 0,9 mℓ/min on each line needs to be maintained at all times. The condition of the tubes and couplings (especially at the pump rollers and bulkhead connector areas) should be checked every 3 months.

Component details:

Peristaltic pump:	Watson Marlow Microcassette pumphead 304 MCX, 10 rpm. Supplier: Aeromix (Pty) Ltd
Valves:	Asco sub-miniature solenoid valve, 2/2 way, normally closed, 1/8" brass, No. WPSC8225A4, 24VDC Supplier: Sprecher & Schuh
Tubes:	Watson Marlow 1,14 mm ID silicone tubing, No. 503S/rr Supplier: Aeromix (Pty) Ltd

CHAPTER 6

CONCLUSIONS

Worldwide, radioisotope production, and specifically gas target technology, is a very specialized field. As was discussed in Chapter 2, gas target technology applications, requirements and conditions at the different radioisotope production and research centres vary drastically. Each centre normally designs and develops its own systems in order to satisfy its own specific needs. The technology often demands close integration of various fields, especially in engineering and physics. The design and development processes therefore constantly require input from and compromise between these fields.

As indicated in Chapter 4, the design of the system was subjected to numerous fixed parameters within which it had to work. This made obtaining single, simple solutions extremely difficult and demanded many trade-offs. Despite these factors, all the original objectives, as formulated in Chapter 3, were accomplished. The first series of experimental production runs with the gas target, as recorded in Chapter 5, proved that both the expected mechanical specifications and the Rb production yield could be achieved. The system was then phased into the production programme, while the old RbCl system was gradually phased out. During this period, operating and other personnel involved were trained under production conditions. Physics data were also collected whilst changing various production parameters. Although the system is now in full-scale use for delivering ^{81}Rb to hospitals, data collection and experimentation are still continuing in order to optimize operations.

The Radioisotope Production Group at the NAC is constantly challenged to develop new or improved methods for the production of radioisotopes as the beam-time demand and therefore the competition for beam—time between the various user groups increases. Due to the high beam generation costs, beam—time schedules and beam utilization have to be optimized, and the introduction of the new krypton gas target system for the production of ^{81}Rb will substantially increase the time available for other production and experimental runs. The higher production yield of the new system compared to the old solid RbCl target system also makes provision for an expected future increase in the demand for ^{81}Rb/^{81m}Kr from the end users.

The successful completion of the project now necessitates the manufacture of additional krypton gas targets. Furthermore, the feasibility of further improvements or automation on the control system should be investigated. The routine maintenance programme of the gas target system also has to be introduced.

The design and development of the krypton gas target system was a project which not only demanded an efficient and reliable operational system, but also a database of knowledge in the field of gas target technology for future reference. As a consequence of the fact that all the separate components within the system were individually developed, sufficient knowledge was also gained for using these components for other similar applications.

In conclusion, the krypton gas target system is now an integral component of the production facilities at the NAC and has paved the technology path for, amongst others, a xenon gas target system which is at present seriously considered for the production of ^{127}Xe, a radioisotope utilized in the medical field.

APPENDIX A1

MASS CALCULATION OF GAS TARGET

Mass of stainless steel components:

The volumes of the stainless steel components first need to be calculated.

Volume of struts:

$$V_{S1} = \frac{\pi}{4} D^2 \times L \times 4 \text{ off}$$

$$= \frac{\pi}{4} \times 10^2 \times 218 \times 4$$

$$= 68,487 \times 10^3 \text{ mm}^3$$

Volume of face plate:

$$V_{S2} = \text{volume of plate} - \text{volume of hole}$$

$$= (\ell \times b \times t) - \frac{\pi}{4} \times D^2 \times t$$

$$= 130 \times 130 \times 10 - \frac{\pi}{4} \times 31^2 \times 10$$

$$= 161,452 \times 10^3 \text{ mm}^3$$

Volume of inner vessel cone:

$$V_{S3} = \frac{\pi}{12} h \left[(D_1^2 + D_1 d_1 + d_1^2) - (D_2^2 + D_2 d_2 + d_2^2) \right]$$

$$= \frac{\pi}{12} \times 162 \left[(82^2 + 82 \times 27 + 27^2) - (80^2 + 80 \times 25 + 25^2) \right]$$

$$= 27,228 \times 10^3 \text{ mm}^3$$

Volume of cooling jacket cone:

$$V_{S4} = \frac{\pi}{12} h \left[(D_1^2 + D_1 d_1 + d_1^2) - (D_2^2 + D_2 d_2 + d_2^2) \right]$$

$$= \frac{\pi}{12} \times 162 \left[(88^2 + 88 \times 33 + 33^2) - (86^2 + 86 \times 31 + 31^2) \right]$$

$$= 30,282 \times 10^3 \text{ mm}^3$$

Volume of small end cap:

$$V_{S5} = \frac{\pi}{4} \times D^2 \times L$$

$$= \frac{\pi}{4} \times 34^2 \times 1$$

$$= 907,920 \text{ mm}^3$$

Volume of large end cap:

$$V_{S6} = \frac{\pi}{4} \times D^2 \times L$$

$$= \frac{\pi}{4} \times 116^2 \times 1$$

$$= 10,568 \times 10^3 \text{ mm}^3$$

Volume of cooling jacket ring:

$$V_{S7} = \frac{\pi}{4} \times (D^2 - d^2) \times L$$

$$= \frac{\pi}{4} \times (100^2 - 75^2) \times 10$$

$$= 34,361 \times 10^3 \text{ mm}^3$$

Volume of valves:

$$V_{S8} = (\ell \times b \times h) \times 2 \text{ off}$$

$$= 19 \times 19 \times 19 \times 2$$

$$= 13718 \text{ mm}^3$$

Total volume of stainless steel components:

$$V_S = V_{S1} + V_{S2} \text{.........} + V_{S8}$$

$$= 347,004 \times 10^3 \text{ mm}^3$$

Density of stainless steel (Gr 316) $= 8000 \text{ kg/m}^3$ [Jac86]

Total mass of stainless steel:

$$M_S = D \times V$$

$$= 8 \times 10^{-6} \times 347{,}004 \times 10^3$$

$$= 2{,}776 \text{ kg}$$

Mass of aluminium components:

The volumes of the aluminium components first need to be calculated.

Volume of base:

$$V_{A1} = (\ell \times b \times t)$$

$$= 140 \times 130 \times 19$$

$$= 345{,}8 \times 10^3 \text{ mm}^3$$

Volume of beam-stop:

$$V_{A2} = \frac{\pi}{4} \times D^2 \times L$$

$$= \frac{\pi}{4} \times 74^2 \times 15$$

$$= 64{,}513 \times 10^3 \text{ mm}^3$$

Volume of yoke guides:

$$V_{A3} = \ell \times b \times h \times 2 \text{ off}$$

$$= 30 \times 20 \times 145 \times 2$$

$$= 174 \times 10^3 \text{ mm}^3$$

Volume of window:

$$V_{A4} = \frac{\pi}{4} \times D^2 \times L$$

$$= \frac{\pi}{4} \times 50^2 \times 6$$

$$= 11{,}78 \times 10^3 \text{ mm}^3$$

Total volume of aluminium components:

$$V_A = V_{A1} + V_{A2} + V_{A3} + V_{A4}$$

$$= 596,093 \times 10^3 \text{ mm}^3$$

Density of aluminium (Gr 6082) $= 2710 \text{ kg/m}^3$ [Jac86]

Total mass of aluminium:

$$M_A = D \times V$$

$$= 2,71 \times 10^{-6} \times 596,093 \times 10^3$$

$$= 1,615 \text{ kg}$$

Mass of krypton gas:

Volume of krypton gas:

$$V_K = 7\ell$$

Density of krypton gas $= 3,478 \text{ g}/\ell$ @ 20°C [Crc87]

Mass of krypton gas:

$$M_K = D \times V$$

$$= 3,478 \times 7$$

$$= 24,346 \text{ g}$$

Total mass of gas target:

$$M_T = M_S + M_A + M_K$$

$$= 4,42 \text{ kg.}$$

APPENDIX A2

TARGET POWER DENSITY CALCULATIONS

Power density of water–cooled front entrance area:

Power absorbed:

$$P = V \times I$$

where P = power absorbed in Watts

V = energy received in MeV

I = beam current in μA

Therefore P = 13,22 × 60

= 793,2 W

Area heated by beam:

Beam diameter = 1 cm

Therefore beam area A = $\frac{\pi}{4} \times D^2$

= $\frac{\pi}{4} \times 1^2$

= 0,785 cm^2

Two interfaces (entrance window and front end cap) are cooled simultaneously:

Thus total area = 2 × 0,785

= 1,57 cm^2

Power density:

$$P_D = \frac{P}{A}$$

where P_D = power density in W/cm^2

P = power absorbed in Watts

A = area heated by beam in cm^2

Therefore $P_D = \frac{793,2}{1,57}$

$\qquad = 505,2 \ W/cm^2$

Power density of inner vessel:

Power absorbed:

$P \ = \ V \times I$

where P $=$ power absorbed in Watts

$\qquad$ V $=$ energy received in MeV

$\qquad$ I $=$ beam current in μA

Therefore,

$P \ = \ 8,02 \times 60$

$\quad = \ 481,2 \ W$

Vessel area heated by beam:

Frustum of cone:

$A_1 \ = \ \frac{\pi}{2} \, m(D + d)$

where $A_1 =$ area

$\qquad$ D $=$ large end diameter

$\qquad$ d $=$ small end diameter

and m is given by:

$$= \ \sqrt{\left[\frac{D-d}{2}\right]^2 + h^2}$$

where m $=$ tapered height of cone

$\qquad$ h $=$ perpendicular height of cone

Therefore m $= \sqrt{\left[\dfrac{8-2,5}{2}\right]^2 + 16,2^2}$

$= 16,43$ cm

Thus A_1 $= \dfrac{\pi}{2} \times 16,43 \times (8 + 2,5)$

$= 271,0$ cm²

Rear end cap:

Blank diameter $= 11,8$ cm

Therefore $A_2 = \dfrac{\pi}{4} \times D^2$

$= \dfrac{\pi}{4} \times 11,8^2$

$= 109,4$ cm²

Front end cap:

Blank diameter $= 3,7$ cm

Therefore $A_3 = \dfrac{\pi}{4} \times D^2$

$= \dfrac{\pi}{4} \times 3,7^2$

$= 10,8$ cm²

Total surface area of inner vessel:

$A_T = A_1 + A_2 + A_3$

$= 271,0 + 109,4 + 10,8$

$= 391,2$ cm²

Power density:

$P_D = \dfrac{P}{A}$

where P_D = power density in W/cm²

P = power absorbed in Watts

A = area heated by beam in cm²

Therefore,

$$P_D = \frac{481,2}{391,2}$$

$$= 1,23 \text{ W/cm}^2$$

Power density of beam-stop:

Power absorbed:

$$P = V \times I$$

where P = power absorbed in Watts

V = energy received in MeV

I = beam current in μA

$$P = 44,48 \times 60$$

$$= 2668,8 \text{ W}$$

Area heated by beam:

Beam diameter = 5 cm

$$\text{Therefore beam area A} = \frac{\pi}{4} \times D^2$$

$$= \frac{\pi}{4} \times 5^2$$

$$= 19,6 \text{ cm}^2$$

Power density:

$$P_D = \frac{P}{A}$$

where P_D = power density in W/cm²

$\quad$ P $\quad$ = power absorbed in Watts

$\quad$ A $\quad$ = area heated by beam in cm²

Therefore,

$$P_D = \frac{2668,8}{19,6}$$

$$= 136,2 \text{ W/cm}^2.$$

REFERENCES

For further information on the National Accelerator Centre, annual reports are available from:

The Librarian
NAC
P O Box 72
Faure
7131

Annual report no's:

NAC/AR/75–01	NAC/AR/81–01	NAC/AR/87–01
NAC/AR/76–01	NAC/AR/82–01	NAC/AR/88–01
NAC/AR/77–01	NAC/AR/83–01	NAC/AR/89–01
NAC/AR/78–01	NAC/AR/84–01	NAC/AR/90–01
NAC/AR/79–01	NAC/AR/85–01	NAC/AR/91–01
NAC/AR/80–01	NAC/AR/86–01	NAC/AR/92–01

[Ang67]   Angst and Pfister. 1967. *Elastomer Specifications Catalogue.* Angst and Pfister AG, Zürich, Austria.

[Bar85]   Barron R.F. 1985. *Cryogenic Systems.* 2nd Edition. Oxford Science Publications.

[Bjo84]   Björnstad T. 1984. *The Production of* ^{81m}Kr *Generators at the Oslo Cyclotron.* University of Oslo Report 84-02.

[Bmi89]   Bureau for Mechanical Engineering. 1989. *Report BM 89/75.* University of Stellenbosch.

[Bur79]   Burgerjon J.J. 1979. *500 MeV Radio Gas Target for Positron Emission Tomography.* TRIUMF Report TRI-DN-79-2.

[Crc87]   CRC. 1987. *Handbook of Chemistry and Physics.* 67th Edition. Ed. Weast R.C. CRC Press, Inc.

[Dab90]   Dab.   1990.   *Horizontal Centrifugal Electric Pumps* — Catalogue. Interdab, Mestrino, Italy.

[Del90]   Delevan. 1990. *Industrial Nozzles and Accessories Catalogue.* Delevan Ltd, Cheshire, U.K.

[Fes90]   Festo.   1990.   *Pneumatics Product Range Catalogue.* Festo (Pty) Ltd, Johannesburg, RSA.

[Gie83]   Gieck K. 1983. *Engineering Formulas.* 4th Edition, McGraw-Hill.

[Goo91]   Goodall R.   1991.   Private Communications.   MRC Cyclotron Unit, Hammersmith Hospital, London.

[Haa91]   Haasbroek F.J. 1991. Private Communications. NAC.

[Has81]   Haskel.   1981.   *An Introduction to Air Driven Liquid Pumps* — M–LP Brochure. Haskel Energy Systems Ltd., Sunderland, UK.

[Has86]   Haskel. 1986. *An Introduction to Air Driven Gas Booster Compressors* — M–GB Gas Booster Compressor Brochure. Haskel Energy Systems Ltd., Sunderland, UK.

[Hea88]   Headline Filters.   1988.   *Compressed Air Filters Catalogue.* Headline Filters Ltd., Maidstone, Kent, U.K.

[Hea89]   Hearn E.J.   1989.   *Mechanics of Materials.*   2nd Edition, Pergamon Press. 19 (1,2).

[Hol82]   Holman J.P. 1982. *Heat Transfer.* 5th Edition, McGraw-Hill.

[Hum88]   Human T.M.   1988.   *The Design and Development of a Microprocessor Based Control System for an Electric Rail Transport System.* Masters Diploma Thesis, Cape Technikon.

[Jac86]   Jacksons Metals.   1986.   *Ferrous and Non-Ferrous Metals* — Stocklist. Jacksons Metals (Pty) Ltd., Sandton, RSA.

[Mar83] March. 1983. *Seal-Less Magnetic Drive Pump* – Catalogue. March Manufacturing Inc. Glenview, Illinois, U.S.A.

[Mil89a] Mills S.J., Nortier F.M., Rautenbach W.L., Smit H.A. and Steyn G.F. 1989. *A multi-purpose target station for radioisotope production at medium energies*. In Proc. 12th Int. Conf. on Cyclotrons and their Applications, Berlin. Eds. Martin B. and Ziegler K. 1991. World Scientific, Singapore, p. 527.

[Mil89b] Mills S.J., Nortier F.M., Rautenbach W.L. and Steyn G.F. 1989. *A Versatile Cooling Water System for Radioisotope Production Targets in Tandem*. In Proc. 12th Int. Conf. on Cyclotrons and their Applications, Berlin. Eds. Martin B. and Ziegler K. 1991. World Scientific, Singapore, p. 523.

[Mil92] Mills S.J. 1992. Private Communications. NAC.

[Ost67] Ostergaard D.E. 1967. *Advanced Diemaking*. Resources and Materials of the National Tool, Die and Precision Machining Assn. McGraw-Hill. p. 126-142.

[Par71] Parker. 1971. *O-Ring Cross Reference* – Catalogue. Parker Seal Co., Culver City, California, USA.

[Rut85] Ruth T.J., Adam M.J., Burgerjon J.J., Lenz J. and Pate B.D. *A Gas Target for Radionuclide Production with 500 MeV Protons*. TRIUMF Report TRI-PP-85-23, Vancouver, Canada

[Sch81] Schwartz W. 1981. *Electropolishing*. In Plating and Surface Finishing. Ed. Swalheim D.A., p. 42-45, AES Update, New York, USA.

[Sch90] Scheidereiter C. 1990. Private Communications. Plastronics (Pty) Ltd, Cape Town.

[Ste90] Steyn G.F. 1990. Private Communications. NAC.

[Ste91]   Steyn G.F., Mills S.J., Nortier F.M. and Haasbroek F.J. 1991. *Integral Excitation Functions for $^{nat}Kr+p$ up to 116 MeV and Optimization of the Production of ^{81}Rb for ^{81m}Kr Generators.* Appl. Radiat. Isot. 42. p. 361-370.

[Ste92]   Stevens C.J., Fisch R.K., Steyn G.F. 1992. *Software Developed for the Remote Control of a High-Pressure Krypton Gas Target System.* NAC Report NAC/I/92-02.

[Swa88]   Swagelok, Whitey, Nupro, Cajon, Sno-Trik. 1988. *Fittings, Valves and Couplings* — Catalogue. The Swagelok Companies. USA.

[Ver83]   VEW. 1983. *Vereinigte Edelstahlwerke Aktiengesellschaft* — Manual. VEW, Vienna, Austria.

[Von76]   Von Witsch W. and Willaschek J.G. 1976. *High-Pressure Gas Target for the Production of Intense Fast-Neutron Beams.* Nuclear Instruments and Methods, **138**, p. 13-17. North Holland Publishing Co.

[Wat86]   Waters S.L., Clark J.C., Horlock P.L., Brown C., Bett R. and Sims H.E. 1986. *Production of ^{81}Rb using a 60 MeV Proton Beam. Target Development and Aspects of Recovery.* Journal of Labelled Compounds and Radiopharmaceuticals, **23**, p. 10-12.